Title
Two proteins that cycle asynchronously between nuclei and centrosomes

Author
Oegema, Karen,

Publication Date
1997

Peer reviewed|Thesis/dissertation

Two Proteins that Cycle Asynchronously Between Nuclei and Centrosomes: *Drosophila* CP190 and CP60

by

Karen Oegema

DISSERTATION

Submitted in partial satisfaction of the requirements for the degree of

DOCTOR OF PHILOSOPHY

in

Cell Biology

in the

GRADUATE DIVISION

of the

UNIVERSITY OF CALIFORNIA

San Francisco

I dedicate this thesis to my parents

Ted and Carol Oegema

for their encouragement and perseverance,

and to Arshad Desai

for his help and friendship.

Acknowledgments

I would like to thank Bruce Alberts for providing the best of environments in which to be a graduate student, for being the source of the joy of doing science that drew me to his lab, and for encouraging us to take the high and long (but instructive) road.

I would like to thank Tim Mitchison for his practical advice and encouragement, for being the chair of my orals and thesis committees and for being a mentor to me. Contact with Tim and his lab has enabled me to learn much of what I know about how to do science.

I would like to thank Chris Field for watching over me during graduate school, for providing me with many opportunities and for being an adult role model in the midst of chaos.

I would also like to thank the entire Alberts lab, past and present. It has been an honor to be connected to so many wonderful people and excellent scientists.

Thank you to Becky Kellum and Kevin Hacker for friendship and for accompanying me on an absolutely excellent vacation to Costa Rica, to Bill Theurkauf for being a supportive bay-mate, to Michelle Moritz for her patient friendship and to Yixian Zheng for her zany influence.

Thank you also to Mercedes Rojas for being my friend and for helping me with my Spanish and to Raffi Aroian for organizing lab social events, for being a great source of encouragement and for teaching me what it means to bond with your organism.

Many thanks to Jack Barry for helping me learn protein purification, for exposing me to opera and for keeping us up to date on the latest news and gossip.

I want to thank Doug Kellogg for getting me started in the Alberts lab, for making life fun, and for always having time to talk to me, and Bill Sullivan for his genuinely good attitude towards science and life in general and for always being a source of perspective during my graduate career. When everything seemed completely bogus - talking to Bill always made me feel better about life and excited about my work (but did not necessarily result in bogosity reduction). Thank you also for allowing me to bear the torch or idiocy for a few years - before it came to rest in its rightful home in Santa Cruz.

Thank you to Bin Liu for his quirky influence and for sticking it out with me as a graduate student in the Alberts lab and to Bob Schrock for being a good lab citizen and a totally nice guy.

I would also like to thank Paul Peluso for many late night junk food runs, sushi, good music, and for keeping me up to date on Ffh and FtsY and Wallace Marshall for being the ideal collaborator.

Finally I would like to thank my parents and my brother Jeff for endless love and support during my endless education,

Arshad Desai for being himself and my best friend, and Wally and Little Guy for affectionately hanging with me through it all.

Two Proteins that Cycle Asynchronously Between Nuclei and Centrosomes: *Drosophila* CP190 and CP60

Karen Oegema

Abstract

CP190 and CP60 are two Drosophila proteins of unknown function that shuttle between centrosomes and nuclei in a cell cycle-dependent manner. Both CP190 and CP60 are able to attain and maintain their centrosomal localization in the absence of microtubules. We have quantitated the relative timing of the localizations of CP190 and CP60 using time lapse 3D wide field microscopy after injection of fluorescently labeled fusion proteins. CP190 is found in nuclei during interphase and at centrosomes during mitosis. The oscillation of CP60 between nuclei and centrosomes is similar but temporally delayed. CP60 accumulates at centrosomes during anaphase, reaching peak levels by telophase and localizes to nuclei gradually during interphase, reaching peak levels just before nuclear envelope breakdown. Once in the nucleus, both CP190 and CP60 form fibrous intranuclear networks; however, they do not co-localize extensively with each other or with DNA.

To characterize the regions of CP190 responsible for its dynamic behavior, we injected smaller rhodamine-labeled fusion proteins spanning most of CP190 into early Drosophila embryos and followed their localizations using time-lapse confocal microscopy. A single bipartite 19-amino acid nuclear localization signal responsible for the nuclear localization of our fusion proteins was identified. Robust centrosomal localization is conferred by a separate region of 124 amino acids.

We have also characterized the protein complexes containing CP190, CP60 and γ-tubulin in concentrated Drosophila embryo extracts. γ-tubulin is

found in two distinct but related complexes, neither of which contain CP190 or CP60. The larger γ-tubulin containing complex (MW about 3,000,000 daltons) can be converted to a smaller γ-tubulin containing complex (about 240,000 daltons) by treatment with high salt. γ-tubulin fails to co-immunoprecipitate with CP190 or CP60 from concentrated extracts, and neither CP190 nor CP60 co-immunoprecipitates with γ-tubulin. Comparison between native CP190 and CP60 in extracts and comparable bacterially expressed fusion proteins reveals that both native CP60 and CP190 form large, asymmetric oligomers. Experiments in which extracts are analyzed on sucrose gradients following immunodepletion of CP190 or CP60 demonstrate that most of the CP60 in extracts associates with CP190.

Tim Mitchison, Ph.D.
Committee chairman

Bruce Alberts, Ph.D.
Advisor

Two Proteins that Cycle Asynchronously Between Nuclei and Centrosomes: *Drosophila* CP190 and CP60

Table Of Contents

List of Tables

Chapter 4

List of Figures

Chapter 1

Chapter 2

Chapter 3

Chapter 4

Appendix

The Rockefeller
University Press
1114 First Avenue, 4th Floor
New York, New York 10021
(212) 327-7938
Fax (212) 327-8587

2 July 1996

Dear Dr. Oegema:

We shall be glad to grant you permission for the reproduction of the material referred to in your letter of 28 June 1996*.

Our only requirements are that you also obtain permission from the author(s) and give suitable acknowledgment to the source in the following manner: Reproduced from **The Journal of Cell Biology, year, vol., pp.** by copyright permission of The Rockefeller University Press.

Sincerely yours,

THE JOURNAL OF
CELL BIOLOGY

Iris Vallecilla
Permissions

Dr. Karen Oegema
University of CA-San Francisco
Dept. Biochemistry/Biophysics
Box 0448
San Francisco, CA 94143-0448

P.S. Since you are the author, a credit line is our only requirement.

*JCB-vol:131,1261-1273,(yr?). article for use in dissertation.

MOLECULAR BIOLOGY OF THE CELL

PUBLICATIONS OFFICE • 9650 ROCKVILLE PIKE • BETHESDA, MARYLAND 20814-3992
TELEPHONE (301) 530-7153 • FAX (301) 571-8304

Rosalba A. Kampman
Managing Editor

July 22, 1996

Dr. Karen Oegema
Department of Biochemistry
and Biophysics
Box 0448
U. of Calif., San Francisco
San Francisco, CA 94143

Dear Dr. Oegema:

We are happy to grant you permission for the reproduction of the material* referred to in your letter of June 18, 1996.

Our only requirement is that you give suitable acknowledgement to the source in the following manner: "Reproduced from *Molecular Biology of the Cell*, year, volume number, page numbers by copyright permission of the American Society for Cell Biology".

Sincerely yours,

Rosalba A. Kampman
Managing Editor

**Molecular Biology of the Cell*, 1995, Volume 6, pp. 1673-1684

Introduction

In the late 19th century two cytologists, Van Beneden and Boveri, independently concluded that the structure at the focus of the mitotic astral fiber array was a permanent organelle that persists during vegetative growth (Wilson, 1925). In his 1924 text, "The Cell in Development and Heredity", E.B. Wilson summarized what was then known about centrosomes (see Fig. 1).

"The general term *central body* is applied to a structure which forms the focus of the aster or astral system during mitotic cell-division, and hence is often spoken of as the *division-center*. In many cases this body persists during the vegetative or "resting" period of the cell, and is handed on by division to the daughter-cells without loss of its identity..... Its most constant and essential component is the *centriole*, a minute granule or rod, often double, in some cases lying naked in the cytoplasm, more often surrounded by a cytoplasmic investment of various degrees of complexity."

Since its discovery more than a century ago, the centrosome has continued to intrigue cell biologists. Over the past thirty years, electron microscopy has greatly improved the resolution of our view of the centrosome. We now know that centrosomes consist of a pair of intricately detailed centriolar cylinders, each consisting of nine triplet microtubules, surrounded by an electron dense cloud of pericentriolar material (PCM) that is the origin of the microtubules nucleated by the centrosome (Gould and Borisy, 1977, Keryer, et al., 1984, reviewed in Kalnins, 1992).

The structural dynamics of centrosomes during the cell cycle have also been characterized. The centriolar cylinders duplicate once per cell cycle in concert with changes in the surrounding PCM that are thought to provide the structural basis for the very different interphase and mitotic microtubule

assemblies (see Fig. 2). In interphase tissue culture cells, the PCM contains small electron-opaque aggregates, or satellites, that surround the parent centriole. During prophase, the satellites disappear and are replaced by a large mitotic "halo" of lighter staining material that surrounds the parent centriole and nucleates the abundant mitotic microtubule array (Robbins, et al., 1968, Rieder and Borisy, 1982, Vorobjev and Chentsov, 1982). In one study, the nucleating capacity of centrosomes from mitotic cells was found to be about 5 fold higher than that of centrosomes from interphase cells (Kuriyama and Borisy, 1981).

Isolated centrosomes can nucleate microtubules in vitro and can template the protofilament number of the microtubules they nucleate (Mitchison and Kirschner, 1984, Evans, et al., 1985). Recently, EM tomography of centrosomes isolated from *Drosophila* embryos has dramatically altered our structural picture of the centrosome, allowing the visualization of microtubule nucleating sites within the pericentriolar material (Moritz, et al., 1995). The microtubule nucleating activity of the PCM is now ascribed to the presence of γ-tubulin containing ring complexes (γ-TuRCs) that can nucleate microtubules when isolated in vitro and that appear as rings in intact centrosomes (see Fig. 3; Moritz, et al., 1995, Zheng, et al., 1995).

We can conclude, at the very least, that the centrosome is a dynamic organelle that can duplicate, nucleate microtubules, template the protofilament number of nucleated microtubules, organize/anchor microtubules, and that can change in a cell cycle dependent way so that more microtubules are nucleated during mitosis than during interphase. By virtue of its ability to nucleate microtubules, the centrosome also determines the number, and to some extent the distribution, of the microtubules in animal cells. The centrosome nucleated microtubule arrays, in turn, direct the events of mitosis and have a central role in

the organization of the interior of the cell during interphase (for reviews see Mazia, 1987, Kellogg, et al., 1994, Schatten, 1994, Vorobjev and Nadezhdina, 1987).

The problem facing the current generation of cell biologists is to understand the centrosome at a molecular level in the context of the cell. To do this we need to identify and characterize the molecules that comprise the structural scaffold and microtubule nucleating elements as well as centrosomal components involved in a number of dynamic processes including: centrosome duplication and separation, the observed cell cycle dependent changes in the nucleating capacity of centrosomes, the interaction of the centrosome with the nucleus and with spindle poles, and the organization and dynamics of microtubule arrays.

The identification of centrosomal components has been slow due to the centrosome's small size and paucity which make biochemical approaches difficult and to their involvement in very general mitotic events which increases the difficulty of genetic approaches. Further complicating the issue is the fact that the centrosome, as the origin of the cell's nucleated microtubules, is also a hub for intracellular traffic. Schatten discusses this problem in his 1994 review.

" A significant difficulty in determining which centrosomal proteins and other components are integral and invarient is that the centrosome serves as a hub of intracellular trafficking. If we view the cell as a tangle of highways leading into, through, and out of the centrosome, then an analogy with Rome might be appropriate. Products destined for Naples (or, say, the apical cellular surface) must pass through Rome (i.e. the centrosome) from their site of production in Milan (or the Golgi-endoplasmic reticulum complex). Isolation of the greater Rome complex would be expected to result in the isolation of the highway and

rail systems into and out of Rome, as well as that of all the trucks and other carriers with their cargoes. This analogy illustrates a serious problem in the characterization of the centrosome, since the centrosome carries with it a significant amount of the cytoplasm and yet it is not sufficient to define the centrosome as some fractional component of the entire cytoplasm."

Acknowledging this problem, we define the "core" centrosome as the structure that remains when microtubules have been depolymerized. We can use this test to divide the proteins that are found to accumulate at centrosomes into two groups: those that require microtubules for their centrosomal localization and those capable of localizing to centrosomes independent of the nucleated microtubule array. The first group is likely to include proteins that function to organize the spindle pole, as well as proteins that accumulate at the centrosome due to its role as a hub for intracellular trafficking. Examples of proteins in the first group include include centractin, a component of the dynein containing dynactin complex (Trina Schroer, personal communication), NCD, a minus end directed motor protein, (Endow, et al., 1994), and NuMA, a protein important for spindle pole integrity (also called centrophilin, SP-H and SPN; Price and Pettijohn, 1986, Kallajoki, et al., 1991, Tousson, et al., 1991).

A small group of proteins that do not require microtubules for their centrosomal localization have been identified. Known components of core centrosomes include: pericentrin, γ-tubulin, Xklp2, centrosomin, CP190 and CP60. Antibodies from an autoimmune serum from a patient with scleroderma (designated 5051) were used to clone pericentrin. Pericentrin is a highly conserved, 220 kDa, largely coiled-coil protein that antibody injection experiments suggest may have a role in the structural organization and cohesiveness of the PCM (Doxsey, et al., 1994). Xklp2 is a recently identified kinesin, cloned in a PCR screen of a Xenopus library, that is potentially involved

in centrosome separation and spindle assembly (Boleti, et al., 1996). Centrosomin is a novel structural protein with three leucine zipper motifs and several coiled-coil domains that was identified using an immunopurification method to clone target genes of the homeotic transcription factor Antennapedia in *Drosophila* (Heuer, et al., 1995). Centrosomin localizes to centrosomes throughout the cell cycle in preblastoderm embryos and only to mitotic centrosomes in postblastoderm embryos (Li and Kaufman, 1996). Loss of zygotic centrosomin expression causes a variety of developmental phenotypes and animals mosaic for centrosomin expression exhibit defects indicative of a block in cell proliferation. Embryos that lack maternal as well as zygotic centrosomin also display defects in nuclear division, chromosome alignment and microtubule organization (Li and Kaufman, 1996).

The identification of γ-tubulin as a suppressor of a β-tubulin mutation in *Aspergillus nidulans* has been an important lead in attempts to understand microtubule nucleation by centrosomes (Oakley and Oakley, 1989). γ-tubulin is a highly conserved member of the tubulin family that localizes to centrosomes and to spindle pole bodies (the functional centrosome equivalent in fungi) and is required for spindle assembly and progression through mitosis (Oakley, et al., 1990, Stearns, et al., 1991, Zheng, et al., 1991). Injection of tissue culture cells with antibodies to γ-tubulin inhibits microtubule nucleation from centrosomes (Joshi, et al., 1992) and recruitment of γ-tubulin to sperm basal bodies is required for aster formation in Xenopus egg extracts (Felix, et al., 1994, Stearns and Kirschner, 1994). Recently, a γ-tubulin containing ring complex (γ-TuRC), capable of nucleating microtubules *in vitro* and of capping their minus ends, was purified from *Xenopus* extracts (Zheng, et al., 1995). γ-tubulin containing rings of the same dimensions (25 nm in diameter) have been visualized in the PCM by EM tomography both in the presence and absence of nucleated microtubules (Moritz,

et al., 1995). These results have lead to the seeded model of microtubule nucleation (Fig. 4; Zheng, et al., 1995) to explain how centrosomes are able to template the protofilament number of nucleated microtubules.

Although the identification of γ-tubulin has resulted in a great deal of progress towards understanding microtubule nucleation, still very little is known about either centrosome duplication or the maturation of centrosomes that occurs at the transition between interphase and mitosis in animal cells. Phosphorylation has been proposed to play a role in the mitotic maturation of centrosomes (Buendia, et al., 1992, Vandre and Borisy, 1989, Bailly, et al., 1989, Centonze and Borisy, 1990, Engle, et al., 1988), and the epitope recognized by the MPM-2 antibody (which reacts with a subset of mitotic phosphoproteins) localizes to centrosomes in a microtubule independent fashion during mitosis (Vandre and Borisy, 1989), In addition, treatment with phosphatase or MPM-2 antibody inhibits microtubule nucleation from mitotic centrosomes (Centonze and Borisy, 1990). Centrosome duplication remains completely mysterious.

Our laboratory has taken a biochemical approach to identify cytoskeletal proteins in *Drosophila* embryos. *Drosophila* embryos were chosen as a starting material because large quantities of embryos are easily available and the cytoskeletal proteins required for the rapid syncytial divisions are maternally deposited and are therefore both abundant and largely soluble. We also hope that genetic studies, available in *Drosophila*, will facilitate the functional characterization of identified proteins.

We have used microtubule affinity chromatography and immunocytology to identify and characterize microtubule binding proteins from *Drosophila* embryo extracts (Kellogg, et al., 1989). This approach has lead to the identification of several novel centrosome components. One centrosomal protein identified in this manner is CP190. CP190 has been cloned and sequenced

(Whitfield, et al., 1995); the sequence predicts a novel protein of 1,096 amino acids with an isoelectric point of 4.5 and a molecular weight of 122kD (CP190 runs aberrently on SDS-polyacrylamide gels at 190kDa). Native CP190 localizes primarily to nuclei during interphase and to centrosomes during mitosis (Frasch, et al., 1986, Whitfield, et al., 1988).

Our laboratory extended this work using immunoaffinity chromatography to identify CP190 binding proteins (Kellogg and Alberts, 1992). One protein identified in this way is CP60. Like CP190, CP60 alternates between nuclei and centrosomes in a cell cycle-dependent manner (Kellogg and Alberts, 1992). CP60 has been cloned and sequenced; the sequence predicts a novel protein of 440 amino acids that contains six consensus sites for phophorylation by cyclin-dependent kinases and a sequence of amino acids similar to the "destruction box" that targets cyclins for proteolysis at the end of mitosis (Kellogg, et al., 1995).

This thesis describes the characterization and molecular dissection of CP190 and CP60 that we have done in an attempt to elucidate the functions of these proteins in *Drosophila* embryos.

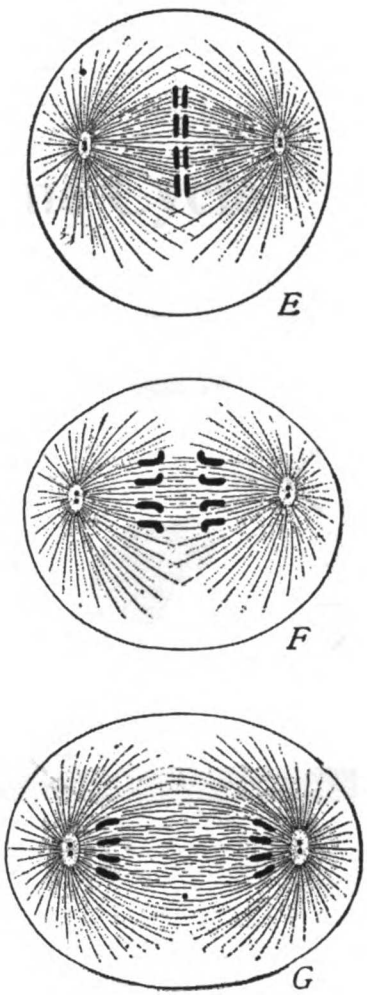

Figure 1- The Central Bodies during mitosis (1924)

Figure 2- The centrosome cycle

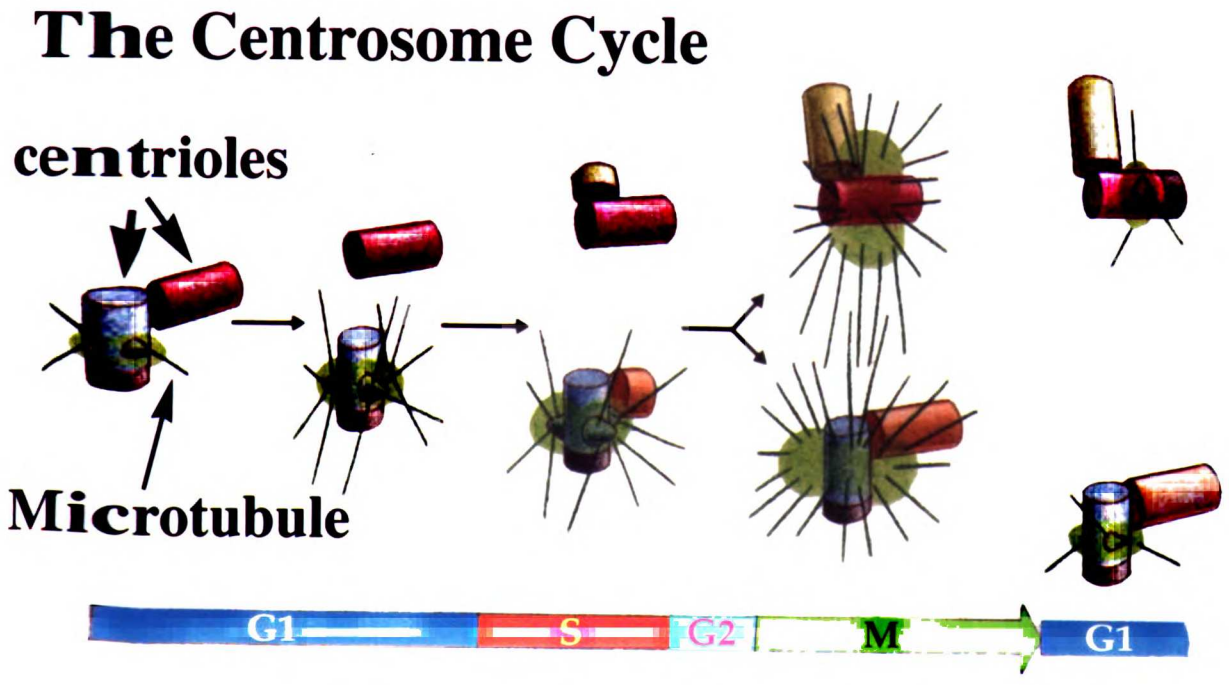

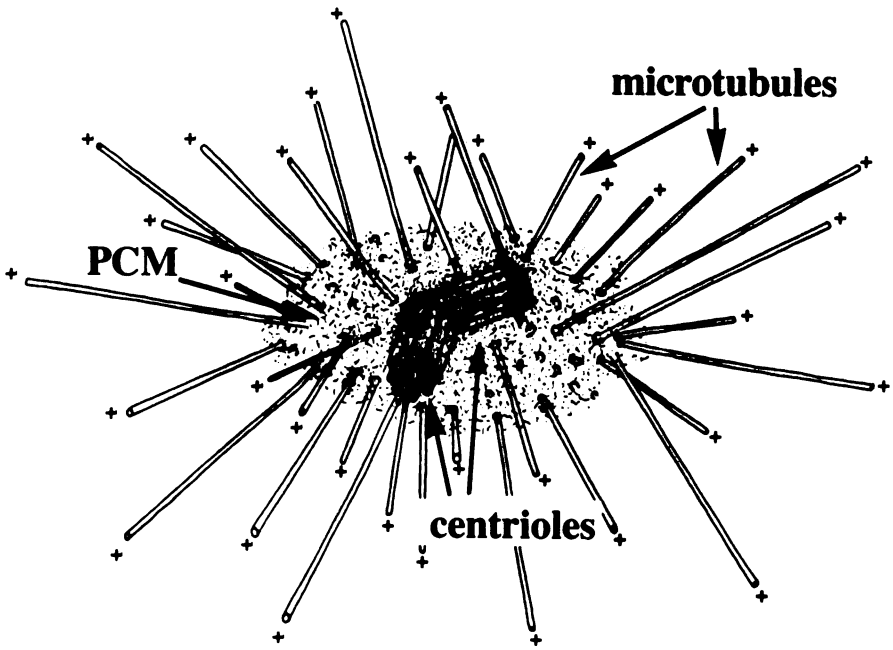

Figure 3- The centrosome (1995)
γ-TuRC= pink rings

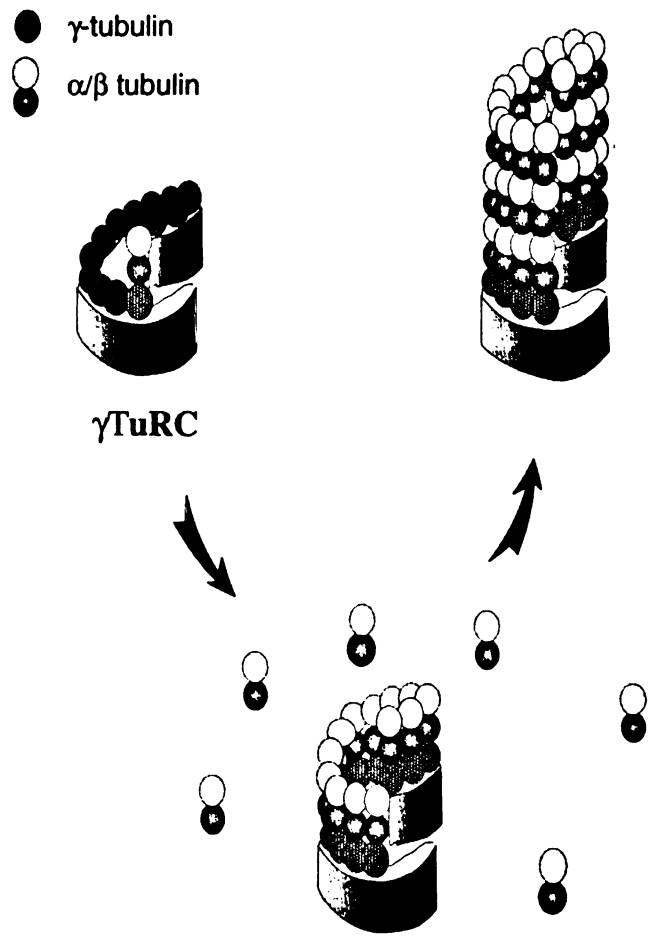

Figure 4- The seeded nucleation model.

Chapter 2

Characterization of the localization patterns of CP190 and CP60

Two Proteins that Cycle Asynchronously Between Nuclei and Centrosomes: Drosophila CP60 and CP190

Karen Oegema*+, Wallace Marshall*, John Sedat and Bruce Alberts

Department of Biochemistry and Biophysics
University of California, San Francisco
San Francisco, CA 94143-0448

* Note- These two authors contributed equally to this work

+ To whom correspondence should be addressed. Telephone: (415) 476-4581; Fax (415) 476-0806

Running Title: CP190 and CP60 cycle asynchronously

Abstract

CP190 and CP60 are two *Drosophila* proteins of unknown function that shuttle between centrosomes and nuclei in a cell cycle-dependent manner. These two proteins are physically associated in vitro, and both will localize to centrosomes even in the absence of microtubules. We injected fluorescently labeled, bacterially expressed CP190 and CP60 into living *Drosophila* embryos and followed their behaviour during the rapid syncytial blastoderm divisions (nuclear cycles 10-13). During interphase, CP190 is found in nuclei. Immediately following nuclear envelope breakdown, CP190 localizes to centrosomes where it remains until telophase, thereafter accumulating in reforming nuclei. Quantitative 3D wide-field fluorescence microscopy shows that this cycle is delayed for CP60. Unlike CP190, CP60 accumulates at centrosomes primarily during anaphase, where it remains into early interphase. During nuclear cycles 12 and 13, CP60 accumulates gradually in nuclei during interphase, reaching peak levels just before nuclear envelope breakdown. During nuclear cycles 10 and 11, CP60 accumulates primarily after nuclear envelope breakdown, suggesting that CP60 binds to an unknown nuclear structure that persists into mitosis. Once in the nucleus, both CP190 and CP60 appear to form fibrous intranuclear networks; however, they do not co-localize extensively with each other or with DNA.

Introduction

In animal cells, centrosome nucleated microtubule arrays are essential for a wide variety of cellular processes including cell division and chromosome segregation, directed cell movement, and interphase cytoplasmic organization (for reviews see Mazia, 1987; Vorobjev and Nadezhdina, 1987; Schatten, 1994; Kellogg, et al., 1994). Studies using electron microscopy have shown that centrosomes consist of a pair of centriolar cylinders surrounded by a cloud of pericentriolar material (PCM) that is the source of the nucleated microtubules (Gould and Borisy, 1977; Keryer, et al., 1984; Rieder and Borisy, 1982; Vorobjev and Chentsov, 1982). Isolated centrosomes can nucleate microtubules in vitro and can template the protofilament number of the microtubules they nucleate (Evans, et al., 1985) The microtubule nucleating activity of the PCM is due to the presence of γ-tubulin containing ring complexes (γ-TuRCs) that can nucleate microtubules when isolated in vitro and that can be visualized in intact centrosomes by EM tomography (Moritz, et al., 1995; Zheng, et al., 1995).

The centrosome is structurally very dynamic, changing continuously in a cell cycle-dependent manner. The centriolar cylinders duplicate once per cell cycle in concert with changes in the surrounding PCM that are thought to provide the structural basis for the very different interphase and mitotic microtubule assemblies. In interphase tissue culture cells, the PCM contains small electron-opaque aggregates, or satellites, that surround the parent centriole. During prophase, the satellites disappear and are replaced by a large mitotic "halo" of lighter staining material that surrounds the parent centriole

and nucleates the abundant mitotic microtubule array (Robbins, et al., 1968; Rieder and Borisy, 1982; Vorobjev and Chentsov, 1982). In one study, the nucleating capacity of centrosomes from mitotic cells was found to be about 5 fold higher than that of centrosomes from interphase cells (Kuriyama and Borisy, 1981).

At a molecular level, very little is known about either centrosome duplication or the maturation of centrosomes that occurs at the transition between interphase and mitosis in animal cells. Phosphorylation has been proposed to play a role in the mitotic maturation of centrosomes (Buendia, et al., 1992; Vandre and Borisy, 1989; Bailly, et al., 1989; Centonze and Borisy, 1990; Engle, et al., 1988), and the epitope recognized by the MPM-2 antibody (which reacts with a subset of mitotic phosphoproteins) localizes to centrosomes in a microtubule independent fashion during mitosis (Vandre and Borisy, 1989). In addition, treatment with phosphatase or MPM-2 antibody inhibits microtubule nucleation from mitotic centrosomes (Centonze and Borisy, 1990).

Further understanding of these cell cycle-dependent centrosomal processes will require the isolation of well-defined centrosomal components and the study of their dynamics at centrosomes. CP190 and CP60 are two such proteins. These proteins shuttle to and from the centrosome in a cell-cycle dependent manner (Frasch, et al., 1986; Whitfield, et al., 1988; Kellogg, et al., 1995) and both proteins are able to attain and maintain their centrosomal localizations in the absence of microtubules, suggesting that they are core components of the pericentriolar material (Raff, et al., 1993; Oegema, et al., 1995). Other proteins that can localize to centrosomes independent of the nucleated microtubule array include: pericentrin, (Doxsey, et al., 1994), the kinesin family member Xklp2 (Boleti, et al., 1996), centrosomin (Li and

Kaufman, 1996) and γ-tubulin (Raff, et al., 1993). Examples of proteins that require microtubules for their localizations to spindle poles include NuMA (also called centrophilin, SP-H and SPN), and NCD, a minus end-directed microtubule motor protein (Price and Pettijohn, 1986; Kallajoki, et al., 1991; Tousson, et al., 1991; Endow, et al., 1994).

The cloning and sequencing of CP190 reveals that it is a novel protein of 1096 amino acids, with a cluster of four putative zinc fingers located roughly in the middle of the predicted protein (Whitfield, et al., 1995). Native CP190 shuttles between nuclei and centrosomes (Frasch, et al., 1986; Whitfield, et al., 1995; Whitfield, et al., 1988) and the regions of this protein responsible for its nuclear and centrosomal localizations have been identified (Oegema, et al., 1995).

CP60 was identified by immunoaffinity chromatography on columns constructed from anti-CP190 antibodies (Kellogg and Alberts, 1992). Like CP190, CP60 localizes to nuclei and to centrosomes in a cell cycle-dependent manner (Kellogg, et al., 1995). CP60 has been cloned and sequenced and shares no significant amino acid homology with CP190 or with any other known protein; it contains 6 consensus cdc2 phosphorylation sites and is phosphorylated in vivo (Kellogg, et al., 1995).

To begin to get a molecular handle on the cell cycle-dependent changes that occur at centrosomes, we have compared the localizations of CP190 and CP60 both by high resolution light microscopy (in fixed embryos) and by quantitative 3D wide-field fluorescence time-lapse microscopy (in live embryos following injection of the fluorescently labeled proteins). We find that, although CP60 was identified by its biochemical association with CP190, the two proteins have very different temporal and spatial localization patterns in *Drosophila* embryos.

Materials and methods

Work with Fluorescent Fusion Proteins

The expression, purification and fluorescent labeling of the CP190 and CP60 fusion proteins were performed as described previously, as were embyro injection and confocal microscopy (Oegema, et al., 1995).

Wide-Field Three-Dimensional Microscopy

Three-dimensional images of living embryos were obtained by wide-field fluorescence microscopy (Hiraoka, et al., 1991) using a Olympus 60X objective with a numerical aperture of 1.4. The computer-controlled stage was stepped in vertical increments of 0.75 μM, and at each vertical position, one 256x256 pixel optical section was acquired for each wavelength, using a cooled CCD. A total of 16 optical sections in each wavelength (fluorescein and rhodamine) were collected to form a single 3D multiwavelength image. The stage was then reset to the initial position and the process repeated continuously, to form a time-lapse series. Using this scheme, one two-wavelength 3D image was collected every 52 seconds. The fixed embryos were examined the same way, except that 512x512 pixel optical sections were taken. For the high resolution micrographs of fixed material optical sections were taken every 0.2 μm. Following image acquisition, out of focus blur was removed using constrained iterative deconvolution (Agard, et al., 1989).

Quantitation of Fluorescence Intensity

In order to quantify changes in total fluorescence in centrosomes and nuclei, all centrosomes and nuclei were defined by tracing their outlines using an interactive modeling program (Chen, et al., 1995). The outlines thus defined were used to classify each pixel in the image as nuclear, centrosomal, or cytoplasmic background. In each section, the average cytoplasmic background was calculated and then subtracted from each nuclear pixel in order to reduce the contribution of scattered light to the measurements. Because out-of-focus light from the nuclei occasionally overlapped a centrosome even after deconvolution, the average intensity of all pixels falling outside a centrosome but within 0.35 μm of the centrosomal boundary was computed and subtracted from each pixel in the centrosome. The total intensity contributed by all centrosomal and nuclear pixels was then calculated separately for each wavelength.

Embryo Fixation and Immunofluorescence

Embryos were fixed in 37% formaldehyde as described (Theurkauf, 1992). The rabbit anti-CP60 antibody used has been described (Kellogg et al., 1995). The goat anti-CP190 antibody used was prepared by immunizing a goat with a total of 4 mg of a maltose binding protein-fusion with CP190 amino acids 606-870, a fragment of CP190 previously described as 190c (Kellogg and Alberts, 1992). Immunizations and bleeds were carried out by the Berkeley Antibody Company (Richmond, CA). The antibodies were affinity purified on a column of immobilized GST-190c prepared as described (Kellogg and Alberts, 1992) according to standard techniques (Harlow and Lane, 1988). donkey fluorescein anti-goat and Texas red anti-rabbit were obtained from Jackson ImmunoResearch Laboratories, Inc (West Grove, PA).

Fluorescence in situ hybridization

Fluorescence in situ hybridization (FISH) with a digoxygenin-labeled rDNA probe (made by Abby Dernburg, UCSF) was carried out in fixed embryos using a modified version (Dernburg et al., in press) of a previously published method (Hiraoka et al., 1993). Embryos were returned to room temperature for all subsequent steps. Embryos were washed four times in 2X SSCT (0.3 M CaCl, 0.03 M Na_3 citrate, 0.1%Tween-20), blocked with 6 mg/ml normal goat serum (Jackson Immunoresearch Laboratories, West Grove, PA) in 2X SSCT for 4 hours, and were then incubated overnight with rabbit anti-CP60 antibody at 1.3 μg/ml in 2X SSCT. The embryos were then washed four times in 2X SSCT (1 hour per wash), incubated for 4 hours with fluorescein rat-anti-digoxygenin (1:8000) and rhodamine donkey-anti-rabbit (diluted 1:200) in 2X SSCT. (Both secondary antibodys were obtained from Jackson Immunoresearch). Embryos were washed three times for 10 min and then overnight in 2X SSCT before washing for 30 min in 2XSSCT and staining for 10 min in 0.5 μg/ml DAPI in 2X SSCT. Embryos were then washed two times in 50 mM Tris-HCl, pH 8.5 and mounted in antifade mounting medium (Vectashield, Vector Laboratories, Inc., Burlingame, CA).

Preparation of Nuclear Matrices

Schneider cells were cultured at 25° C in D22 insect medium (Sigma Chemical Co.) supplemented with 10% fetal calf serum. Approximately 6.5 x 10^8 cells were pelleted in a clinical centrifuge for 3 min at 860g. The pellet was washed once in PBS and then resuspended in 50 ml of 10 mM Tris-Cl, pH 7.4, 10 mM NaCl, 5 mM $MgCl_2$, 1/1000 protease inhibitor stock, 0.1 mM PMSF and allowed to swell for 5 min at room temperature before repelleting . (Protease inhibitor stock is 1.6 mg/ml benzamidine HCl and 1 mg/ml each

phenanthroline, aprotinin, leupeptin and pepstatin A). The cell pellet was resuspended in 10 ml of 0°C lysis buffer (15 mM Tris-Cl, pH 7.4, 80 mM KCl, 5 mM $MgCl_2$, 0.1% digitonin, 1/100 protease inhibitor stock, 1 mM PMSF), immediately transferred to a 15 ml glass dounce and homogenized by 10-15 strokes with a tight pestle. The lysate was spun at 1000g for 10 min at 4°C. Pelleted nuclei were washed twice with 40 ml of 5 mM Tris-Cl, pH 7.4, 2 mM KCl, 5 mM $MgCl_2$, 0.1% digitonin, 1/100 protease inhibitor stock, 1 mM PMSF. Pelleted nuclei were resuspended in 1 ml of digestion buffer (10 mM Tris-Cl, pH 7.4, 50 mM NaCl, 300 mM sucrose, 3 mM $MgCl_2$, 1 mM Na_3EGTA, 1 mM PMSF, 1/100 protease inhibitor stock and 0.5% v/v Triton X-100) and digested at 37°C for 20 min in the presence of 100 U/ml RNase free DNase (Boehringer-Mannheim Biochemicals, Indianapolis, IN). Ammonium sulfate was added at 25°C from a 1M stock solution to a final concentration of 0.25M. The nuclei were pelleted as above and resuspended in 500 ul of digestion buffer. NaCl was added to a final concentration of 2M from a 4M NaCl stock in digestion buffer. Nuclei were held on ice for 10 min before pelleting the matrices and resuspending them in 800 ul of digestion buffer.

Immunofluorescence of Nuclei and Nuclear Matrices

Nuclei or matrices were diluted 1:150 in PME (10 mM K PIPES, pH 6.8, 5 mM $MgCl_2$, 5 mM Na_3EGTA, 1/100 protease inhibitor stock), layered onto a 5 ml cushion of 30% glycerol in PME and pelleted onto polylysine coated coverslips at 10,000 rpm for 15 min in a Beckman JS13.1 rotor at 4°C. The coverslips were fixed in 2% formaldehyde in PBS for 5 min, post-fixed in -20°C methanol for 5 min and rehydrated in TBST (20 mM Tris-Cl, pH 7.4, 150 mM NaCl, 0.1% TritonX-100). The coverslips were then processed for immunofluorescence as described (Evans, et al., 1985).

Western Blotting

To prepare samples for western blotting, 50 ul samples were taken of nuclei, nuclear matrices, total lysate and cytoplasm. $CaCl_2$ was added to 2 mM, 1/20 volume of 2 mg/ml micrococcal nuclease was added and the samples were held on ice for 30 min. Load buffer (60 mM Tris-Cl, pH 6.8, 2% SDS, 20 mM DTT) was added to 1 ml and the samples were heated at 90°C for 3 min. Samples were precipitated by the addition of 0.2 volumes of 100% trichloracetic acid and were resuspended in sample buffer and sonicated for 1 min in a waterbath sonicator. Samples of lysate, cytoplasm, nuclei and matrices corresponding to 9 μg of crude lysate were separated on an 8.5% (CP190, CP60 and topo II) or a 10-15% (histones) polyacrylamide gradient gel and were western blotted for Topo II, CP190, CP60 and histones. Western blotting was performed as described (Kellogg et al., 1989) using mouse monoclonal antibodies to topoisomerase II (Swedlow et al., 1993) or histones (mab 052, Chemicon Industries), or the affinity purified rabbit anti-CP60, and goat anti-190 antibodies described earlier . Signals were detected by Enhanced Chemiluminscence (Amersham).

Results

CP190 and CP60 fusion proteins have different patterns of nuclear and centrosomal localization in embyros

To allow us to follow the behaviour of CP190 and CP60 in live embyros, early embryos (before nuclear cycles 10-13) were co-injected with either rhodamine-labeled CP60 or CP190 fusion protein mixed with

fluorescein labeled 40,000 MW dextran. The dextran is excluded from nuclei with intact nuclear envelopes, and it therefore provides a marker for nuclear envelope breakdown and reformation (Kalpin, et al., 1994).

Shown in Figure 1A is a time lapse series of confocal images taken of a CP190 injected embryo, beginning in interphase of nuclear cycle 12, timed relative to nuclear envelope breakdown. In interphase, (-21s), the labeled dextran is excluded from nuclei, making them visible as black circles against a background of cytoplasmic dextran; at this time, the CP190 is localized to nuclei. Upon nuclear envelope breakdown, the CP190 begins to move to centrosomes and, by + 34s, the centrosomal fluorescence has reached nearly maximal intensity. CP190 remains at centrosomes throughout mitosis until telophase, when it begins to accumulate in the reforming nuclei (345s). Although some CP190 remains attached to nuclear structures during mitosis, the intensity of its nuclear localization is drastically reduced by metaphase (143s).

Figure 1B shows a similar time lapse series of confocal images taken of an embryo injected with CP60. Unlike CP190, CP60 never completely disappears from centrosomes during interphase, although its centrosomal localization becomes very weak. CP60 remains attached to residual nuclear structures after nuclear envelope breakdown, and there is no immediate accumulation of CP60 at centrosomes (see Fig. 1B, 0 and 51s). CP60 begins to accumulate dramatically at centrosomes at anaphase (see Fig. 1B, 196s) and remains prominently at centrosomes throughout telophase (327s) and, at reduced intensity, into early interphase (485s). CP60 moves to nuclei gradually during interphase.

In order to compare the localizations of CP190 and CP60 directly, we have also injected embryos with a mixture of rhodamine-labeled CP190 and

fluorescein-labeled 6XHis CP60 fusion proteins; these results are shown in Fig. 2. The differences in the timing of the centrosomal and nuclear localizations of these proteins are again evident. CP190 accumulates at centrosomes primarily between nuclear envelope breakdown and metaphase (see Fig 2. timepoints between 0 and +124 s) wheras CP60 is barely detectable at metaphase (Fig. 2, +124s). CP60 accumulates at centrosomes between the onset of anaphase and telophase, when CP190 levels appear not to change (Fig. 2, timepoints between 222s and 311s). In telophase, CP190 begins to localize to reforming nuclei while CP60 remains only at centrosomes. The CP60 begins to disappear from centrosomes and to accumulate in nuclei during middle to late interphase.

Quantitation of the localization patterns of CP190 and CP60 using wide-field 3D microscopy

To quantitate the localization patterns of the CP190 and CP60 fusion proteins in live embryos, time-lapse three dimensional images of living embryos were collected using wide-field fluorescence microscopy after injection of fluorescein labeled CP190 and rhodamine-labeled CP60 6XHis fusion proteins. One two-wavelength 3D image was collected every 52 seconds (see methods). A stereo pair of one such image, taken of an embryo in metaphase of nuclear cycle 12, is shown in Fig. 3A. After computational processing to remove out of focus information, all of the centrosomes and nuclei in each field were manually outlined in every focal plane of each timepoint. Total centrosomal and nuclear fluorescence for the field was then calculated for each timepoint. We quantitated centrosomal and nuclear fluorescence for two embyros and obtained identical results. The results for

one of these embryos, followed between prometaphase of cycle 12 and the beginning of cycle 14, are graphed in Fig. 3B.

As expected, the temporal localizations of CP190 and CP60 are asynchronous both at centrosomes and in nuclei. CP190 centrosomal fluorescence peaks during prometaphase immediately following nuclear envelope breakdown and remains high throughout mitosis (See Fig. 3B, top panel timepoints 0-5 and 18-25). Some CP60 accumulates at centrosomes between nuclear envelope breakdown and metaphase (see Fig. 3B, top panel, time points 0-2 and 18-21), but the majority of the centrosomal CP60 accumulates during anaphase and telophase (timepoints 3-5 and 22-25). CP60 fusion protein remains at centrosomes well into interphase; CP190, in contrast, was not detectable at centrosomes during most of interphase. CP190 nuclear fluorescence begins to increase in telophase and reaches maximal intensity early in interphase (see Fig. 3(B) timepoints 5-18); in interphase of cycle 13, the accumulation of CP60 nuclear fluorescence only reaches peak levels just before nuclear envelope breakdown.

Quantitation of centrosomal fluorescence in fixed embryos corroborates the trends seen in live embryos

The CP190 and CP60 fusion proteins had been bacterially expressed, purified and labeled with fluorophores, any of which could alter their properties compared to the native proteins. In addition, the 6XHis CP190 fusion protein contained only the C-terminal 85% of the protein (addition of the N-terminal 166 amino acids makes the protein insoluble in bacteria). We therefore wanted to determine if the endogenous CP60 and CP190 behave in the same manner as the injected fusion proteins.

Fixed embryos were incubated with goat anti-CP190 and rabbit anti-CP60, and were processed in a single batch for immunofluorescence. Three dimensional images were obtained from the fixed embryos in a manner identical to that used for the live embryos except larger (512 x 512 pixel) optical sections were taken. We collected data from 2 embryos for each stage of the cell-cycle cycle 12 and from 5 embryos for each stage of the cell-cycle in cycle 13. To avoid bias in embryo selection, embryos were selected and classified as being in interphase, metaphase, anaphase or telophase by their DAPI staining patterns. A portion of a single opical section for one field of nuclei from an embryo representative of each cell cycle state between telophase of cycle 12 and telophase of cycle 13 is shown in Fig. 4A. We found that the localization patterns of the endogenous CP190 and CP60 were qualitatively similar to the localization patterns obtained with the injected labeled fusion proteins. For example, native CP190 is present in telophase nuclei (see Fig. 4A) when no CP60 is detectable in nuclei, and endogenous CP60 shows relatively weak centrosomal localization in metaphase embryos.

In Fig. 4B we plot the average values for centrosomal fluorescence as a function of cell cycle state. Athough the time resolution is poor, the fixed data confirms our live results. The CP190 centrosomal fluorescence reaches peak levels by metaphase wheras the centrosomal fluorescence of CP60 increases substantially between metaphase and anaphase, peaking at telophase. Although we did not quantitate the changes in nuclear fluorescence during interphase, the nuclear staining in the fixed images was consistent with our live data.

CP60 is present in nuclei after nuclear envelope breakdown

Although the localization patterns described above for CP190 and CP60 are similar in all of the syncytial blastoderm nuclear cycles (nuclear cycles 10-13) there are some differences. During the shorter nuclear cycles 10 and 11, there always appears to be at least some CP190 at centrosomes throughout the entire cell cycle. In the longer cycles, 12 and 13, CP190 completely disappears from centrosomes during interphase- as judged by our inability to detect centrosomal CP190 in embryos double labeled for another centrosomal marker, such as γ-tubulin or CP60 (data not shown).

A second difference observed seems more profound. A time-lapse series of confocal images of an embryo in nuclear cycle 11 that had been co-injected with CP60 and 40,000 MW fluorescein dextran is shown in Figure 5A. Wheras CP60 appears to accumulate in nuclei before nuclear envelope breakdown in the later nuclear cycles, CP60 localizes to nuclei primarily after nuclear envelope breakdown in the nuclear cycles 10 and 11. [Compare the nuclear CP60 in cycle 11 before (-35s), and after (+30s) nuclear envelope breakdown in Fig. 5A with the nuclear CP60 in cycle 12 before (-40s) and after (+50s) nuclear envelope breakdown in Fig. 1B]. Results in fixed embryos are consistent with the live data in this regard (Figure 5B).

Within the nucleus, CP190 and CP60 do not co-localize with each other or with DNA

The in vitro association observed between CP190 and CP60 encouraged us to look at their nuclear localizations at higher resolution to determine if these two proteins co-localize in nuclei. Appropriate sections from interphase and mitotic cycle 13 nuclei stained for CP190, CP60 and DNA are shown in Figure 6. Both CP190 and CP60 appear "fibrous" within the nucleus

but, although there are some regions of overlap, CP190 and CP60 do not co-localize extensively within nuclei. In addition, neither CP190 nor CP60 visibly co-localizes with DNA. During mitosis, the patterns of CP190 and CP60 are similar in character to their patterns during interphase and both proteins appear to be excluded from the region around the chromosomes. Previous work has also shown that CP60 and CP190 do not co-localize with microtubules in the region of the spindle (Oegema, et al., 1995). Cumulatively, these results suggest that CP190 and CP60 are binding to some residual nuclear structures that persist into mitosis.

In older embryos, CP190 and CP60 co-localize to spots within the nucleus

In embryos older than cycle 14 (post-cellular blastoderm), CP190 and CP60 have been reported to co-localize to spots within the nucleus (Kellogg et. al., 1995). High resolution optical sections of a region from such an embryo stained for CP190, CP60 and DNA are shown at low and high magnification in Figure 7A. The nuclear localization of much of the CP190 and CP60 is similar to that in Fig. 6, except some of the CP60 and CP190 now co-localize to 1-3 prominent spots within each nucleus. These spots do not correspond to DNA that we can detect by DAPI staining. To determine if these spots are associated with the nucleolus, embryos were fixed and stained for CP190 and CP60 simultaneously with hybridization of a probe recognizing ribosomal RNA. Four sample nuclei are shown in Fig. 7B (DNA is in blue, CP190 and CP60 are in pink and the ribosomal RNA probe is shown in green). We conclude that that the CP190/CP60 spots are also not co-incident with the nucleolus.

CP190 and CP60 cofractionate with nuclear matrix preparations

The fibrous localization patterns of CP190 and CP60 within nuclei, combined with the fact that CP60 (and CP190 to a lesser extent) localizes to the nucleus even after nuclear envelope breakdown, suggested that CP190 and CP60 might be associated with structural elements within the nucleus. To determine if CP190 and CP60 are components of the conventionally defined "nuclear matrix" fraction, nuclei were isolated from *Drosophila* tissue culture cells, treated with DNase and extracted with high salt to remove the DNA and associated proteins. Western blots following the procedure confirm that, while histones are completely extracted , CP190 and CP60 remain in the nuclear matrix fraction along with the expected topoisomerase II (Figure 8A). Figure 8B shows immunofluorescence of isolated nuclei and nuclear matricies stained for either CP190 or CP60 and DNA. The DNA was completely removed by our extraction procedure wheras CP60 and CP190 appear unaffected. We obtained similar results for nuclei isolated from *Drosophila* embryos (data not shown).

Discussion

Although CP60 was initially identified by virtue of its biochemical association with CP190 and both CP60 and CP190 localize to nuclei and to centrosomes (Kellogg et al., 1992; Kellogg et al., 1995), our results show that the timing of their localization is significantly different. In addition, within the nucleus, CP190 and CP60 have different spatial localization patterns.

Experiments in both live and fixed embryos demonstrate that CP190 accumulates at centrosomes immediately following nuclear envelope breakdown, reaching peak levels before metaphase. CP60, in contrast,

accumulates at centrosomes primarily during anaphase reaching peak levels by telophase. Therefore, CP190 is prominently at centrosomes between nuclear envelope breakdown and telophase while CP60 localizes to centrosomes later, between anaphase and early interphase.

The accumulation of CP60 in nuclei also lags that of CP190. CP190 accumulates in nuclei as they reform in telophase reaching peak levels early in interphase. In contrast, CP60 accumulates in nuclei gradually during interphase reaching peak levels just before nuclear envelope breakdown in nuclear cycles 12 and 13. In the earlier shorter nuclear cycles, 10 and 11, CP60 accumulates in nuclei primarily after nuclear envelope breakdown. This could be due to the shorter amount of time spent in interphase in these cycles or to the different timing of a regulatory event. Because CP190 always accumulates before CP60, both at centrosomes and in nuclei, it is possible that CP190 has a role in the recruitment of CP60 to centrosomes, to nuclei, or to both structures. But we also find that CP60 lingers both at centrosomes and in nuclei after the majority of the CP190 is gone, suggesting that CP60 may not require CP190 to remain localized to these structures.

By high resolution 3D wide-field microscopy in fixed embryos, CP190 and CP60 appear "fibrous" within the interphase nucleus. We find that the majority of CP60 and CP190 do not co-localize in nuclei, nor does either protein co-localize extensively with visible DNA. We thought that co-localization with DNA was a possibility because CP190 contains 4 putative zinc fingers and antibodies to CP190 and CP60 were previously found to recognize bands on isolated salivary gland chromosomes (Whitfield et al., 1995). Our results do not rule out the possibility that CP190 and CP60 interact with DNA at discrete sites, but do reveal that CP190 and CP60 do not co-

localize extensively with DNA. In addition, since the fibrous patterns of CP60 and CP190 in the nucleus persist into mitosis, when chromosomes are completely separated from the CP190 and CP60 networks, the fibrous appearance of their localizations cannot be explained merely as volumes within the nucleus excluded by interphase chromatin. In older embryos (post syncytial blastoderm) CP190 and CP60 co-localize to a few prominent spots within nuclei (see Figure 7). These spots do not co-localize with blocks of heterochromatin, visible by DAPI staining, or with the nucleolus; they thus define a novel sub-nuclear structure.

Interestingly, the localization patterns of CP190 and CP60 in nuclei during metaphase are remarkably similar to their localization patterns during interphase, suggesting that CP190 and CP60 may be associating with unknown nuclear structures that persist into mitosis. Consistent with a localization to residual nuclear structures, previous work has shown that CP190 and CP60 do not co-localize with microtubules in the region of the spindle (Oegema et al., 1995). In addition, in nuclear cycles 10 and 11, CP60 localizes to nuclei rapidly after nuclear envelope breakdown suggesting that it is diffusing into the nucleus and binding to some nuclear structure.

Consistent with their nuclear localizations, both CP190 and CP60 are found in conventional nuclear matrix preparations. The relevance of nuclear matrix preparations to actual cellular structures in vivo has long been a matter of controversy. Here we demonstrate that two matrix components, CP60 and CP190, form a fibrous network in intact cells (Fig. 6). In particular, the retention of CP60 in the nucleus following nuclear envelope breakdown (Fig. 1B) and the localization of CP60 to nuclei after nuclear envelope breakdown in nuclear cycles 10 and 11 (Figure 5A) imply that CP60 is bound to a large insoluble structure, i.e. a "nuclear matrix", in living cells.

The centrosome cycle in *Drosophila* embryos has been described in detail (Callaini and Riparbelli, 1990) and is slightly different than that of somatic tissue culture cells in which centrosomes divide during interphase. In *Drosophila* embryos, the centriolar cylinders lose their perpendicular orientation in late metaphase, consistent with preparation for centrosome division; the centrosomes then become visibly less compact in early anaphase, forming ovoid plates by late anaphase. During telophase, the duplicated centrosomes physically separate. CP190, present at centrosomes immediately following nuclear envelope breakdown, could possibly function in the transition of the centrosomes from their interphase location and functions next to the nuclear envelope to their new roles at spindle poles. The localization of CP60 to centrosomes between anaphase and early interphase coincides with the period of centrosome duplication and separation, making possible some role in these processes.

Our results clearly show that CP190 and CP60 have different temporal and spatial localization patterns, suggesting that the interaction between CP190 and CP60 is complex and likely to be regulated in a cell cycle-specific manner. Studies on CP190 and CP60 in extracts are consistent with the observed complexity of their localization patterns. CP60 contains 6 consensus cdc2 phosphorylation sites and western blotting of extracts reveals the existence of multiple phosphorylated forms in vivo (Kellogg et al., 1995). In addition, a kinase present in elutes from anti-CP190 immunoaffinity columns can phosphorylate CP60 in vitro (Kellogg et al., 1995), suggesting that the phosphorylation of CP60 could be in part regulated by its association with CP190. Bacterially expressed CP60 forms a higher order oligomer, which is also formed by a poorly phosphorylated form of CP60 predominant in concentrated *Drosophila* extracts (Oegema et al., submitted for publication).

One speculative possibility, for example, is that the dephosphorylation of CP60 during anaphase releases it from its attatchment to residual nuclear structures and allows CP60 to oligomerize at centrosomes.

We have shown that CP190 and CP60 are two proteins that localize in an alternating asynchronous fashion to the pericentriolar material and to the nucleus. CP190 and CP60 may function sequentially in a process that occurs at centrosomes and could be sequestered in nuclei when they are not needed; alternatively CP190 and CP60 could function both at centrosomes and in nuclei. Genetic studies will hopefully result in clarification of the functions of CP190 and CP60 in embryos.

Acknowledgements:

We would like to thank Arshad Desai and Doug Kellogg for critical reading of the manuscript. This work was supported by grants from the National Institutes of Health to B.M.A (GM23928) and to J.W.S (GM-225101-16). W.F.M was additionally supported by a Howard Hughes Medical Institute predoctoral fellowship.

References

Agard, D., Hiraoka, Y., Shaw, P., and Sedat, J. (1989). Fluorescence microscopy in three dimensions. Meth. Cell. Biol. *30*, 353-377.

Bailly, E., Doree, M., Nurse, P., and Bornens, M. (1989). p34cdc2 is located in both nucleus and cytoplasm; part is centrosomally associated at G2/M and enters vesicles at anaphase. Embo J. *8,* 3985-95.

Boleti, H., Karsenti, E., and Vernos, I. (1996). Xklp2, a novel Xenopus centrosomal kinesin-like protein required for centrosome separation during mitosis. Cell. *84,* 49-59.

Buendia, B., Draetta, G., and Karsenti, E. (1992). Regulation of the microtubule nucleating activity of centrosomes in Xenopus egg extracts: role of cyclin A-associated protein kinase. J Cell Biol. *116,* 1431-42.

Centonze, V. E., and Borisy, G. G. (1990). Nucleation of microtubules from mitotic centrosomes is modulated by a phosphorylated epitope. J Cell Sci. *95,* 405-11.

Chen, H., Swedlow, J., Grote, M., Sedat, J., and Agard, D. (1995). The collection, processing, and display of digital three-dimensional images of biological specimens. In: Handbook of Biological Confocal Microscopy, ed. J. Pawley, New York: Plenum, 197-210.

Doxsey, S. J., Stein, P., Evans, L., Calarco, P. D., and Kirschner, M. (1994). Pericentrin, a highly conserved centrosome protein involved in microtubule organization. Cell. *76,* 639-50.

Endow, S., Chandra, R., Komma, D., Yamamoto, A., and Salmon, E. (1994). Mutants of the Drosophila ncd microtubule motor protein cause centrosomal and spindle pole defects in mitosis. J Cell Sci. *82,* 155-172.

Engle, D. B., Doonan, J. H., and Morris, N. R. (1988). Cell-cycle modulation of MPM-2-specific spindle pole body phosphorylation in Aspergillus nidulans. Cell Motil Cytoskeleton. *10,* 434-7.

Evans, L., Mitchison, T., and Kirschner, M. (1985). Influence of the centrosome on the structure of nucleated microtubules. J Cell Biol. *100,* 1185-91.

Frasch, M., Glover, D. M., and Saumweber, H. (1986). Nuclear antigens follow different pathways into daughter nuclei during mitosis in early Drosophila embryos. J Cell Sci. *82,* 155-72.

Gould, R. R., and Borisy, G. G. (1977). The pericentriolar material in Chinese hamster ovary cells nucleates microtubule formation. J Cell Biol.*73,* 601-15.

Hiraoka, Y., Swedlow, J. R., Paddy, M. R., Agard, D. A., and Sedat, J. W. (1991). Three-dimensional multiple-wavelength fluorescence microscopy for the structural analysis of biological phenomena. Semin Cell Biol. *2,* 153-65.

Kallajoki, M., Weber, K., and Osborn, M. (1991). A 210 kDa nuclear matrix protein is a functional part of the mitotic spindle; a microinjection study using SPN monoclonal antibodies. Embo J. *10,* 3351-62.

Kalpin, R. F., Daily, D. R., and Sullivan, W. (1994). Use of dextran beads for live analysis of the nuclear division and nuclear envelope breakdown/reformation cycles in the Drosophila embryo. Biotechniques. *17*, 730, 732-3.

Kellogg, D. R., and Alberts, B. M. (1992). Purification of a multiprotein complex containing centrosomal proteins from the Drosophila embryo by chromatography with low-affinity polyclonal antibodies. Mol Biol Cell. *3*, 1-11.

Kellogg, D. R., Field, C. M., and Alberts, B. M. (1989). Identification of microtubule-associated proteins in the centrosome, spindle, and kinetochore of the early Drosophila embryo. J Cell Biol. *109*, 2977-91.

Kellogg, D. R., Moritz, M., and Alberts, B. M. (1994). The centrosome and cellular organization. Annu Rev Biochem. *63*, 639-74.

Kellogg, D. R., Oegema, K., Raff, J., Schneider, K., and Alberts, B. M. (1995). CP60: a microtubule-associated protein that is localized to the centrosome in a cell cycle-specific manner. Mol Biol Cell. *6*, 1673-84.

Keryer, G., Ris, H., and Borisy, G. G. (1984). Centriole distribution during tripolar mitosis in Chinese hamster ovary cells. J Cell Biol. *98*, 2222-9.

Kuriyama, R., and Borisy, G. G. (1981). Microtubule-nucleating activity of centrosomes in Chinese hamster ovary cells is independent of the centriole cycle but coupled to the mitotic cycle. J Cell Biol. *91*, 822-6.

Li, K., and Kaufman, T. (1996). The homeotic target gene centrosomin encodes an essential centrosomal component. Cell. *85,* 585-596.

Mazia, D. (1987). The chromosome cycle and the centrosome cycle in the mitotic cycle. Int Rev Cytol. *100,* 49-92.

Moritz, M., Braunfeld, M. B., Sedat, J. W., Alberts, B., and Agard, D. A. (1995). Microtubule nucleation by gamma-tubulin-containing rings in the centrosome. Nature. *378,* 638-40.

Oegema, K., Whitfield, W. G., and Alberts, B. (1995). The cell cycle-dependent localization of the CP190 centrosomal protein is determined by the coordinate action of two separable domains. J Cell Biol. *131,* 1261-73.

Price, C. M., and Pettijohn, D. E. (1986). Redistribution of the nuclear mitotic apparatus protein (NuMA) during mitosis and nuclear assembly. Properties of purified NuMA protein. Exp Cell Res. *166,* 295-311.

Raff, J. W., Kellogg, D. R., and Alberts, B. M. (1993). Drosophila gamma-tubulin is part of a complex containing two previously identified centrosomal MAPs. J Cell Biol. *121,* 823-35.

Rieder, C., and Borisy, G. (1982). The Centrosome Cycle in PtK2 Cells: Asymmetric Distribution and Structural Changes in the Pericentriolar Material. Biology of the Cell. *44,* 117-132.

Robbins, E., Jentzsch, G., and Micali, A. (1968). The centriole cycle in synchronized HeLa cells. J Cell Biol. *36*, 329-39.

Schatten, G. (1994). The centrosome and its mode of inheritance: the reduction of the centrosome during gametogenesis and its restoration during fertilization. Dev Biol. *165*, 299-335.

Swedlow, J. R., Sedat, J. W., and Agard, D. A. (1993). Multiple chromosomal populations of topoisomerase II detected in vivo by time-lapse, three-dimensional wide-field microscopy. Cell. *73*, 97-108.

Tousson, A., Zeng, C., Brinkley, B. R., and Valdivia, M. M. (1991). Centrophilin: a novel mitotic spindle protein involved in microtubule nucleation. J Cell Biol. *112*, 427-40.

Vandre, D. D., and Borisy, G. G. (1989). Anaphase onset and dephosphorylation of mitotic phosphoproteins occur concomitantly. J Cell Sci. *94*, 245-58.

Vorobjev, I. A., and Chentsov Yu, S. (1982). Centrioles in the cell cycle. I. Epithelial cells. J Cell Biol. *93*, 938-49.

Vorobjev, I. A., and Nadezhdina, E. S. (1987). The centrosome and its role in the organization of microtubules. Int Rev Cytol. *106*, 227-93.

Whitfield, W. G., Chaplin, M. A., Oegema, K., Parry, H., and Glover, D. M. (1995). The 190 kDa centrosome-associated protein of Drosophila

melanogaster contains four zinc finger motifs and binds to specific sites on polytene chromosomes. J Cell Sci. *108,* 3377-87.

Whitfield, W. G., Millar, S. E., Saumweber, H., Frasch, M., and Glover, D. M. (1988). Cloning of a gene encoding an antigen associated with the centrosome in Drosophila. J Cell Sci. *89,* 467-80.

Zheng, Y., Wong, M. L., Alberts, B., and Mitchison, T. (1995). Nucleation of microtubule assembly by a gamma-tubulin-containing ring complex. Nature. *378,* 578-83.

Figure legends

Figure 1:

Confocal micrographs of living embryos co-injected with either rhodamine labeled CP190 or CP60 fusion protein and fluorescein labeled

40,000 MW dextran. Each set of micrographs was selected from a time-lapse series taken of a portion of the embryo's surface during several nuclear cycles. The times to the left of each panel are relative to nuclear envelope breakdown as judged by the ability of nuclei with intact nuclear envelopes to exclude fluorescein dextran.

(A) Co-injection of rhodamine labeled 6XHis CP190 (amino acids 167-1090) and fluorescein labeled 40,000 MW dextran. 21 seconds before nuclear envelope breakdown (-21s), the labeled dextran is excluded from nuclei which are therefore visible as black circles against a background of cytoplasmic dextran. Rhodamine labeled CP190 is localized to nuclei. Immediately following nuclear envelope breakdown, CP190 begins to accumulate at centrosomes. CP190 localizes intensely to centrosomes by 34s after nuclear envelope breakdown. By 143s, the nuclei are in metaphase. The nuclear localization of the CP190 fusion protein is drastically reduced but CP190 remains intensely at centrosomes. During anaphase, CP190 remains at centrosomes (223s and 289s) but by telophase, 345s after nuclear envelope breakdown, CP190 is accumulating in reforming nuclei (nuclei are also visible as small areas that exclude cytoplasmic dextran).

(B) Co-injection of rhodamine labeled 6XHis CP60 (full length) and fluorescein labeled 40,000 MW dextran. 40 seconds before nuclear envelope breakdown, CP60 is found primarily in nuclei although we can always see some CP60 at centrosomes. Upon nuclear envelope breakdown (0s), the nuclear CP60 is defomed slightly due to the fomation of the microtubule spindle. By metaphase (138s), the intensity of nuclear localization has been reduced and a small amount of CP60 has accumulated at centrosomes. Between metaphase (138s) and anaphase (196s) the majority of CP60's accumulation at centrosomes occurs. CP60 remains at centrosomes

prominently during telophase (327s) and at reduced intensity into early interphase (485s). In middle to late interphase, CP60 accumulates in nuclei but is still present at centrosomes with much reduced intensity. Scale bars are 10 μm.

Figure 2:

Confocal micrographs of a living embryo co-injected with rhodamine labeled CP190 (amino acids 167-1090) and fluorescein labeled CP60 6XHis fusion proteins. The times shown to the left of each panel are from nuclear envelope breakdown, as judged by the first appearance of CP190 at centrosomes. CP190 accumulates at centrosomes immediately following nuclear envelope breakdown and has reached peak levels by metaphase (see 124s). Very little CP60 has collected at centrosomes by metaphase (124s) but there is a dramatic increase in the amount of centrosomal CP60 at the metaphase to anaphase transition (compare amount of CP60 at centrosomes between 124 and 222s). In telophase, CP190 begins to accumulate in reforming nuclei while CP60 remains centrosomal (311s). In middle to late interphase CP60 joins CP190 in nuclei (678s). Scale bar is 10 μm.

Figure 3:

Quanitation of the asynchronous nuclear and centrosomal localizations of CP190 and CP60 in living embryos using wide-field 3D microscopy. Drosophila embryos were sequentially injected with fluorescein labeled CP190 (amino acids 167-1090) and rhodamine labeled CP60 6XHis fusion proteins. Time-lapse three dimensional images of living embryos were collected using wide-field fluorescence microscopy. A total of 16 256x256 pixel optical sections were taken at 0.75 μm vertical increments for each

wavelength at every time point. In this way, one two-wavelength 3D image was collected every 52 seconds. A stereo pair of one such dual wavelength image, metaphase of nuclear cycle 12, is shown in (A). Scale bar is 2 μm.

The total amount of centrosomal and nuclear fluorescence was quantified between prometaphase of cycle 12 and the beginning of cycle 14; the results are graphed in (B). Timepoint 0 is prometaphase of nuclear cycle 12.

Figure 4:

Comparison of the localizations of native CP190 and CP60 in fixed embryos using wide-field 3D microscopy. Fixed embryos were incubated with goat anti-CP190 and rabbit anti-CP60, each at 2 ug/ml and were processed in one batch for immunofluorescence. Images were obtained from the fixed embryos in a manner identical to that used for the live embryos except 512x512 pixel optical sections were collected. We collected data from 2 embryos for each cell cycle state in cycle 12 and from 5 embryos for each cell-cycle state in cycle 13. To avoid bias in embryo selection, embryos were selected and classified as to their cell cycle state by their DAPI staining pattern. A portion of one opical section from one embryo for each cell cycle state between telophase of cycle12 and telophase of cycle13 is shown in (A). Scale bar is 10 μm. Our fixed data was consistent with our results in live embryos.

Quantitation of the centrosomal fluorescence of CP190 and CP60 vs. cell cycle state was done in a manner identical to the live quantitation. Shown in (B) vs. cell cycle state is the average total centrosomal fluorescence per field of nuclei. Consistent with our live results, we see an apparent lag in the accumulation of CP60 at centrosomes. CP190 acheives peak levels by metaphase and CP60 between anaphase and telophase. The centrosomal fluorecence of CP190 in prophase is low because of the low time resolution of

the fixed experiment. Embryos were selected on the basis of their DNA, so prophase embryos included both embryos that had not yet broken down their nuclear envelopes as well as those in the process of doing so.

Figure 5:

The localization of CP60 in nuclear cycles 10 and 11. (A) Confocal micrographs of a living embryo co-injected with rhodamine labeled 6XHis CP60 and fluorescein labeled 40,000 MW dextran in nuclear cycle 11. Times to the left of the panels are relative to nuclear envelope breakdown. In nuclear cycles 10 and 11, the localization pattern of CP60 at centrosomes is similar to that in nuclear cycles 12 and 13 but CP60 appears to accumulate in nuclei primarily after nuclear envelope breakdown in these early, shorter, cycles (compare the amount of CP60 in nuclei before, -35s, and after, +30s, nuclear envelope breakdown). Scale bar 10 μm. The other difference we have observed is that CP190 appears to localize to centrosomes throughout interphase in cycles 10 and 11 wheras in cycles 12 and 13 CP190 disappears from centrosomes during interphase. Data from fixed embryos in nuclear cycles 10 and 11 are consistent with the live data. Shown in (B) is a nucleus from an embryo in prophase of cycle 11 stained for CP190, CP60 and DNA. CP190 is at centrosomes even though the nuclear envelope has not yet broken down and there is no CP60 in the nucleus. Scale bar 5 μm.

Figure 6:

Immunofluorescence of CP190 and CP60 in nuclei using high resolution wide-field 3D microscopy. Data was taken by an identical procedure as that used in figure 4 except optical sections were taken every 0.2 μm for improved resolution. Shown are sections taken from interphase and

mitotic nuclei in nuclear cycle 13 stained for CP190, CP60 and DNA. In the merged images CP190 is in green, CP60 in red and DNA in blue. CP190 and CP60 have a "fibrous" appearance within the nucleus. Although there are some regions of overlap, CP190 and CP60 do not appear to co-localize extensively in nuclei during interphase nor do either CP190 or CP60 co-localize with DNA. During mitosis the localization patterns of CP190 and CP60 are similar in character to their localizations during interphase suggesting that this localization does not require chromatin and may represent binding to residual nuclear structures. Neither CP190 nor CP60 co-localizes with mitotic chromatin. Scale bar is 2 μm.

Figure 7:

Immunofluorescence of interphase nuclei in one of the post cycle 14 mitotic domains using high resolution wide-field 3D microscopy. In embryos post cycle 14, CP190 and CP60 are often seen co-localizing to non-centrosomal spots within the nucleus- usually between 1 and 3 prominent spots per nucleus. Shown in (A) on the left is a section taken through the middle of a field of interphase post cycle 14 nuclei stained for CP190, CP60 and DNA. In the merged images, CP190 is in green, CP60 in red and DNA in blue. As in the younger embyos, CP190 and CP60 have a "fibrous" appearance within the nucleus but, although their localizations overlap, they are not identical. CP190 and CP60 do not appear to co-localize with visible DNA in these nuclei. Scale bar is 2 μm. On the right is a higher magnification view of one of the nuclei from the field on the left showing one of the prominent CP190/CP60 staining spots within the nucleus. Scale bar 1μm.

(B) Post cycle 14 spots do not correspond to the nucleolus. Shown are 4 examples of post cycle 14 nuclei stained for DNA (blue), the CP60/CP190 spots

(pink), and with a probe recongnizing ribosomal DNA (green). Scale bar 10 μm.

Figure 8:

Nuclear matrix preps. Nuclei were isolated from Schneider cells and the DNA and histones extracted with DNase and high salt to yield the nuclear matrix fraction (see Methods). Fractions from the preparation of the nuclear matricies were western blotted (A), and nuclei and matrices were processed for immunofluorescece (B). The DNA was effectively extracted by our procedure, as were the histones, but CP190 and CP60 were not extracted. Scale bars 10 μm.

Figure 1A
Oegema et al.

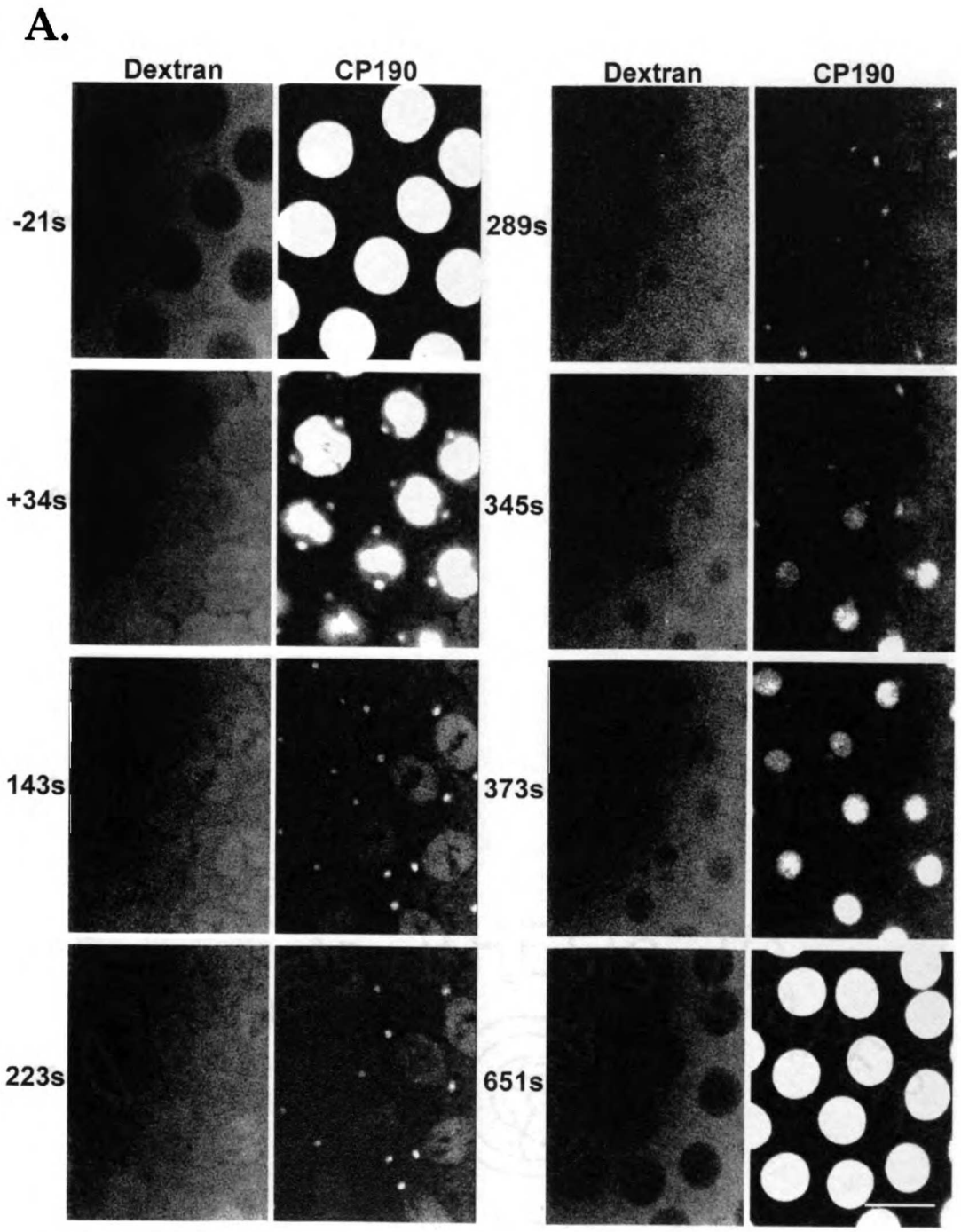

Figure 1B
Oegema et al.

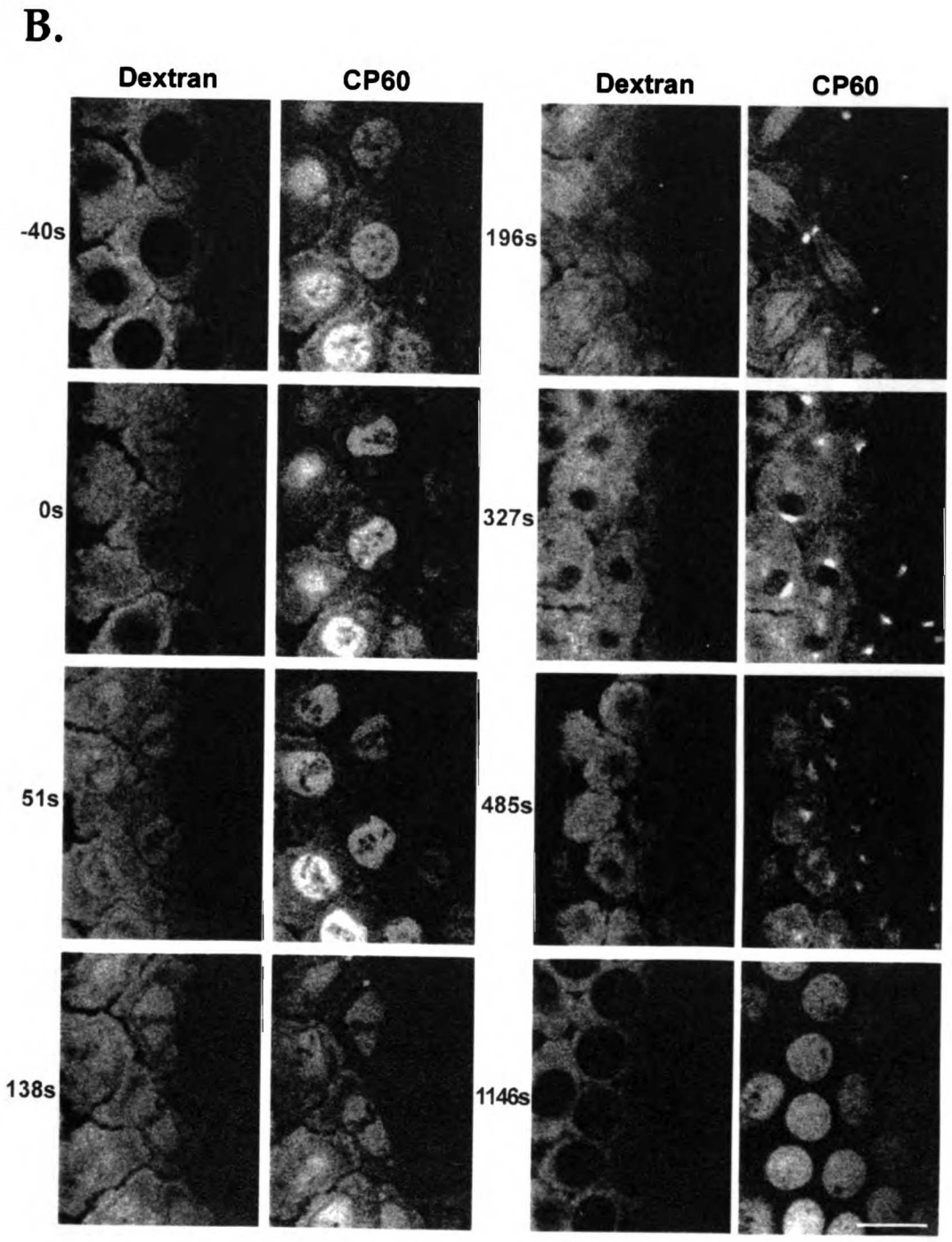

Figure 2
Oegema et al.

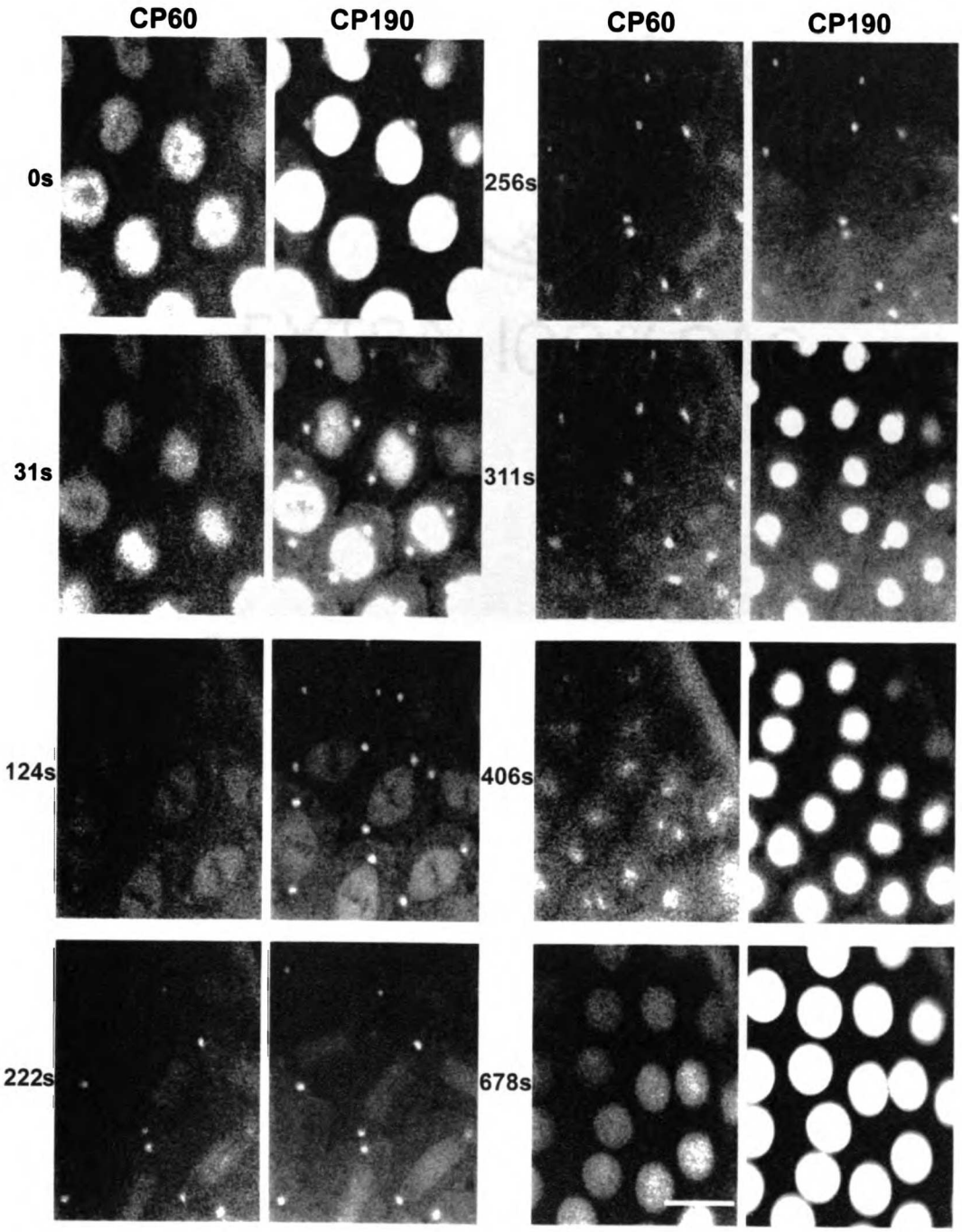

Figure 3A
Oegema et al.

A.

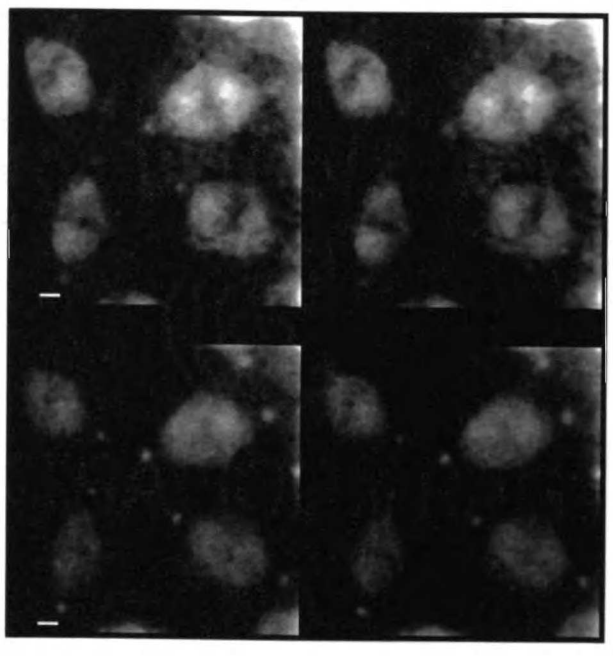

Figure 3B
Oegema et al.

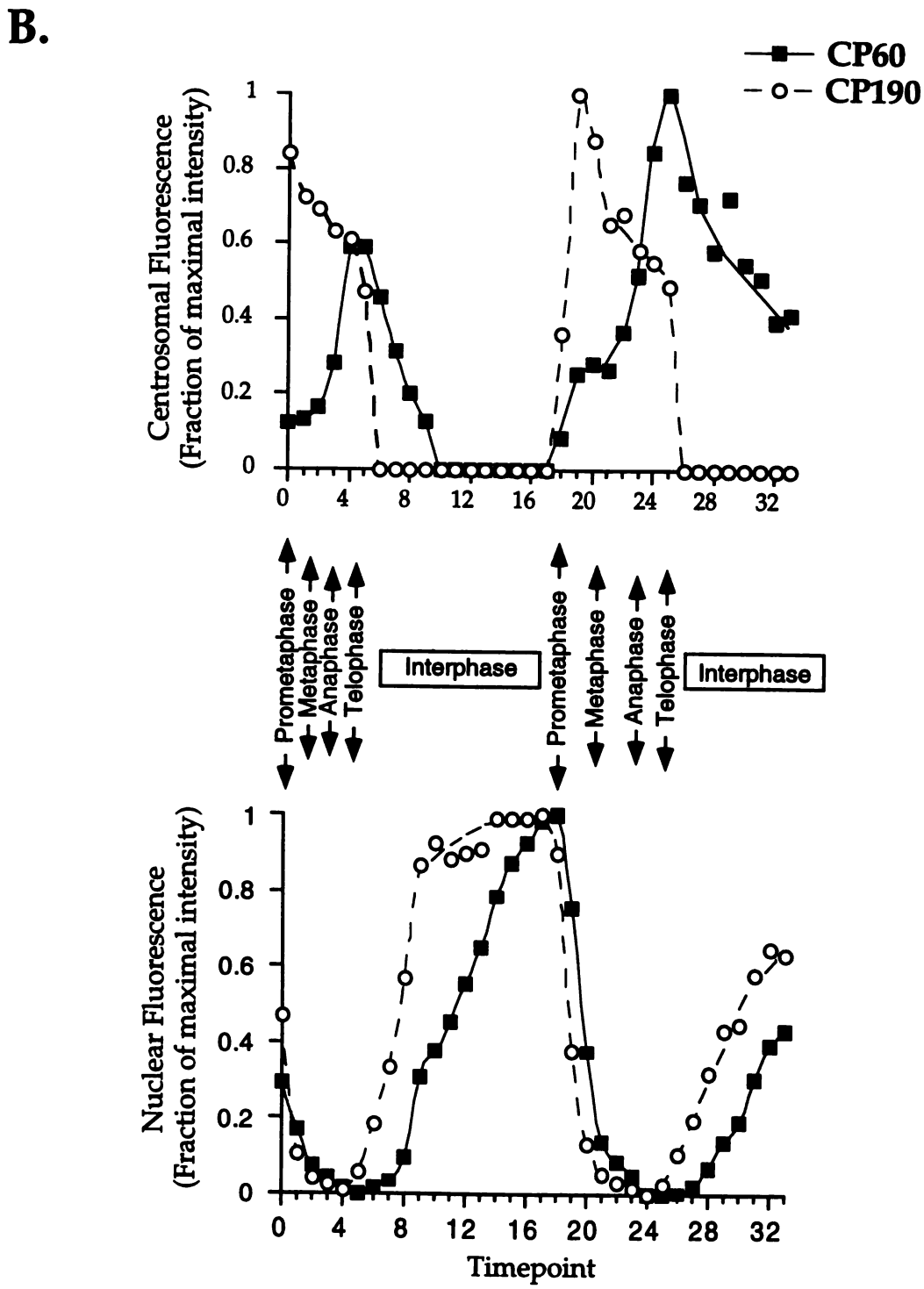

Figure 4A
Oegema et al.

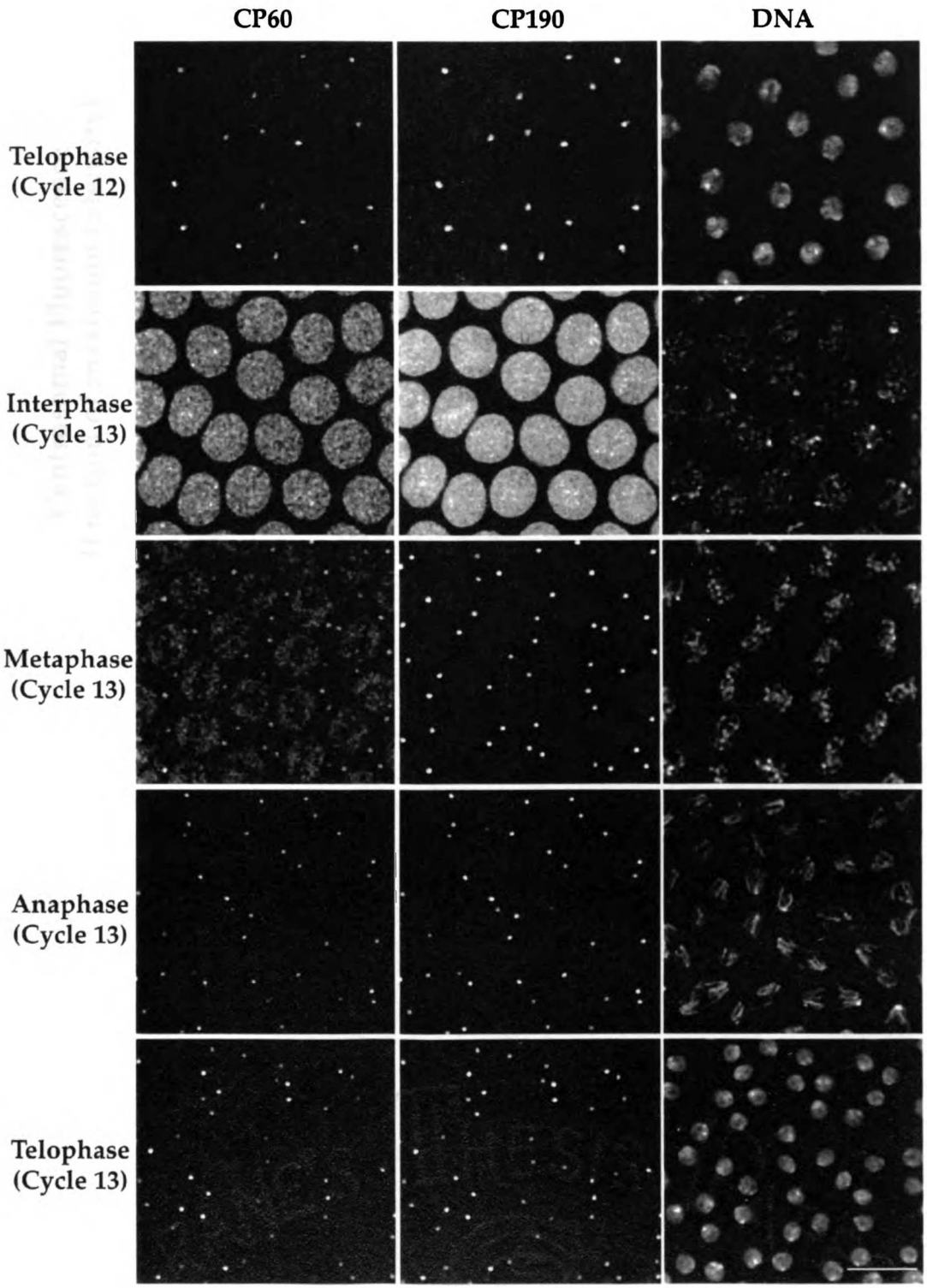

Figure 4B
Oegema et al.

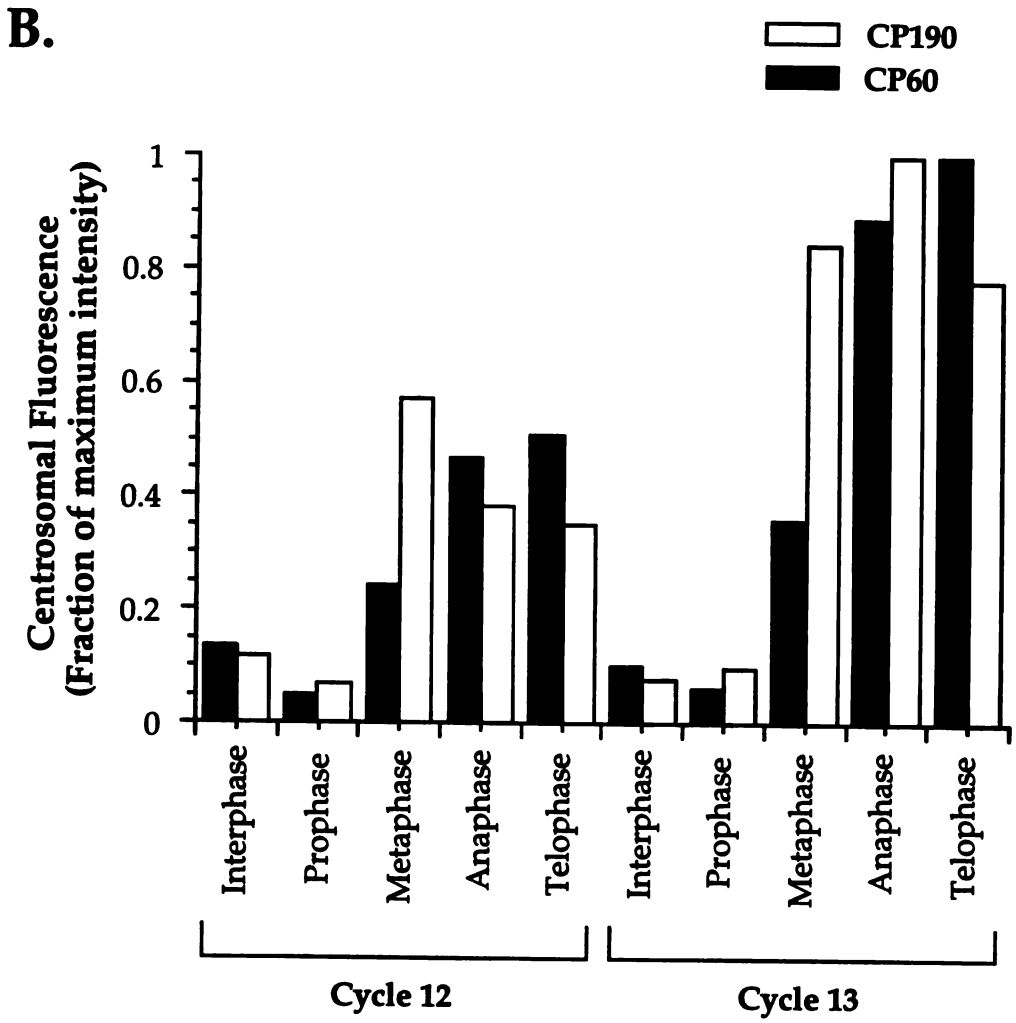

Figure 5
Oegema et al.

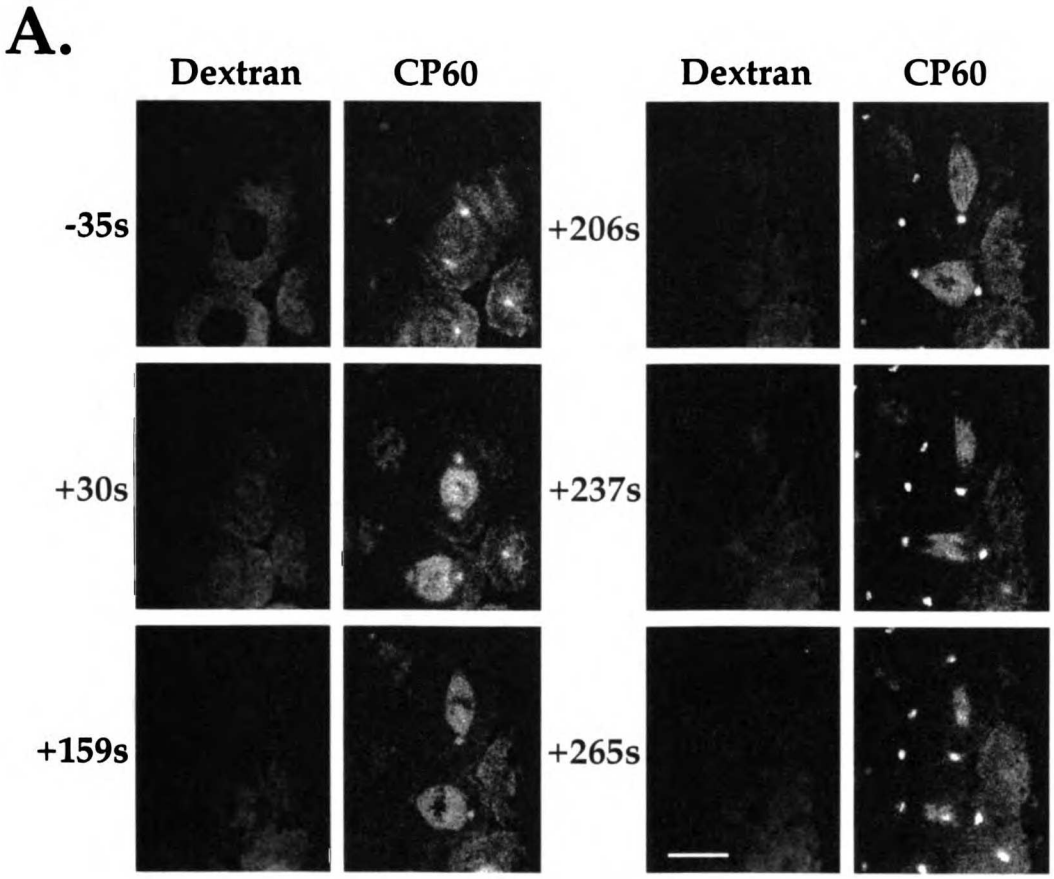

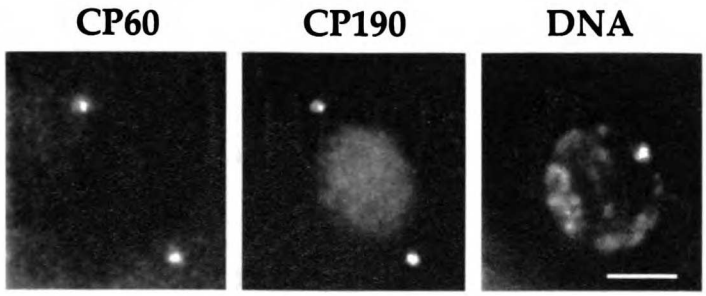

Figure 6
Oegema et al.

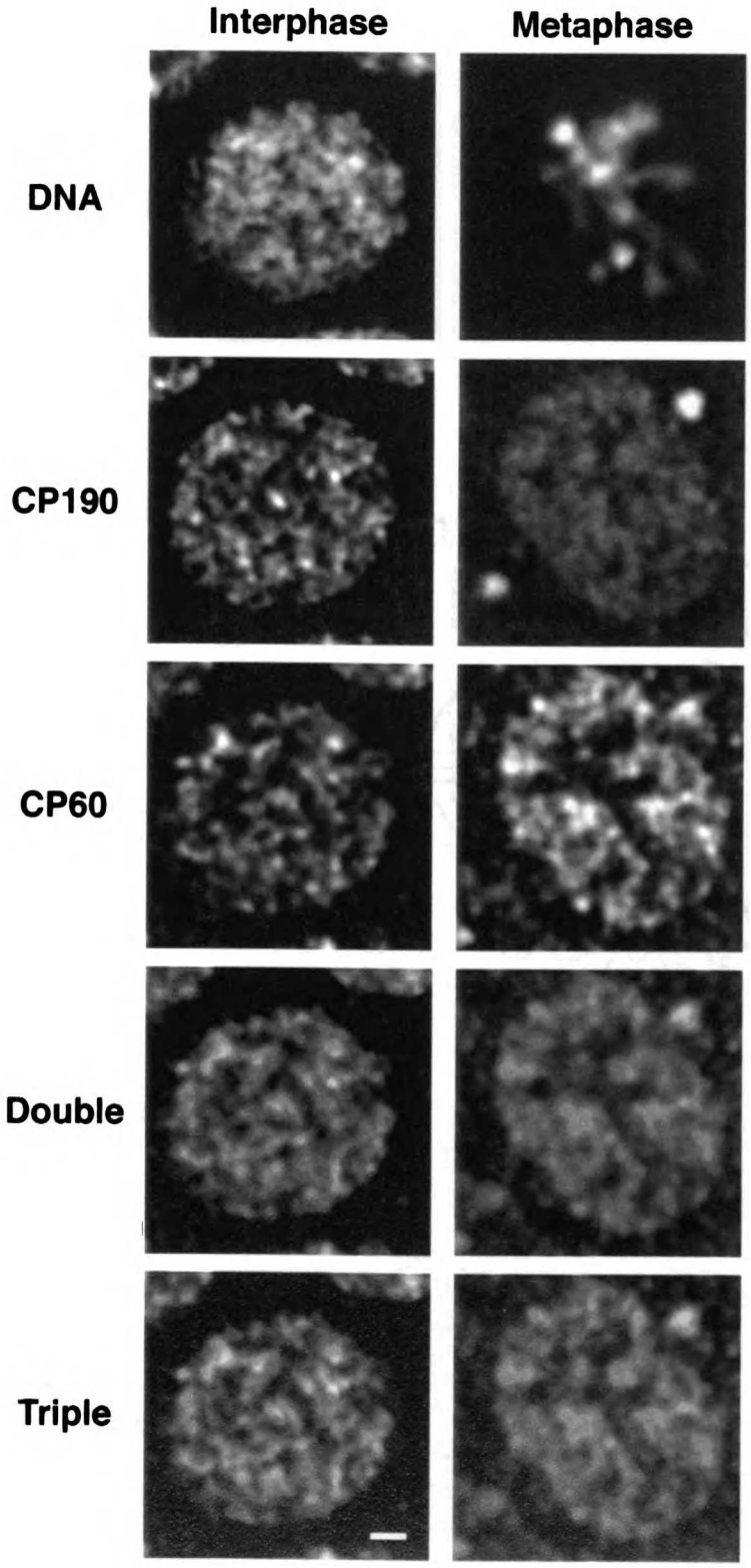

Figure 7A
Oegema et al.

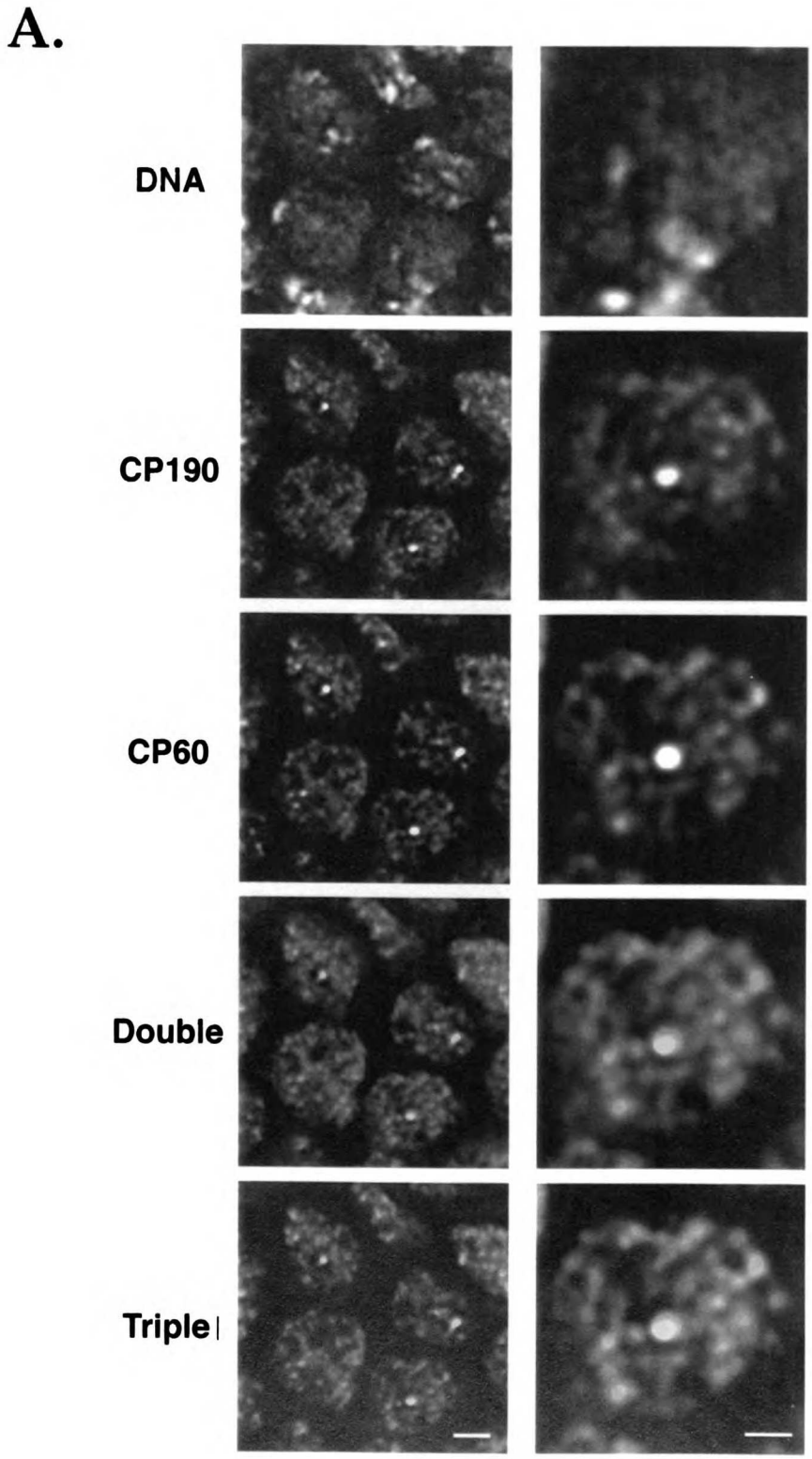

Figure 7B
Oegema et al.

B.

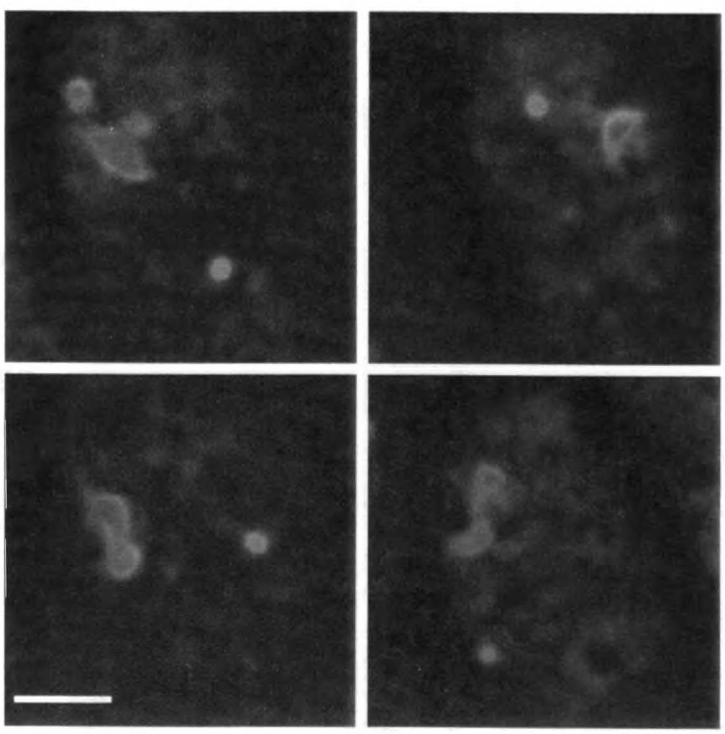

Figure 8A
Oegema et al.

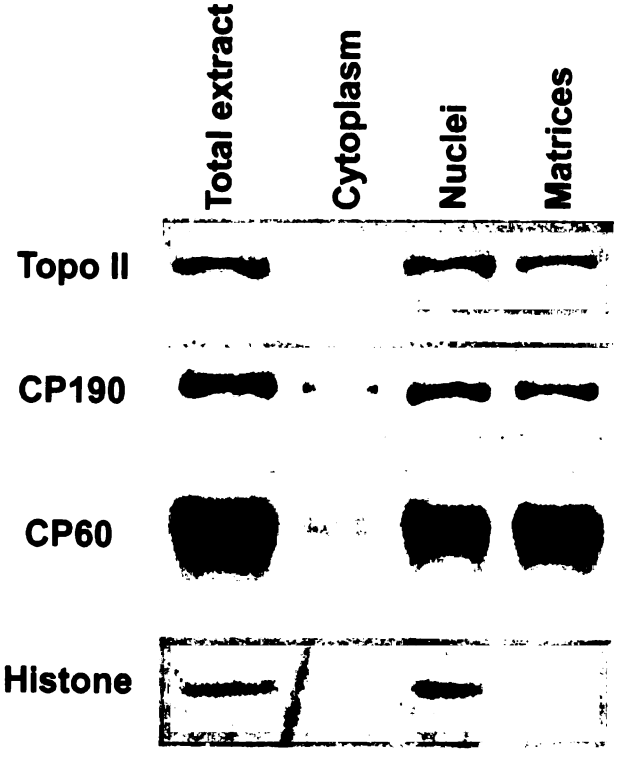

Figure 8B
Oegema et al.

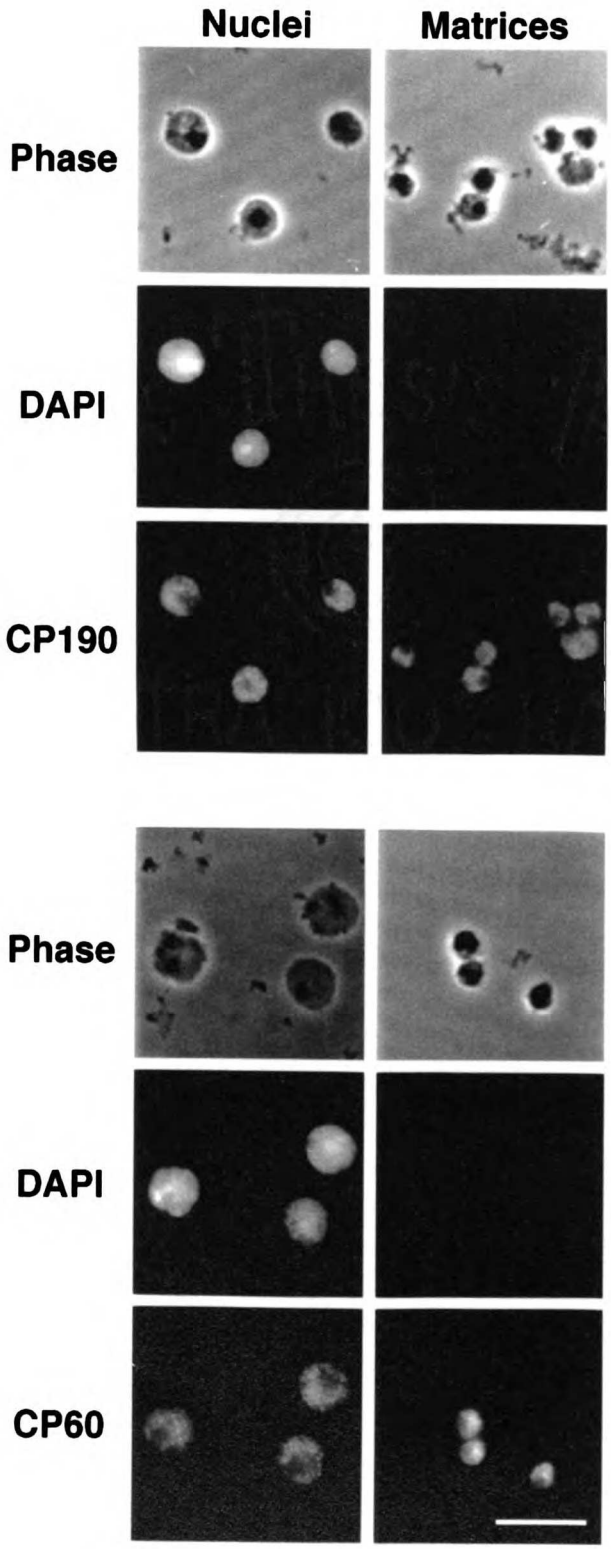

Chapter 3

Identification of the domains of CP190 responsible for its nuclear and centrosomal localizations

The Cell Cycle–dependent Localization of the CP190 Centrosomal Protein Is Determined by the Coordinate Action of Two Separable Domains

Karen Oegema,* William G. F. Whitfield,‡ and Bruce Alberts*

*Department of Biochemistry and Biophysics, University of California, San Francisco, San Francisco, California 94143-0448; and ‡Department of Biological Sciences, University of Dundee, Dundee DD1 4HN, Scotland, U.K.

Abstract. CP190, a protein of 1,096 amino acids from *Drosophila melanogaster*, oscillates in a cell cycle–specific manner between the nucleus during interphase, and the centrosome during mitosis. To characterize the regions of CP190 responsible for its dynamic behavior, we injected rhodamine-labeled fusion proteins spanning most of CP190 into early Drosophila embryos, where their localizations were characterized using time-lapse fluorescence confocal microscopy. A single bipartite 19–amino acid nuclear localization signal was detected that causes nuclear localization. Robust centrosomal localization is conferred by a separate region of 124 amino acids; two adjacent, nonoverlapping fusion proteins containing distinct portions of this region show weaker centrosomal localization. Fusion proteins that contain both nuclear and centrosomal localization sequences oscillate between the nucleus and the centrosome in a manner identical to native CP190. Fusion proteins containing only the centrosome localization sequence are found at centrosomes throughout the cell cycle, suggesting that CP190 is actively recruited away from the centrosome by its movement into the nucleus during interphase. Both native and bacterially expressed CP190 cosediment with microtubules in vitro. Tests with fusion proteins show that the domain responsible for microtubule binding overlaps the domain required for centrosomal localization. CP60, a protein identified by its association with CP190, also localizes to centrosomes and to nuclei in a cell cycle–dependent manner. Experiments in which colchicine is used to depolymerize microtubules in the early *Drosophila* embryo demonstrate that both CP190 and CP60 are able to attain and maintain their centrosomal localization in the absence of microtubules.

Centrosomes are the major microtubule organizing centers found in animal cells. Properties intrinsic to centrosomes include the capacity to duplicate as well as the ability to nucleate and organize microtubule arrays. These arrays, in turn, are essential for a variety of cellular processes including cell division and chromosome segregation, directed cell movement, and general cytoplasmic organization (for reviews see Mazia, 1987; Vorobjev and Nadezhdina, 1987; Schatten, 1994; Kellogg et al., 1994). Despite their importance and the fact that they have been studied for over a century, centrosomes remain a mystery. We still do not understand how centrosomes nucleate microtubules, how they duplicate and separate, or how the changes in centrosome composition and structure that accompany the transition from interphase to mitosis occur.

Our knowledge of the centrosome is largely phenomenological. A molecular characterization of the centrosome has been elusive due to its small size and paucity, which make biochemical purification difficult, and to its involvement in very general organizational processes, which makes genetic approaches problematic. Nevertheless, progress is being made. A number of centrosomal components have already been identified and their cDNAs cloned. Components of the spindle pole body, the centrosome equivalent in yeast and Aspergillus, have also been identified and clues to their function have been obtained from the analysis of mutants (for reviews on known centrosomal components see Kalt and Schliwa, 1993; Kimble and Kuriyama, 1992).

We identified a protein originally called DMAP190 (Drosophila microtubule associated protein of 190 kD) using a combination of microtubule affinity chromatography and immunocytology in *Drosophila* embryos (Kellogg et al., 1989). DMAP190 is a microtubule-associated protein that is recruited to centrosomes at the onset of mitosis. DMAP190 was found to be identical to the antigen recognized by the Bx63 antibody, which was uncovered in a bank of monoclonal antibodies made to *Drosophila* nuclei (Whitfield et al., 1988; Frasch et al., 1986). In agreement

Address correspondence to K. Oegema, Department of Biochemistry and Biophysics, University of California, San Francisco, San Francisco, CA 94143-0448. Ph.: (415) 476-4581. Fax: (415) 476-0806.

with other workers in the field, we now call this protein CP190 (for centrosomal protein of 190 kD).

CP190 has been cloned and sequenced (Whitfield et al., 1995; GenBank/EMBL/DDBJ accession number Z50021); the sequence predicts a novel protein of 1,096 amino acids with an isoelectric point of 4.5 and a molecular weight of 120 kD. CP190 shares a low level of amino acid identity (<15%) over a considerable portion of its length with a class of proteins including neurofilaments, myosin heavy chain, and MAP-2. This homology is thought to result from the presence of extensive tracts of α helical structure that CP190 is predicted to contain. Although most of the proteins in this class possess coiled–coil structural motifs, CP190 does not contain the heptad repeats expected in a coiled–coil structure. Sequence comparisons have also identified a cluster of four putative zinc fingers between amino acids 472 and 590, roughly in the middle of the predicted protein (Whitfield et al., 1995). Native CP190 is found in nuclei during interphase. At prophase, upon nuclear envelope breakdown, CP190 rapidly accumulates at centrosomes where it remains throughout mitosis; beginning at telophase, CP190 is again imported into reforming nuclei (Frasch et al., 1986; Whitfield et al., 1988; Oegema, K., B. Alberts, J. W. Sedat, and W. S. Marshall, manuscript in preparation).

Immunoaffinity chromatography using columns constructed from anti-CP190 antibodies identified a group of proteins that interact with CP190 (Kellogg et al., 1992). One of these, CP60 (centrosomal protein of 60 kD) has been cloned and sequenced (Kellogg et al., 1995). CP60 exhibits behavior similar to CP190; CP60 is found in eluates from microtubule affinity columns and localizes to nuclei and to centrosomes in a cell cycle–dependent manner (Kellogg et al., 1992, 1995). However, CP60 shares no significant amino acid homology with CP190 or with any other known proteins (Kellogg et al., 1995).

Our objectives in this work are twofold: to determine how CP190 achieves its dynamic cell cycle–dependent pattern of centrosomal and nuclear localization and to gain insight into the function of CP190 and CP60 in the *Drosophila* embryo. These studies are a first step towards understanding the cell cycle–dependent changes in structure and function that occur at centrosomes. In this work, we focus on the identification of regions of CP190 important for its dynamic localization pattern and on an examination of the mechanism by which CP190 and CP60 localize to centrosomes in vivo.

Materials and Methods

Expression and Purification of CP190 Fusion Proteins

Two types of fusion proteins were used in these experiments: 6XHis tagged fusion proteins were made using the QIA express pQE9 vector (Stuber, 1990) from Qiagen (Chatsworth, CA) and fusions with glutathione-*S*-transferase (GST)[1] were made using the pGEX-2T vector (Smith, 1988) with a modified polylinker. An oligonucleotide was synthesized and ligated between the BamHI and EcoRI sites of pGEX-2T to create the final sequence GGATCCGGTACCAGATCTCGAGTCGACAAGCTTGGAATTC. The new polylinker thus contains the following restriction enzyme cutting sites in order: BamHI, KpnI, BglII, XhoI, SalI, HindIII, and EcoRI. To generate the fragments of the CP190 DNA sequence that were cloned to produce fusion proteins, we performed nested PCR using a cDNA library as the template (Brown and Kafatos, 1988; Sambrook et al., 1989) and Vent DNA polymerase (New England Biolabs, Beverly, MA). The primers for PCR were derived by reference to the CP190 cDNA sequence (Whitfield et al., 1995) and they contained BglII and HindIII sites at their 5' ends. The PCR products were cloned into either the BamHI/HindIII sites in the pQE9 vector or the BglII/HindIII sites in the modified pGEX-2T vector. The 6XHis fusion proteins therefore begin with the sequence MRGSHHHHHHGS. Transformation was into *Escherichia coli* M15(pREP4) for pQE9-CP190 constructs or *E. coli* TG-1 for pGEX-2T-CP190 constructs.

A Ni-NTA resin (Qiagen) was used to purify the 6XHis fusion proteins. Chromatography was carried out according to the manufacturer's specifications with some modifications. The extract buffer was often supplemented with 2 M urea, since it significantly improves fusion protein solubility. Columns were eluted in 1-ml fractions in a buffer containing 250 mM imidazole (Sigma Chemical Co., St. Louis, MO). GST fusion proteins were purified as in (Smith, 1988) with some buffer modifications. Proteins were eluted in 50 mM Na phosphate, pH 8.0, 500 mM NaCl, 10 mM 2-mercaptoethanol, 5 mM reduced glutathione (Sigma Chemical Co.). Both 6XHis and GST fusion proteins were further purified on a Superose 12 gel filtration column equilibrated into FPLC buffer (50 mM Na phosphate, pH 8.0, 250 mM NaCl, 1 mM 2-mercaptoethanol) using a fast protein liquid chromatography (FPLC) system (Pharmacia Fine Chemicals, Piscataway, NJ).

The 6XHis fusion protein concentrations were determined by measuring their OD_{280} in FPLC buffer using extinction coefficients calculated from their primary amino acid sequence (Gill and von Hippel, 1989). The GST fusion protein concentrations were determined relative to bovine serum albumin using the Bradford assay (Bradford, 1976).

Expression and Purification of CP60 Full-length Fusion Protein

Full-length 6XHis CP60 fusion protein was produced using the pREST vector from Invitrogen (San Diego, CA). Nested PCR was performed as above using primers from the CP60 cDNA sequence (Kellogg et al., 1995). The primers contained BglII and HindIII sites at their 5'ends and the resulting fragment was cloned into pRSETB. Transformation was into *E. coli* BL21(DE3)plysS. Purification was as above except that a Superose 6 gel filtration column was used in place of the Superose 12 column.

Fluorescent Labeling of Fusion Proteins

To label fusion proteins, 0.75 μl of 12.5 mg/ml tetramethyl-rhodamine-NHS ester (Molecular Probes, Eugene OR), dissolved in either *N,N*-dimethylformamide or dimethylsulfoxide, was added to 75 μl of fusion protein (1–5 mg/ml) in FPLC buffer. The mixture was incubated on ice for 5 min, and 7.5 μl of 2 M potassium glutamate, pH 8.0 and 0.75 μl of 0.5 M dithiothreitol were added to stop the reaction. To remove free rhodamine, each labeled fusion protein was then transferred into injection buffer using a small spin column of Bio-Gel P-6 resin that excluded the protein (Bio-Rad Laboratories, Hercules, CA). The injection buffers used were 50 mM Hepes, pH 7.6, 250 mM KCl for the 6XHis fusion proteins and 50 mM Hepes, pH 7.6, 100 mM KCl for the GST fusion proteins. The extent of labeling was assayed by spectroscopy; if the protein was over or under labeled the procedure was repeated varying the amount of rhodamine added. (Proteins were considered over labeled if the absorption peak at 522 nm, due to rhodamine dimers, was equivalent to or higher than the absorption at 556 nm). Labeling stoichiometries were determined using a value of 50,000 M^{-1} cm^{-1} for tetramethyl rhodamine (Molecular Probes, Eugene, OR) and were generally between 0.15 and 0.5 rhodamine/protein monomer.

Embryo Injection and Confocal Microscopy

Embryos were manually dechorionated and injected at 50% egg length according to standard procedures (Santamaria, 1986). The concentrations of the injected labeled fusion proteins were between 2 and 15 mg/ml, and the volume injected was approximately 1–2% of the embryo's total volume (Foe and Alberts, 1983). When added as a second marker, 40,000-mol wt fluorescein dextran (Molecular Probes, Eugene, OR) was injected at con-

1. *Abbreviations used in this paper*: FPLC, fast protein liquid chromatography; GST, glutathione-*S*-transferase; MAP, microtubule-associated protein; NLS, nuclear localization signal.

centrations between 0.15 and 2 mg/ml. Time-lapse confocal microscopy was performed using a Nikon Optiphot fluorescence microscope equipped with the Bio-Rad MRC 600 laser scanning confocal attachment. All images were collected using a Nikon 60× Plan Apo lens with a numerical aperture of 1.4. Embryo injection and screening was performed on a Nikon Diaphot inverted microscope equipped with an epifluorescence attachment.

Fixation and Immunofluorescence

Embryos were fixed in 37% formaldehyde as described (Theurkauf, 1992). Vitelline membranes were removed with methanol. The rabbit anti-CP60 antibody used has been described (Kellogg et al., 1995). The rabbit anti-CP190 antibody used was prepared by immunizing a rabbit with a total of 1.5 mg of a 6XHis fusion with CP190 amino acids 385–508, prepared as described above. Immunizations and bleeds were carried out by the Berkeley Antibody Company (Richmond, CA). The antibodies were affinity purified on a column of immobilized 6XHis CP190 amino acids 385–508, prepared as described (Kellogg and Alberts, 1992) according to standard techniques (Harlow and Lane, 1988). Donkey Cy5 anti-rabbit and fluorescein anti-mouse antibodies were obtained from Jackson ImmunoResearch Laboratories, Inc. (West Grove, PA).

Bead Cosedimentation Assays (Native CP190)

Antibodies were coupled to Affi-prep protein A beads (Bio-Rad Laboratories, Hercules, CA) at 0.5 mg/ml using dimethylpimelimidate as described (Harlow and Lane, 1988). Rabbit antibodies to CP190 amino acids 2299–2554 were prepared as described above. Random rabbit IgG was obtained from Jackson ImmunoResearch Laboratories, Inc. (West Grove, PA). A total of 100 μl of beads were incubated for 1 h at 4°C with 3 ml of *Drosophila* embryo extract prepared as in (Kellogg and Alberts, 1992) except that only two volumes of buffer containing 100 mM KCl were used to re-suspend the embryos. The beads were then extensively washed with 50 mM Hepes, pH 7.6, 1 M KCl, 1 mM Na_3 EGTA, 1 mM $MgCl_2$, 10% glycerol, 0.05% NP-40, plus 1:200 protease inhibitor stock (Kellogg et al., 1989). Cycled tubulin at 15 mg/ml in BRB80 (80 mM potassium Pipes, pH 6.8, 1 mM $MgCl_2$, 1 mM Na_3 EGTA) was polymerized by the addition of an equal volume of BRB80, 20% dimethylsulfoxide, 2 mM GTP at 37°C. The microtubules were stabilized following polymerization by the addition of taxol to 100 μM. Microtubules (5 μl) were diluted into 125 μl of equilibration buffer (20 mM potassium Pipes, pH 6.8, 50 mM potassium acetate, 1 mM $MgCl_2$, 1 mM Na_3 EGTA) plus 0.1% Tween 20 before incubation with 50 μl of beads for 20 min at room temperature. The beads were centrifuged through 10 ml sucrose step gradients consisting of 5 ml of 70% sucrose and 5 ml of 30% sucrose in equilibration buffer plus 0.1% Tween 20 using a table top centrifuge (International Equipment Company, Needham Heights, MA) at top speed for 10 min. Proteins pelleted with beads were analyzed by SDS–polyacrylamide gel electrophoresis.

Microtubule Cosedimentation Assays (Bacterially Expressed Fusion Proteins)

To 30 μg of each fusion protein in FPLC buffer, we added 13 μg of the T4 bacteriophage gene 45 protein (Morris et al., 1979) as a carrier. The volume of each sample was brought up to 66 μl with FPLC buffer, which was then exchanged for equilibration buffer using spin desalting columns. The fusion proteins were centrifuged at 100,000 rpm for 10 min in the TLA 100 rotor (Beckman Instruments, Fullerton, CA). Cycled tubulin at 18.5 mg/ml in BRB80 was used to prepare taxol stabilized microtubules as described above. Fusion protein (10 μl) was mixed with 80 μl of equilibration buffer containing 200 μg/ml gene 45 protein (as carrier) and either 10 μl of microtubules or 10 μl of control buffer. The mixtures were layered over 100 μl cushions of 80 mM potassium Pipes, pH 6.8, 1 mM $MgCl_2$, 1 mM Na_3 EGTA, 50% glycerol, and were then centrifuged at 100,000 rpm for 10 min in the TLA 100 ultracentrifuge. Supernatants and pellets were then analyzed by electrophoresis on 13.5% polyacrylamide gels.

Microtubule Bundling Assays

Cycled tubulin (8 μl of 10 mg/ml) and rhodamine-labeled cycled tubulin (2 μl of 10 mg/ml) were added to 10 μl of BRB80 plus 2 mM GTP. The tubulin was allowed to polymerize at 37°C for 20 min. Labeled microtubules were stabilized by the addition of 80 μl of BRB80 plus 20 μM taxol. Fusion protein (1 μl of 0.5 mg/ml in 50 mM potassium phosphate, pH 8.0, 300 mM KCl, 1 mM 2-mercaptoethanol) was mixed with 2 μl of rhodamine-labeled microtubules. The mixture was incubated at room temperature for 10 min and then diluted 1:25 into BRB80, 60% glycerol, 0.1% glutaraldehyde, plus an oxygen scavenging system (50 μg/ml catalase, 100 μg/ml glucose oxidase, 12.5 mM glucose), and mounted for viewing under the fluorescence microscope.

The tubulin used in the experiments described in this paper was purified from bovine brain according to Mitchison et al. (1984), through the phosphocellulose chromatography step. As judged by SDS–polyacrylamide gel electrophoresis, it is free of detectable microtubule associated proteins (MAPs).

Results

Identification of Protein Domains Responsible for the Centrosomal and Nuclear Localizations of CP190

After PCR was used to amplify six overlapping fragments of the CP190 cDNA, these fragments were cloned into the vector pQE9 to construct a series of fusion proteins (Fig. 1), each with a 12-amino acid tag containing 6-histidine residues at its amino terminus. Each of the fusion proteins is denoted by its CP190 amino acid numbers; (Whitfield et al., 1995). These fusion proteins were soluble and could be purified under native conditions; however, fusion proteins including amino acids 1-166 were insoluble and were

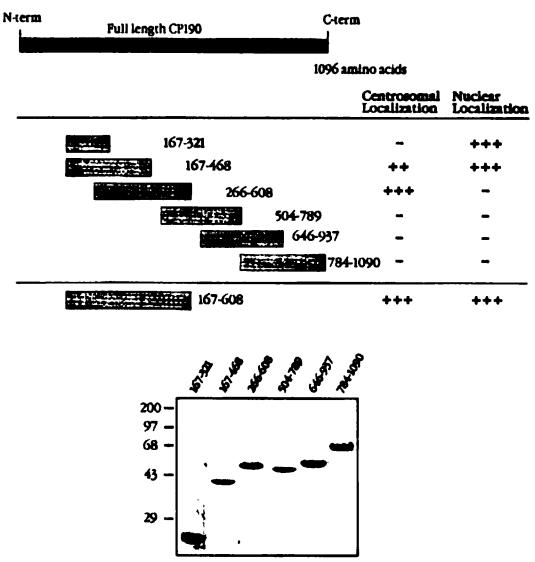

Figure 1. A map of the 6XHis tagged fusion proteins used in injection experiments. Purified fusion proteins containing the indicated sequences from CP190 (amino acid numbers are shown) were rhodamine-labeled and injected into syncytial *Drosophila* embryos. The columns to the right summarize the localization of each fusion protein, as observed by time-lapse confocal microscopy. In the inset, each of the purified fusion proteins has been analyzed by SDS–polyacrylamide gel electrophoresis (13.5% polyacrylamide) and detected by staining with Coomassie blue. The size of markers in kilodaltons is indicated in the left margin. For the injection experiments, the highest concentration tested was often limited by the solubility of the fusion protein. The maximum concentration injected was 4.6, 4.5, 5.6, 7.3, 13.6, 15.0, and 3.0 mg/ml for each fusion protein, as listed from top to bottom in the figure: each protein showing positive localization gave consistent results at concentrations of 1.5–2.0 mg/ml and higher.

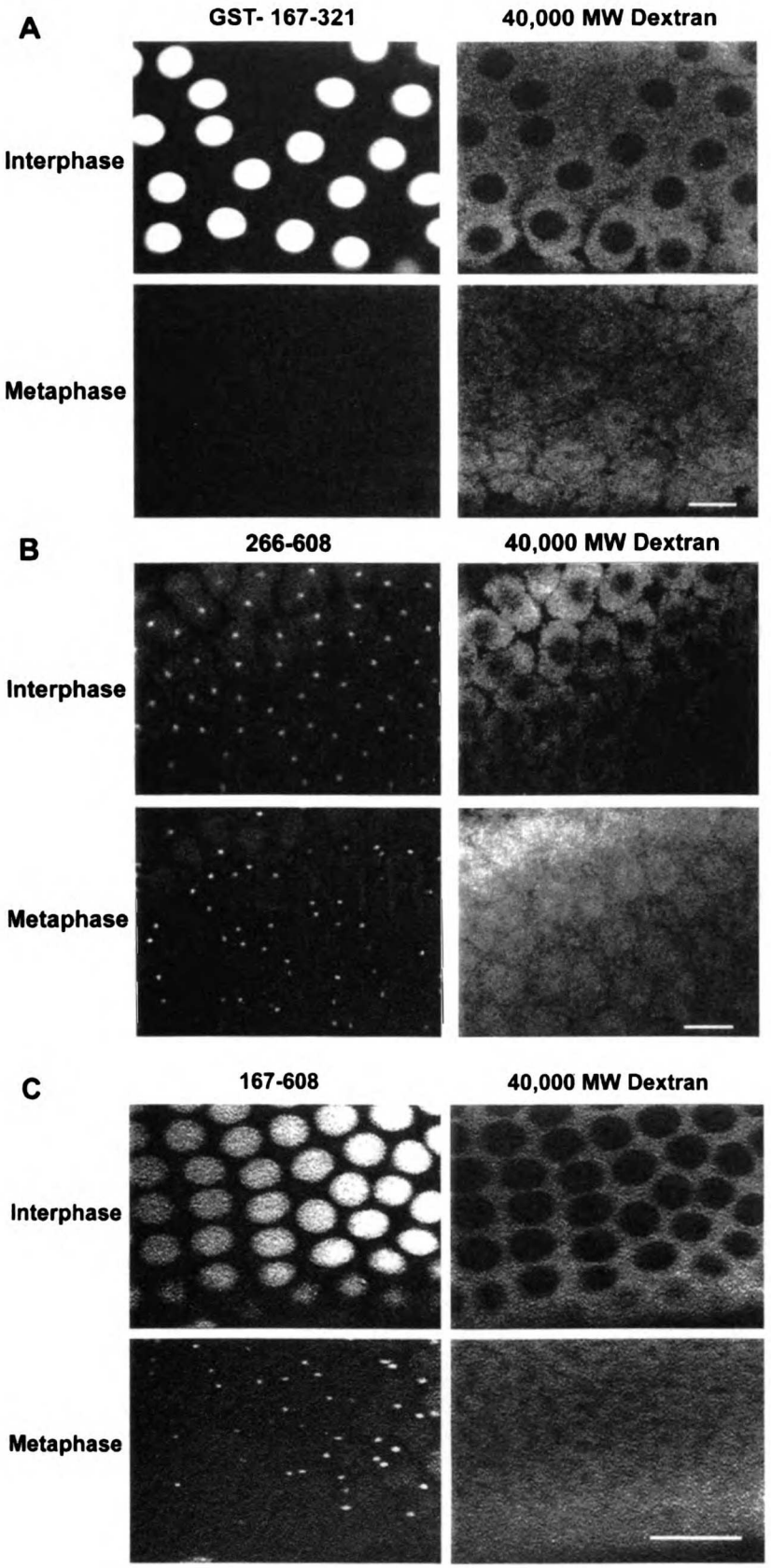

Figure 2. Injection of CP190 fusion proteins reveals three different localization patterns. Confocal micrographs of living embryos co-injected with rhodamine-labeled fusion protein and fluorescein-labeled 40,000-mol wt dextran. Each set of micrographs was selected from a time-lapse series taken of a portion of the embryo's surface during several cell cycles. The localization patterns are classified according to the localization of the fusion proteins during interphase and mitosis (interphase localization/mitotic localization). Shown here for each fusion protein are interphase (*top*) and metaphase (*bottom*) of the same cell cycle. Rhodamine-labeled fusion protein is on the left and fluorescein-labeled dextran is on the right. The 40,000-mol wt dextran was injected at concentrations of 0.15–0.3 mg/ml; the fusion proteins were injected at a concentration of 1.7 mg/ml. Examples of the three localization patterns obtained are shown: (*a*) Co-injection of rhodamine labeled GST-167-321 and 40,000-mol wt fluorescein dextran. GST-167-321 has a nuclear/cytoplasmic localization pattern; it is imported into nuclei as they reform in telophase and is completely localized in nuclei by interphase. Upon nuclear envelope breakdown, the fusion protein immediately disperses into the cytoplasm. Because the 40,000-mol wt dextran is excluded from nuclei as they reform, the nuclei appear as black holes against a cytoplasmic background of dextran. Upon nuclear envelope breakdown, the dextran immediately diffuses into the nuclei. (*b*) 266-608 is an example of a centrosomal/centrosomal pattern of localization; it is found at centrosomes at constant levels throughout the cell cycle. (*c*) 167-608 is an example of a protein that cycles between nuclei and centrosomes giving a nuclear/centrosomal localization pattern. This protein accumulates in nuclei during telophase and remains there throughout interphase; upon nuclear envelope breakdown, it immediately begins to accumulate at centrosomes. The centrosomal localization peaks by metaphase and remains relatively constant until the subsequent telophase. Bars, 10 μm.

therefore not pursued. We purified the overlapping fusion proteins in Fig. 1 by Ni-NTA agarose affinity chromatography followed by passage over a FPLC Superose 12 sizing column. The sizing column step removed aggregated fusion protein and truncated products and was often essential to get functional proteins. After fluorescent labeling of the purified fusion proteins with *N*-hydroxysuccinimidyl rhodamine at low stoichiometry, we injected them into *Drosophila* embryos during or just prior to the late syncytial nuclear divisions (cycles 10–14); fluorescein-labeled 40,000-mol wt dextran was co-injected to serve as a cell cycle marker (Kalpin et al., 1994).

At early stages of *Drosophila* development, the embryo is a syncytium, so injected protein can diffuse via the common cytoplasm to the hundreds of nuclei present. By cycle 10, the nuclei have migrated to form a uniform monolayer just beneath the cortex (Foe and Alberts, 1983), simplifying their visualization. We followed these nuclei and their associated centrosomes using fluorescent time-lapse confocal microscopy. During interphase, the nuclei appear in the fluorescein channel as black holes that exclude dextran. At prometaphase, when the nuclear envelope breaks down, dextran floods into the nucleus, thus allowing us to accurately assess the cell cycle state of the injected embryos (Fig. 2).

Injection of each of the labeled fusion proteins resulted in either no localization or one of three localization patterns that we have designated nuclear/cytoplasmic, nuclear/centrosomal, and centrosomal/centrosomal, according to their locations during interphase and mitosis (interphase localization/mitotic localization). The first pattern, nuclear/cytoplasmic, is exemplified by fusion protein 167-321 (Fig. 1). This fusion protein is localized to the cytoplasm during mitosis, and is imported into reforming nuclei in telophase where it remains throughout interphase. Upon nuclear envelope breakdown, fusion protein 167-321 disperses evenly throughout the cytoplasm where it remains throughout mitosis. The localization of this portion of CP190 when injected as a GST fusion protein was identical to that of the smaller 6XHis fusion protein (see Fig. 2 *a*, GST-167-321).

Injection of fusion protein 167-468 resulted in a nuclear/centrosomal pattern of localization, labeling nuclei during interphase and showing weak centrosomal localization during mitosis. Fusion protein 266-608 gave a centrosomal/centrosomal pattern of localization (Fig. 2 *b*), strongly localizing to centrosomes with equal intensity during both interphase and mitosis.

We constructed fusion protein 167-608 (Fig. 1) to see if we could enhance the centrosomal localization of fusion protein 167-468 while maintaining its nuclear/centrosomal pattern of localization. This protein localized to nuclei during interphase and gave a robust centrosomal localization during mitosis, mimicking the localization pattern of the native protein (Fig. 2 *c*).

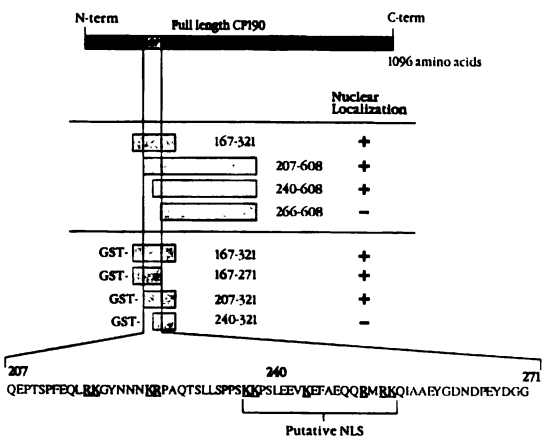

Figure 3. Characterization of the region of CP190 responsible for nuclear localization. Fusion proteins in the region of the nuclear localization domain are diagrammed here. The top 4 fusion proteins were 6XHis tagged and were injected at concentrations of 4.6, 1.3, 3.1 and 2.7 mg/ml (in order from *top* to *bottom*); the bottom four were fusions of small pieces of CP190 with glutathione-*S*-transferase and were injected at concentrations of 3.3, 1.5, 2.3, and 3.8 mg/ml (in order from *top* to *bottom*). Purified fusion proteins were rhodamine-labeled and injected into syncytial *Drosophila* embryos. Nuclear localization was scored by subsequent observation on an inverted fluorescence microscope. From this data, the region that we believe to be responsible for nuclear localization is found between amino acids 207 and 271. The basic residues are underlined. A bipartite NLS is found between amino acids 237 and 255.

Characterization of a Region of CP190 Responsible for Nuclear Localization

Based on our injection data, the region responsible for the nuclear localization of our fusion proteins is located between amino acids 167 and 321. Closer examination of the amino acid sequence in this region identified a potential bipartite nuclear localization signal (NLS) between amino acids 237 and 255 (Fig. 3). A bipartite NLS consists of two

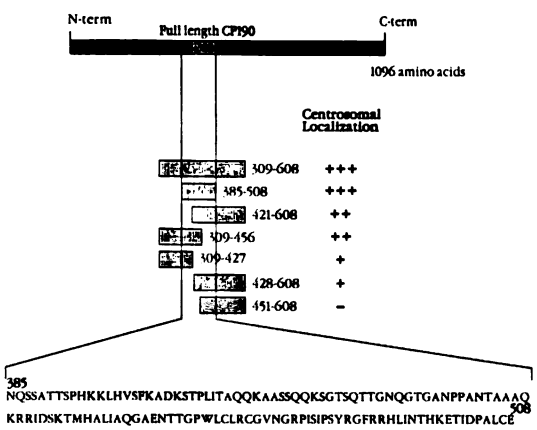

Figure 4. Characterization of the domain(s) of CP190 responsible for its centrosomal localization. The 6XHis tagged fusion proteins diagrammed were rhodamine-labeled and injected into syncytial *Drosophila* embryos. Centrosomal localization was scored by fluorescence confocal microscopy. Two non-overlapping fusion proteins, 309-427 and 428-608, localize to centrosomes, suggesting that the centrosomal localization domain contains multiple independent elements which together cooperate to give robust centrosomal localization.

basic amino acids, followed by a spacer region of approximately 10 amino acids, followed by another region of 5 amino acids, 3 of which are basic; in many cases, the spacer can vary considerably in length (Dingwall and Laskey, 1991). The potential NLS in CP190 has a spacer of 13 amino acids.

The fusion proteins shown in Fig. 3 were labeled with rhodamine and injected into embryos to test whether this potential NLS is responsible for the nuclear localization of our CP190 fusion proteins. Fusion protein 207-608 gave a nuclear/centrosomal localization pattern, confirming that it contains sufficient sequences to target the fusion protein to nuclei during interphase. Fusion protein 240-608 also gave a nuclear/centrosomal localization pattern, even though this construct deletes the upstream element of the bipartite NLS (Fig. 3). The slightly smaller fusion protein 266-608, representing an additional NH_2-terminal deletion of 26 amino acids, however, fails to concentrate in the nucleus. Thus, sequences essential for the nuclear localization of CP190 appear to lie between amino acids 240 and 266.

Some protein fragments were also expressed as fusions with GST. The GST fusion with amino acids 240-321 of CP190 does not localize to the nucleus. How can we explain these results? One possible explanation is that the complete bipartite NLS between amino acids 237 and 255 of CP190 is normally required for the nuclear localization of our fusion proteins, but, in the case of fusion protein 240-608 fused to 6XHis, the amino terminus with its positive charge can fill in for the missing upstream pair of basic amino acids.

Characterization of the Domain of CP190 Responsible for Centrosomal Localization

To determine if we could further delineate the domain of CP190 required to obtain centrosomal localization, smaller fusion proteins were constructed (Fig. 4). A 124–amino acid 6XHis fusion protein corresponding to amino acids 385-508 of CP190 was able to localize well to centrosomes when fluorescently labeled and injected into embryos. As seen previously for the larger fusion protein 266-608, this fusion protein localized to centrosomes constitutively, with equal intensity throughout the cell cycle. Fusion proteins 421-608 and 309-456 contain NH_2- and COOH-terminal deletions, respectively, of part of the 124–amino acid region of 385-508 (see Fig. 4). These protein fragments also localize to centrosomes, although the ratio of centrosomal staining to background cytoplasmic staining is decreased (data not shown). Two nonoverlapping fusion proteins, 309-427 and 428-608 were then constructed. Although both of these proteins localize to centrosomes, this localization is comparatively weak (data not shown). There is no obvious amino acid homology between these two independent regions of CP190. These results suggest that the centrosomal localization domain is complex, spanning at least the 124–amino acid region which allows robust centrosomal local-

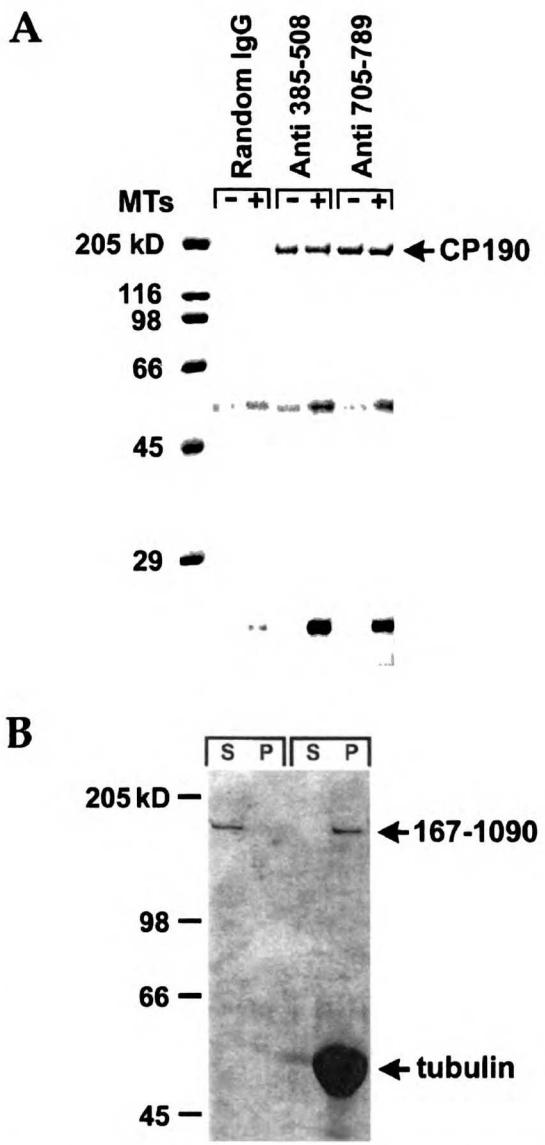

Figure 5. Native and bacterially expressed CP190 bind microtubules. (*a*) Protein A beads coupled to random IgG, anti-CP190 amino acids 385-508 or anti-CP190 amino acids 705-789 were mixed with *Drosophila* embryo extract. The beads were washed extensively with buffer containing 1 M KCl to remove any proteins associated with CP190 and were then mixed with taxol-stabilized microtubules or control buffer before layering on 10 ml sucrose step gradients and pelleting in a table top clinical centrifuge. Pelleted beads were boiled in sample buffer and released proteins were analyzed by SDS–polyacrylamide gel electrophoresis (10% polyacrylamide). (*Top*) Coomassie-stained gel. (*Bottom*) Western blot of the central portion of the gel with the anti-α-tubulin mouse monoclonal DM1α. Western blotting was necessary because IgG heavy chain that leached off the beads runs at the same molecular weight as tubulin. (*b*) The bacterially expressed 6XHis fusion with CP190 amino acids 167-1090 was tested for its ability to cosediment with taxol stabilized microtubules. The supernatants and pellets from sedimentations done in the absence (left two lanes) or presence (right two lanes) of taxol-stabilized microtubules were analyzed by SDS–polyacrylamide gel electrophoresis.

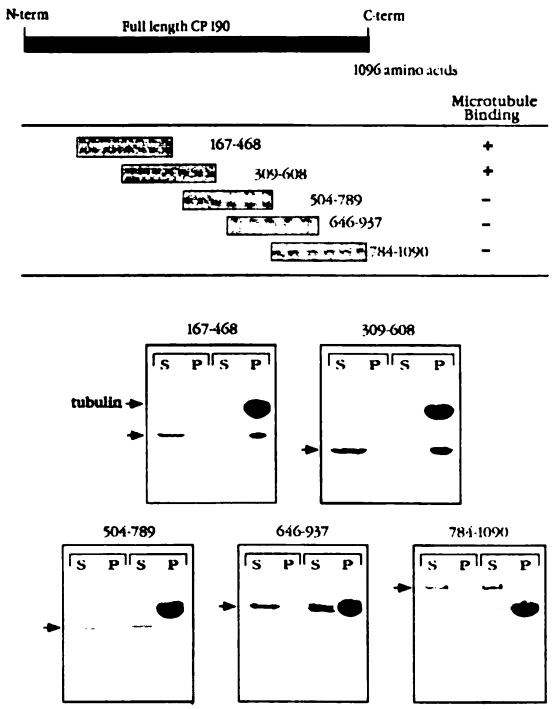

Figure 6. Identification of the region of CP190 important for its microtubule binding. (*Top*) Map of the fusion proteins spanning CP190 that were tested for their ability to cosediment with microtubules. (*Bottom*) The supernatants and pellets from sedimentations done in the absence (left two lanes in each box) or presence (right two lanes in each box) of taxol-stabilized microtubules. The samples were separated by electrophoresis on 13.5% polyacrylamide gels and stained with Coomassie blue. The large band in the right-most lane in each box is tubulin. Fusion proteins 167-468 and 309-608 pellet only in the presence of microtubules. Fusion proteins 504-789, 646-937, and 784-1090 remain in the supernatant with or without microtubules.

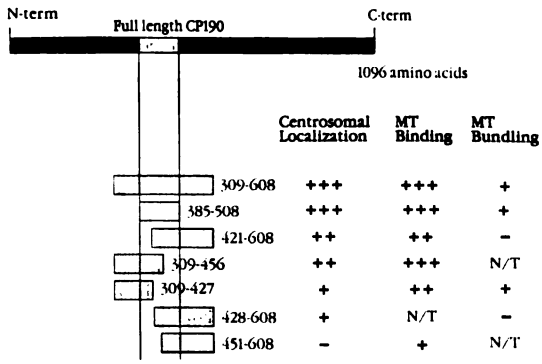

Figure 7. A comparison of microtubule cosedimentation, centrosomal localization and microtubule bundling is shown for fusion proteins in the region of the centrosomal localization domain. The ability of a fusion protein to cosediment with microtubules was qualitatively assessed based on cosedimentation assays done at two salt concentrations. Experiments were carried out in 20 mM K-Pipes, pH 6.8, 50 mM potassium acetate, 1 mM $MgCl_2$, 1 mM Na_3EGTA and in the same buffer plus 50 mM NaCl. Bundling assays were performed as described in the legend to Fig. 8. *N/T* indicates that the fusion protein was not tested in the assay.

ization. No significant homology was found when these 124 amino acids (the amino acids between 385 and 508) were compared alone, or as a part of larger fragments, to known protein databases using the BLAST comparison tool (Atschul et al., 1990). The centrosomal localization domain does overlap slightly with the central domain of CP190 predicted to encode four zinc fingers (Whitfield et al., 1995), since the fusion protein with amino acids 385-508 contains one putative zinc finger. However, this zinc finger can not be required for centrosomal localization since the fragment 309-456, which contains no zinc fingers, also gives good localization to centrosomes.

The Domain of CP190 Responsible for Its Centrosomal Localization Cannot Be Separated from a Region That Confers an Ability to Cosediment with Microtubules

Since CP190 was originally identified by microtubule-affinity chromatography (Kellogg, et al., 1989), we wanted to determine if native CP190 could bind directly to microtubules. To do this, we used protein A beads coupled to anti-CP190 antibody to immunoprecipitate the endogenous protein from *Drosophila* embryo extracts. The beads were subsequently washed with buffer containing 1 M potassium chloride to remove proteins which associate with CP190. The beads were then mixed with microtubules and sedimented at low speed through a sucrose step gradient. Fig. 5 *a* shows the results of such an experiment. CP190 is cleanly immunoprecipitated by both anti-CP190 antibodies (Fig. 5 *a*, last four lanes) but not with random rabbit IgG. Microtubules co-pellet with the CP190 bound beads but not with control beads coupled to random IgG.

Additionally, we found that a bacterially expressed 6XHis fusion protein containing amino acids 167-1090 of CP190 would cosediment with microtubules in vitro (Fig. 5 *b*); the stoichiometry of this binding at saturation was one CP190 167-1090 monomer to between four and five tubulin dimers (data not shown), suggesting that CP190 binds along the lengths of microtubules in vitro. We localized the region of CP190 responsible for microtubule binding by subjecting a series of smaller fusion proteins to the cosedimentation test (Fig. 6). Fusion proteins 167-468 and 309-608 cosedimented quantitatively with microtubules under our conditions, whereas the more COOH-terminal fusion proteins, (504-789, 646-937, and 784-1090), remained in the supernatant both in the presence and absence of microtubules (Fig. 6). We next tested the fusion proteins that were used to narrow down the centrosomal localization domain (Fig. 4) in our cosedimentation assay. As shown in Fig. 7, we were unable to separate the region important for centrosomal localization from the microtubule binding region; in fact, it seems that the ability of a fusion protein to cosediment with microtubules closely parallels its ability to localize to centrosomes.

We also tested some of these fusion proteins to see if they could bundle rhodamine-labeled microtubules. Fusion proteins 309-608, 309-427, and 385-508 caused microtubules to

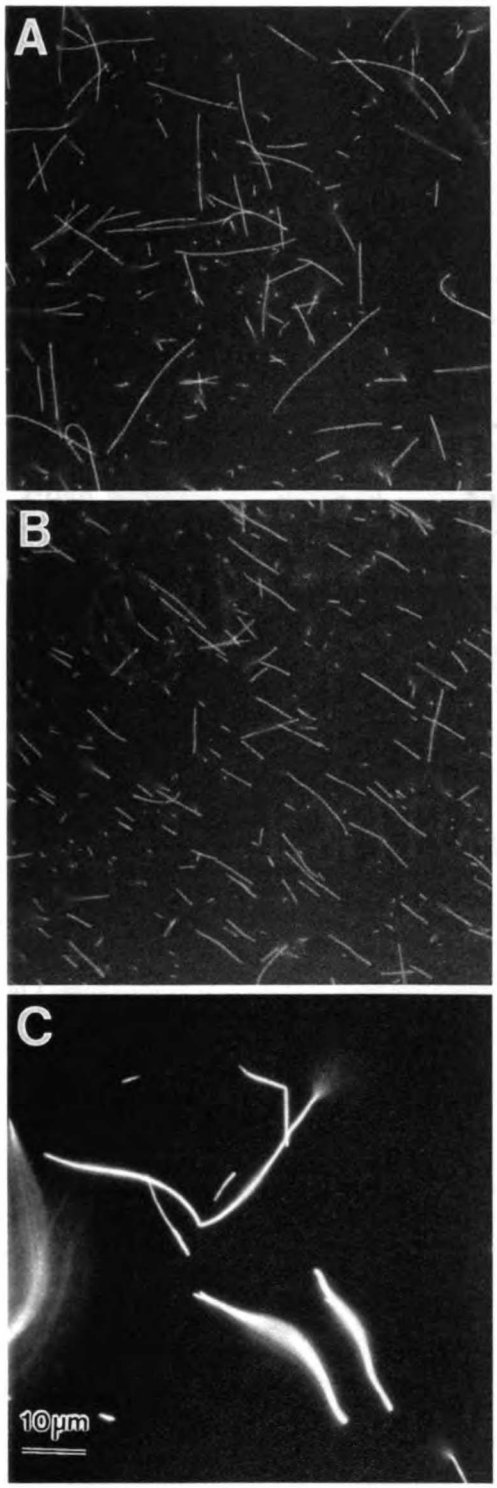

form tight bundles (Fig. 8). This bundling was salt insensitive, as bundles would still form in the presence of 500 mM KCl (data not shown). Fusion proteins 421-608 and 428-608, although able to cosediment with microtubules, were not able to bundle microtubules in our assay. Fig. 7 summarizes the centrosomal localization, microtubule binding and microtubule bundling data for fusion proteins derived from the region of the centrosomal localization domain.

Microtubules Are Not Required for the Accumulation or Maintenance of CP190 or CP60 at Centrosomes

Centrosomal proteins can be divided into two groups: those proteins that require microtubules for their centrosomal localization and those capable of localizing to centrosomes independent of microtubules. The first group is likely to include proteins that function to organize the spindle pole, as well as proteins that accumulate at the centrosome due to its role as a hub for intracellular trafficking. Examples of proteins in the first group include NCD (a minus end–directed microtubule motor protein) and NuMA a protein important for spindle pole integrity (also called centrophilin, SP-H, and SPN), both of which localize to spindle poles in a microtubule-dependent manner (Price and Pettijohn, 1986; Kallajoki et al., 1991; Tousson et al., 1991; Endow et al., 1994). The group of proteins that localize to centrosomes independent of a nucleated microtubule array can be considered components of a "core" centrosome, defined as the structure that remains when microtubules have been depolymerized. Known components of "core" centrosomes include γ-tubulin and pericentrin (Stearns et al., 1991; Zheng et al., 1991; Doxsey et al., 1994).

Since there was a correlation between the centrosomal localization of our fusion proteins and their ability to cosediment with microtubules in vitro, we predicted that the association of CP190 with microtubules might function to localize CP190 to centrosomes in vivo. Moreover, not only does CP60 associate biochemically with CP190 (Kellogg and Alberts, 1992) and likewise localize to nuclei and centrosomes in a cell cycle specific manner, but bacterially expressed CP60, like CP190, binds directly to microtubules in vitro (Kellogg et al., 1995). Therefore, we wanted to determine if either CP60 or CP190 require microtubules to accumulate at centrosomes, rather than being components of "core" centrosomes. Previously, we have shown that there is no apparent difference in the amount of CP190 or CP60 detected by immunofluorescence at centrosomes between control mitotic embryos and colchicine-treated embryos arrested in mitosis (Raff et al., 1993). These experiments demonstrated that CP190 and CP60 remain at centrosomes when microtubules are depolymerized, suggesting that microtubules are not required to maintain their centrosomal

Figure 8. Assaying microtubule bundling. To assay MT bundling, 2 μl of rhodamine-labeled microtubules was mixed with 1 μl of purified fusion protein and the mixture was incubated at room temperature for 10 min before dilution into fix (see Materials and Methods). (*A*) Buffer control microtubules are not bundled. (*B*) fusion protein 428-608 also cannot bundle microtubules. (*C*) Addition of fusion protein 385-508 causes microtubules to form tight bundles (the apparent fraying of the ends of the bundles is misleading, being due to the bundles leaving the plane of focus).

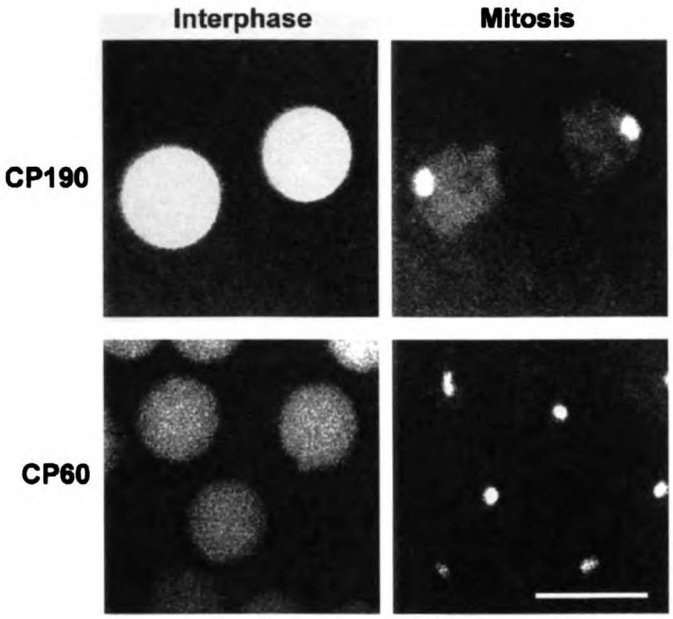

Figure 9. Imaging of CP190 and CP60 in live embryos shows that CP190 and CP60 make the transition from the nucleus to the centrosome even in the absence of microtubules. 6XHis tagged CP60 and 6XHis tagged CP190 (amino acids 167-1090) were purified and labeled with rhodamine. The purified fusion proteins were injected in 50 mM Hepes, 100 mM NaCl, 5 mM colchicine. Immediately following injection, interphase embryos that had imported CP190 or CP60 into their nuclei were selected and followed into mitosis: Z-series were taken on the confocal microscope during interphase and the subsequent colchicine induced arrest. In this way, we were able to watch CP190 and CP60 make the transition from nuclear to centrosomal localization in the absence of microtubules in live embryos. Shown here are projections of these Z-series done using the COMOS software that operates the confocal microscope (BioRad Laboratories). Bar, 10 μm.

localization. However, microtubules could nevertheless have a role in causing the movement of CP190 or CP60 to centrosomes.

To test the effect of microtubule depolymerization on the ability of CP190 and CP60 to accumulate at centrosomes, we co-injected 5 mM colchicine and either purified rhodamine-labeled 6XHis CP60 (full length) or 6XHis CP190 (amino acids 167-1090). The injected embryos were immediately screened to find interphase embryos that had imported the fluorescent CP190 or CP60 into their nuclei. The embryos were then followed using time-lapse confocal microscopy until they entered a colchicine-induced mitotic arrest (Fig. 9). Control embryos were similarly injected and then fixed and stained for microtubules to insure that our treatment was depolymerizing microtubules completely (data not shown). We found that CP190 and CP60 accumulated at centrosomes with normal kinetics in the absence of microtubules, suggesting that microtubule binding plays no role in localizing either CP190 or CP60 to centrosomes.

Neither CP190 nor CP60 Bind along the Length of Microtubules In Vivo

Since neither CP60 nor CP190 require microtubules for transport to centrosomes, we performed double-label immunofluorescence to detect α-tubulin and either CP190 or CP60 in the same embryo. The aim was to determine whether these proteins localize along the lengths of microtubules in vivo, as previously demonstrated for several MAPs (Kreis and Vale, 1993). Neither CP190 nor CP60 could be detected along the lengths of microtubules at any point during the cell cycle (Fig. 10). Although present in the region of the spindle during mitosis, CP190 and CP60 exhibit a granular staining similar in character to their nuclear staining during interphase. If there is an interaction between CP190 or CP60 and microtubules in the spindle, this interaction is not similar to that of conventional MAPs.

Discussion

This paper presents the beginnings of a molecular characterization of CP190. We have identified the regions of CP190 important for its dynamic pattern of nuclear and centrosomal localization inside the cell, as well as for its ability to cosediment with microtubules in vitro. These data, combined with the results of in vivo experiments that test for a role of microtubules in the centrosomal localization of CP190 and CP60, shed light on the mechanism by which these two proteins localize to centrosomes in vivo.

When a set of 6XHis fusion proteins spanning CP190 were bacterially expressed, purified, rhodamine-labeled, and injected into *Drosophila* embryos, the injected proteins either did not localize or exhibited one of three localization patterns which we have designated nuclear/cytoplasmic, nuclear/centrosomal and centrosomal/centrosomal (to represent localizations during interphase and mitosis, respectively). A fusion protein containing amino acids 167–608, ~40% of full-length CP190, localizes to centrosomes during mitosis and to nuclei during interphase, in a manner that closely mimics the localization pattern of the native protein. The region of CP190 between amino acids 167 and 608 was further divided to identify independent domains responsible for centrosomal or nuclear localization. These results are summarized in Fig. 11.

The region responsible for the nuclear localization of our fusion proteins contains a bipartite NLS (Dingwall and Laskey, 1991) between amino acids 237 and 255, suggesting that the nuclear import of CP190 is signal dependent. We also note that CP190 contains a second potential bipartite NLS between amino acids 125 and 144, in a re-

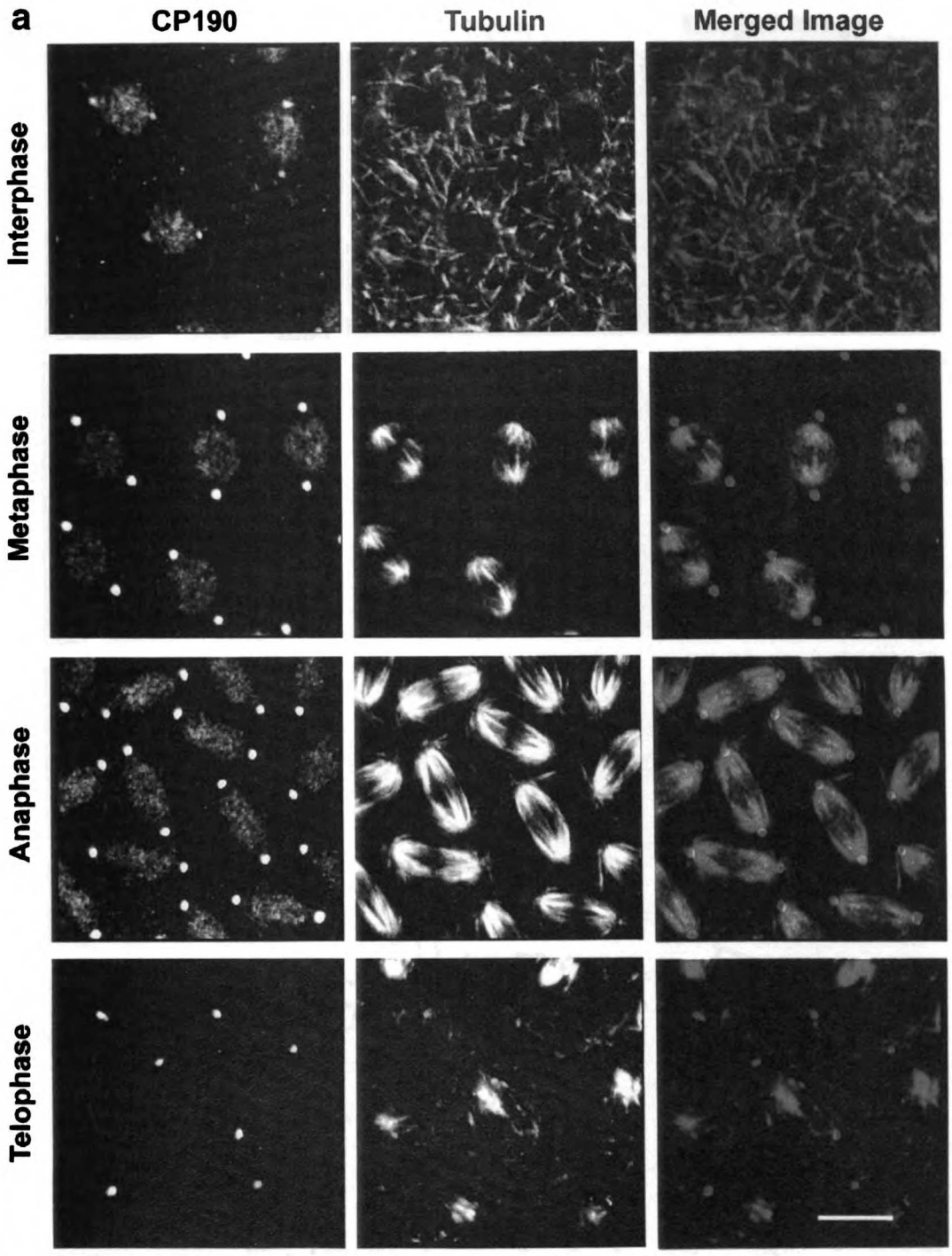

Figure 10. CP60 and CP190 do not co-localize with microtubules in vivo. (*a*) Double label immunofluorescence of CP190 and α-tubulin in syncytial *Drosophila* embryos. (*b*) Double label immunofluorescence of CP60 and α-tubulin in syncytial *Drosophila* embryos. Neither CP190 nor CP60 are found along the lengths of microtubules at any stage of the cell cycle. During mitosis CP190 and CP60 appear to stain residual nuclear structures in the region of the spindle. Bars, 10 μm.

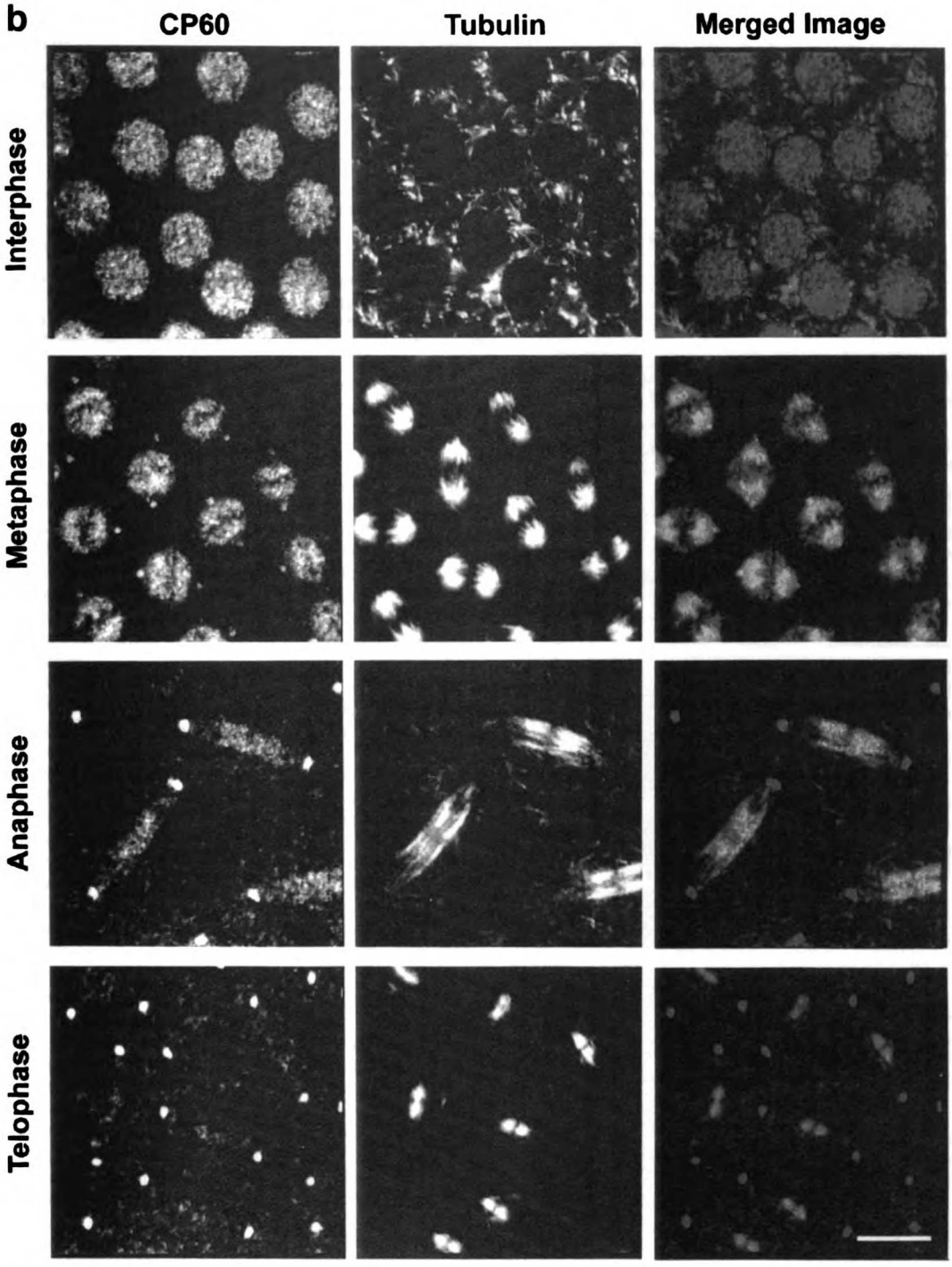

gion of CP190 that we were not able to study due to its insolubility when expressed in bacteria. This additional NLS could also contribute to the nuclear localization of the native protein.

A fusion protein containing the 124 amino acids 385-508 is sufficient for robust localization to centrosomes. Fragments that localize to centrosomes that lack a NLS, such as 266-608 (Fig. 3), remain at centrosomes at constant levels

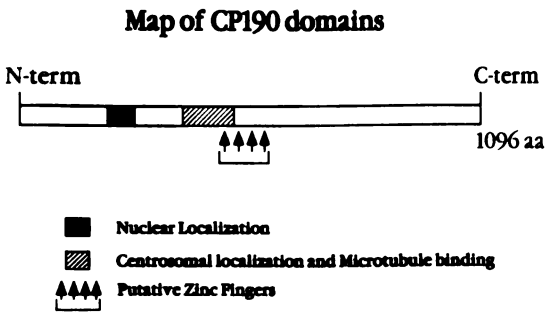

Figure 11. A Map summarizing the locations of the identified domains of CP190. The nuclear localization domain is between amino acids 207 and 271. The region of CP190 between amino acids 385 and 508 is sufficient for both good centrosomal localization and cosedimentation with microtubules in vitro. The region of CP190 between amino acids 472 and 590 contains four putative zinc fingers- the arrows point to the center of each putative zinc finger.

throughout the cell cycle. In contrast, fusion proteins that are only slightly longer, and which contain a NLS, such as 240-608, mimic the localization pattern of the native protein. Thus addition of the 26 amino acids containing the NLS confers the ability to be released from centrosomes during interphase as well as the ability to localize to nuclei. This suggests that CP190 is effectively pulled away from centrosomes during interphase by its sequestration into intact nuclei.

Weak centrosomal localization can be achieved by two adjacent, independent fragments of CP190, each containing a distinct portion of the 124-amino acid domain that produces strong centrosomal localization. There is no significant amino acid homology between the two independent fragments, suggesting the absence of a repeated motif for centrosomal binding. It nevertheless appears that separate parts of the localization domain can confer some centrosomal binding and, when put together, they act cooperatively to give the strong centrosomal localization found in fragments containing the entire domain. (A caveat is that we cannot distinguish between weak localization due to poor folding of our fusion proteins and weak localization due to lack of essential sequences.)

When a *Drosophila* embryo extract is passed over a microtubule affinity column, CP190 interacts with microtubules (Kellogg et al., 1989). This result, however, could reflect binding of CP190 to other proteins that bind directly to microtubules. It is therefore interesting that both native CP190 and a bacterially expressed fusion protein corresponding to the COOH-terminal 85% of CP190 can bind directly to microtubules in vitro. We have narrowed down the microtubule binding domain of CP190 and find that it is inseparable from the region required for centrosomal localization (see Fig. 7). The microtubule binding domain has no detectable homology to other known microtubule binding domains (Lewis et al., 1988; Himmler et al., 1989; Noble et al., 1989; Yang et al., 1989; Irminger-Finger et al., 1990; Aizawa et al., 1991).

Depolymerization of microtubules in vivo using colchicine does not noticeably affect the rate or extent of accumulation of CP190 or CP60 at centrosomes, suggesting that they are members of a very small set of characterized proteins that do not require microtubules to attain or maintain their centrosomal localizations. Many other characterized centrosomal components such as NuMA and NCD require microtubules for their localization to spindle poles or microtubule asters. CP190 and CP60, on the other hand, seem to be cell cycle-dependent components of a "core" centrosome, independent of the nucleated microtubule array. Other known components of core centrosomes include γ-tubulin and pericentrin (Stearns et al., 1991; Zheng et al., 1991; Doxsey et al., 1994).

This raises the important question of the in vivo relevance of the in vitro binding of both CP190 and CP60 to microtubules. By immunofluorescence, there is no obvious colocalization of CP190 or CP60 along the lengths of microtubules in the spindle or during interphase (Fig. 10). We can think of three possibilities to explain our data: (*a*) CP190 and CP60 localize to the centrosome by mechanisms independent of MT binding, but function as microtubule binding proteins at the centrosome. (*b*) The binding of CP190 and CP60 to microtubules observed in vitro reflects a related but different association that is important for the binding of these proteins to centrosomes. For example, CP190 and CP60 could bind to γ-tubulin at the centrosome (Raff et al., 1993). (*c*) The binding of CP190 or CP60 to microtubules could be an in vitro artifact, mediated by positively charged regions on the surface of these proteins.

The identification of the nuclear and centrosomal localization domains of CP190 is a first step towards probing its function; these domains can now be mutated and further analyzed. In addition, we can attempt to block the centrosomal localization of native CP190 in *Drosophila* embryos by the injection of antibodies to the centrosomal localization domain, or by the injection of short CP190 fusion proteins. (Some of the fusion proteins that bind centrosomes could have a dominant negative effect.) Finally, by transforming *Drosophila* with a full-length CP190 carrying point mutations designed to disrupt its nuclear localization sequences, we should be able to retain this protein at the centrosome throughout the cell cycle. If CP190 is sequestered in nuclei during interphase to keep it from interfering with centrosome function, such a mutation should produce a clear phenotype.

K. Oegema thanks Doug Kellogg and Chris Field for technical assistance, for many hours of stimulating discussions, and for encouragement and moral support. We also thank Jack Barry for protein purification assistance and advice. In addition, Michelle Moritz, Raffi Aroian, Tim Mitchison, and Arshad Desai made helpful comments and critically read the manuscript.

This work was supported by National Institutes of Health (National Institutes of Health) grant GM 23928 to B. Alberts. K. Oegema was additionally supported by fellowships from the National Science Foundation and the University of California, San Francisco.

Received for publication 23 June 1995 and in revised form 25 August 1995.

References

Aizawa, H., Y. Emori, A. Mori, H. Murofushi, H. Sakai, and K. Suzuki. 1991. Functional analyses of the domain structure of microtubule-associated protein-4 (MAP-U). *J. Biol. Chem.* 266:9841–9846.

Atschul, S. F., W. Gish, W. Miller, E. W. Myers, and D. J. Lipman. 1990. Basic local alignment search tool. *J. Mol. Biol.* 215:403–410.

Bradford, M. M. 1976. A rapid and sensitive method for the quantitation of microgram quantities of protein utilizing the principle of protein-dye binding. *Anal. Biochem.* 72:248–254.

Brown, N. H., and F. C. Kafatos. 1988. Functional cDNA libraries from *Drosophila* embryos. *J. Mol. Biol.* 116:1431–1442.

Dingwall, C., and R. A. Laskey. 1991. Nuclear targeting sequences--a consensus? *Trends Biochem. Sci.* 16:478–481.

Doxsey, S. J., P. Stein, L. Evans, P. D. Calarco, and M. Kirschner. 1994. Pericentrin, a highly conserved centrosome protein involved in microtubule organization. *Cell.* 76:639–650.

Endow, S. A., R. Chandra, D. J. Komma, A. H. Yamamoto, and E. D. Salmon. 1994. Mutants of the *Drosophila* ncd microtubule motor protein cause centrosomal and spindle pole defects in mitosis. *J. Cell Sci.* 107:859–867.

Foe, V. E., and B. M. Alberts. 1983. Studies of nuclear and cytoplasmic behaviour during the five mitotic cycles that precede gastrulation in *Drosophila* embryogenesis. *J. Cell Sci.* 61:31–70.

Frasch, M., D. M. Glover, and H. Saumweber. 1986. Nuclear antigens follow different pathways into daughter nuclei during mitosis in early *Drosophila* embryos. *J. Cell Sci.* 82:155–172.

Gill, S. C., and P. H. von Hippel. 1989. Calculation of protein extinction coefficients from amino acid sequence data. *Anal. Biochem.* 182:319–326.

Harlow, E., and D. Lane. 1988. Antibodies: A Laboratory Manual. Cold Spring Harbor Laboratory Press, Cold Spring Harbor, NY.

Himmler, A., D. Drechsel, M. W. Kirschner, and D. W. Martin, Jr. 1989. Tau consists of a set of proteins with repeated C-terminal microtubule-binding domains and variable N-terminal domains. *Mol. Cell Biol.* 9:1381–1388.

Irminger-Finger, I., R. A. Laymon, and L. S. Goldstein. 1990. Analysis of the primary sequence and microtubule-binding region of the *Drosophila* 205K MAP. *J. Cell Biol.* 111:2563–2572.

Kallajoki, M., K. Weber, and M. Osborn. 1991. A 210 kDa nuclear matrix protein is a functional part of the mitotic spindle: a microinjection study using SPN monoclonal antibodies. *EMBO J.* 10:3351–3362.

Kalpin, R. F., D. R. Daily, and W. Sullivan. 1994. Use of dextran beads for live analysis of the nuclear division and nuclear envelope breakdown/reformation cycles in the *Drosophila* embryo. *Biotechniques.* 17:730–733.

Kalt, A., and M. Schliwa. 1993. Molecular components of the centrosome. *Trends Cell Biol.* 3:119–128.

Kellogg, D. R., and B. M. Alberts. 1992. Purification of a multiprotein complex containing centrosomal proteins from the Drosophila embryo by chromatography with low-affinity polyclonal antibodies. *Mol. Biol. Cell.* 3:1–11.

Kellogg, D. R., C. M. Field, and B. M. Alberts. 1989. Identification of microtubule-associated proteins in the centrosome, spindle, and kinetochore of the early *Drosophila* embryo. *J. Cell Biol.* 109:2977–2991.

Kellogg, D. R., M. Moritz, and B. M. Alberts. 1994. The centrosome and cellular organization. *Annu. Rev. Biochem.* 63:639–674.

Kellogg, D. R., K. Oegema, J. Raff, K. Schneider, and B. M. Alberts. 1995. CP60: a *Drosophila* microtubule associated protein that is localized to the centrosome in a cell cycle-specific manner. *Mol. Biol. Cell.* In press.

Kimble, M., and R. Kuriyama. 1992. Functional components of microtubule-organizing centers. *Intl. Rev. Cytol.* 136:1–50.

Kreis, T., and R. Vale. 1993. Guidebook to the Cytoskeletal and Motor Proteins. Oxford University Press Inc., New York.

Lewis, S. A., D. H. Wang, and N. J. Cowan. 1988. Microtubule-associated protein MAP2 shares a microtubule binding motif with tau protein. *Science (Wash. DC).* 242:936–939.

Mazia, D. 1987. The chromosome cycle and the centrosome cycle in the mitotic cycle. *Intl. Rev. Cytol.* 100:49–92.

Mitchison, T., and M. Kirschner. 1984. Microtubule assembly nucleated by isolated centrosomes. *Nature (Lond.).* 312:232–237.

Morris, C. F., H. Hama-Inaba, D. Mace, N. K. Sinha, and B. M. Alberts. 1979. Purification of the gene 43, 44, 45 and 62 proteins of the bacteriophage T4 DNA replication apparatus. *J. Biol. Chem.* 254:6787–6796.

Noble, M., S. A. Lewis, and N. J. Cowan. 1989. The microtubule binding domain of microtubule-associated protein MAP1B contains a repeated sequence motif unrelated to that of MAP2 and tau. *J. Cell Biol.* 109:3367–3376.

Price, C. M., and D. E. Pettijohn. 1986. Redistribution of the nuclear mitotic apparatus protein (NuMA) during mitosis and nuclear assembly. Properties of purified NuMA protein. *Exp. Cell Res.* 166:295–311.

Raff, J. W., D. R. Kellogg, and B. M. Alberts. 1993. *Drosophila* gamma-tubulin is part of a complex containing two previously identified centrosomal MAPs. *J. Cell Biol.* 121:823–835.

Sambrook, J., E. F. Fritsch, and T. Maniatis. 1989. Molecular Cloning: a Laboratory Manual. Cold Spring Harbor Laboratory Press, Cold Spring Harbor, NY.

Santamaria, P. 1986. Injecting Eggs. *In Drosophila*: A Practical Approach. IRL Press, Washington DC. 159–174.

Schatten, G. 1994. The centrosome and its mode of inheritance: the reduction of the centrosome during gametogenesis and its restoration during fertilization. *Dev. Biol.* 165:299–335.

Smith, D. B. 1988. Single step purification of polypeptides expressed in *Escherichia coli* as fusions with glutathione S-transferase. *Gene.* 67:31–40.

Stearns, T., L. Evans, and M. Kirschner. 1991. Gamma-tubulin is a highly conserved component of the centrosome. *Cell.* 65:825–836.

Stuber, D., Matile, H., and Garotta, G. 1990. System for high-level production in *Escherichia coli* and rapid purification of recombinant proteins: application to epitope mapping, preparation of antibodies, and structure-function analysis. *In* Immunological Methods, Vol. IV, 121–152.

Theurkauf, W. E. 1992. Behavior of structurally divergent alpha-tubulin isotypes during *Drosophila* embryogenesis: evidence for post-translational regulation of isotype abundance. *Dev. Biol.* 154:205–217.

Tousson, A., C. Zeng, B. R. Brinkley, and M. M. Valdivia. 1991. Centrophilin: a novel mitotic spindle protein involved in microtubule nucleation. *J. Cell Biol.* 112:427–440.

Vorobjev, I. A., and E. S. Nadezhdina. 1987. The centrosome and its role in the organization of microtubules. *Intl. Rev. Cytol.* 106:227–293.

Whitfield, W. G., S. E. Millar, H. Saumweber, M. Frasch, and D. M. Glover. 1988. Cloning of a gene encoding an antigen associated with the centrosome in *Drosophila*. *J. Cell Sci.* 89:467–480.

Whitfield, W. G. F., M. A. Chaplin, K. Oegema, H. Parry, and D. M. Glover. 1995. The 190 kDa centrosome-associated protein of *Drosophila melanogaster* contains four zinc finger motifs and binds to specific sites on polytene chromosomes. *J. Cell Sci.* 108:3377–3387.

Yang, J. T., R. A. Laymon, and L. S. Goldstein. 1989. A three-domain structure of kinesin heavy chain revealed by DNA sequence and microtubule binding analyses. *Cell.* 56:879–889.

Zheng, Y., M. K. Jung, and B. R. Oakley. 1991. Gamma-tubulin is present in *Drosophila melanogaster* and Homo sapiens and is associated with the centrosome. *Cell.* 65:817–823.

Chapter 4

The charcterization of protein complexes containing CP190, CP60 and γ-tubulin in concentrated *Drosophila* embryo extracts

The Characterization of Protein Complexes Containing CP190, CP60 and γ–tubulin in Drosophila Embryo Extracts

Karen Oegema*, Yixian Zheng and Bruce Alberts

Department of Biochemistry and Biophysics
University of California, San Francisco
San Francisco, CA 94143-0448

*To whom correspondence should be addressed. Telephone: (415) 476-4581; Fax (415) 476-0806

Running Title: Centrosomal protein complexes in extract

Abstract

The centrosome is responsible for the nucleation and organization of microtubule arrays in animal cells. As a step toward understanding centrosome structure and function, we have characterized the protein complexes containing three centrosomal proteins, CP190, CP60 and γ–tubulin in concentrated *Drosophila* embryo extracts. In these embyro extracts, γ–tubulin is found in two distinct complexes, neither of which contain CP190 or CP60. The larger γ–tubulin containing complex has a predicted molecular mass of about 3,000,000 daltons and it can be converted to the smaller γ–tubulin containing complex of about 240,000 daltons by treatment with high salt. In concentrated embryo extracts, γ–tubulin fails to co-immunoprecipitate with CP190 or CP60 and neither CP190 nor CP60 co-immunoprecipitate with γ–tubulin. Both bacterially expressed 6XHis CP60 fusion protein and native CP60 form large, asymmetric oligomers. Native CP190 also appears to be an asymmetric oligomer. Experiments in which extracts are analyzed on sucrose gradients following immunodepletion of CP190 or CP60 demonstrate that most of the CP60 is associated with CP190. In summary, our results show that although CP60 is complexed with CP190 in extracts, neither CP190 nor CP60 is complexed with γ–tubulin.

Introduction

In animal cells, centrosome-nucleated microtubule arrays are essential for a wide variety of cellular processes including cell division and chromosome segregation, directed cell movement and general interphase cytoplasmic organization (for reviews see Kellogg et al., 1994, Mazia, 1987, Schatten, 1994, Vorobjev and Nadezhdina, 1987). Studies using electron microscopy have shown that centrosomes consist of a pair of centriolar cylinders surrounded by an electron dense cloud of pericentriolar material (PCM) that is the origin of microtubules nucleated by the centrosome (Keryer et al., 1984, Rieder and Borisy, 1982, Vorobjev and Chentsov, 1982).

Centrosomes are dynamic structures *in vivo*, continuously changing throughout the cell cycle. In addition to centrosome duplication, which occurs once per cell cycle, there is also a maturation of centrosomes that occurs at the transition between interphase and mitosis, accompanied by an increase in the amount of PCM and an increase in the microtubule nucleating capacity of the centrosome (Kuriyama and Borisy, 1981, Rieder and Borisy, 1982). In one study, the nucleating capacity of centrosomes from mitotic cells was about 5 times that of centrosomes from interphase cells (Kuriyama and Borisy, 1981).

Characterization of centrosomes and their dynamics at a molecular level is still in the nascent stages. The identification of centrosomal components is confounded by the fact that the centrosome, as the focus of the cells' microtubule arrays, is also a hub for intracellular trafficking, making it difficult to distinguish actual components of the pericentriolar material from molecules recruited by the nucleated microtubule array. To simplify this

problem, we define the "core" centrosome as the structure that remains when microtubules have been depolymerized.

Pericentrin and γ–tubulin are two known protein components of core centrosomes. Pericentrin is thought to be a structural component of the PCM that may play an essential role in its organization (Doxsey et al., 1994) and γ–tubulin is a highly conserved member of the tubulin family shown to be involved in microtubule nucleation (Joshi et al., 1992, Oakley et al., 1990, Stearns et al., 1991, Zheng et al., 1991). Recently, a γ–tubulin containing ring complex (gTuRC), capable of nucleating microtubules *in vitro* and of capping their minus ends, was purified from *Xenopus* extracts (Zheng et al., 1995). EM tomography on centrosomes isolated from *Drosophila* revealed the presence of rings of γ–tubulin within the PCM in both the presence and absence of nucleated microtubules. In centrosome-nucleated microtubule asters, the γ–tubulin rings are found at the microtubule minus ends (Moritz et al., 1995). These results suggest that the γ–tubulin ring complex is responsible for the microtubule nucleating capacity of the PCM and also reveal how centrosomes can template the protofilament number of the microtubules that they nucleate (Evans et al., 1985, Zheng et al., 1995).

In order to understand the centrosome at a molecular level we need to identify not only the molecules that comprise the structural scaffold and microtubule nucleating elements, but also centrosomal components involved in a number of other dynamic processes including: centrosome duplication and separation, the observed cell cycle dependent changes in the nucleating capacity of centrosomes, the interaction of the centrosome with the nucleus and with spindle poles, and, possibly, the organization and dynamics of microtubule arrays. One example of a component of core centrosomes that may have a role in these functions is Xklp2, a recently

identifed centrosomal kinesin that may be important for centrosome separation and spindle assembly (Boleti et al., 1996).

CP190 and CP60 are two cell cycle-dependent components of core centrosomes identified in *Drosophila*. We originally identified CP190 by microtubule-affinity chromatography and immunocytology in *Drosophila* embryos (Kellogg et al., 1989). CP190 has been cloned and sequenced (Whitfield et al., 1995); the sequence predicts a novel protein of 1,096 amino acids with an isoelectric point of 4.5 and a molecular weight of 122kD (CP190 runs aberrently on SDS-polyacrylamide gels at 190kDa). Native CP190 localizes primarily to nuclei during interphase and to centrosomes during mitosis (Frasch et al., 1986, Whitfield et al., 1988, Oegema et al., submitted for publication) and the domains responsible for the nuclear and centrosomal localizations of CP190 have been identified (Oegema et al., 1995).

CP60 was identified by immunoaffinity chromatography on columns constructed from anti-CP190 antibodies (Kellogg and Alberts, 1992). Like CP190, CP60 alternates between nuclei and centrosomes in a cell cycle-dependent manner, but with somewhat different timing (Kellogg et al., 1995; Oegema et al., submitted for publication). CP60 has been cloned and sequenced; the sequence predicts a novel protein of 440 amino acids that contains six consensus sites for phophorylation by cyclin-dependent kinases and a sequence of amino acids similar to the "destruction box" that targets cyclins for proteolysis at the end of mitosis (Kellogg et al., 1995).

In order to help ascribe function to CP190 and CP60, we have taken a biochemical approach. In this paper we present the biochemical characterization of protein complexes containing CP190, CP60 and γ–tubulin in concentrated *Drosophila* embryo extracts. We find that γ–tubulin is in two distinct, related complexes, neither of which contain CP190 or CP60.

Materials and Methods

Buffers

Extract Buffer is 50 mM HEPES, pH 7.6, 75 mM KCl, 1 mM Na_3EGTA, 1 mM Na_3EDTA, 0.05% NP-40. Protease inhibitor stock contains 1.6 mg/ml benzamidine HCl and 1 mg/ml each phenanthroline, aprotinin, leupeptin and pepstatin A dissolved in ethanol. Gradient Buffer is 50 mM HEPES, pH 7.6, 1 mM $MgCl_2$, 1 mM Na_3EGTA, 1 mM b-mercaptoethanol and protease inhibitor stock (1:200). Column Buffer is 50 mM HEPES, pH 7.6, 1 mM $MgCl_2$, 1 mM Na_3EGTA, 2% w/v glycerol. Phosphate buffered saline (PBS) contains 5.4 mM Na_2HPO_4, 1.8 mM KH_2PO_4, 137 mM NaCl, and 2.7 mM KCl adjusted to pH 7.2. Sample buffer contains 63 mM Tris-HCl, pH 6.8, 3% sodium dodecyl sulfate (SDS), 5% b-mercaptoethanol, 10% glycerol. Tris buffered saline (TBS) is 20 mM Tris-Cl, pH 7.4, 150 mM NaCl. TBST is TBS plus 0.1% Tween-20. PBST is PBS plus 0.1% Tween-20.

Antibodies

The rabbit antibodies to CP60 and to amino acids 385-508 of CP190 have been previously described (Kellogg et al., 1995, Oegema et al., 1995). The rabbit antibody to amino acids 705-789 of CP190 was prepared according to Oegema et al. (1995). One of the rabbit anti-γ–tubulin antibodies used was raised against a full length *Drosophila* γ–tubulin (Zheng,Y., Oakley, C.E., and Oakley,B.R., unpublished experiments) expressed in baculovirus. The second anti γ–tubulin antibody used was raised to the to the C-terminal peptide QIDYPQWSPAVEASKAG of this *Drosophila* γ–tubulin. The production and

purification of both of these antibodies will be described elsewhere (Zheng,Y. and Alberts, B.M., unpublished experiments).

Embryo Fixation and Immunofluorescence

Embryos were fixed in 37% formaldehyde as described (Theurkauf, 1992). Vitelline membranes were removed with methanol. The antibodies used were rabbit anti-CP190 (amino acids 385-508), rabbit anti-CP60 and rabbit anti-γ–tubulin C-terminal peptide. The anti-γ–tubulin antibody was directly labeled with N-hydroxy succinimidyl Cy-5 (Amersham, Arlington Heights, IL) and the anti-CP190 and anti-CP60 antibodies were directly labeled with N-hydroxy succinimidyl fluorescein (Molecular probes, Eugene, OR). Briefly, antibodies at 0.65 mg/ml were buffer exchanged into 0.1 M $NaCO_3$, pH 9.3 before mixing with 1/100 volume of 8.3 mM dye dissolved in DMSO. Antibodies were labeled at 22°C for 30 min before adding 1/10 volume of 2M Potassium glutamate, pH 8.0 to stop the reaction. Antibodies were desalted into PBS, 10% glycerol, 0.02% Sodium azide for storage. Confocal microscopy was performed using a Nikon Optiphot fluorescence microscope equipped with the Bio-Rad MRC 600 laser scanning confocal attachment. All images were collected using a Nikon 60X Plan Apo lens with a numerical aperture of 1.4.

Drosophila extracts

Drosophila embryos between 0 and 4.5 hours old were harvested, dechorionated and washed extensively as previously described (Miller et al., 1989). The embryos were dried by blotting with paper towels and were resupended in 1 volume of Extract Buffer containing protease inhibitor stock (1:50) and 2 mM phenylmethylsulfonyl fluoride. The embryos were

immediately homogenized by several passes of a motor-driven teflon dounce homogenizer. The crude extract was centrifuged for 10 min at 30,000 rpm in a Beckman TLA 100.3 rotor (Fullerton, CA), and was then transferred to new tubes for an 8 min spin at 100,000 rpm in the same rotor. The supernatant below the lipid layer was collected, taking care to avoid the loose pellet at the bottom of the tube.

Sucrose gradient sedimentation and gel filtration chromatography

Sucrose gradients were poured as step gradients (5 X 950 ml steps) that were allowed to diffuse overnight at 4°C before use. They were formed from Gradient Buffer with the sucrose percentages (5-20% or 5-40%) and potassium chloride concentration (75 or 500 mM) indicated in each experiment. A 50-75 ml aliquot of sample was loaded onto each gradient. Gradients were spun at 4°C at 50,000 rpm in a Beckman SW 55 rotor for 4 to 14 hours, as indicated, and were fractionated from the top by hand into 16, 300 ml, fractions. Protein standards (0.5 mg/ml each) were loaded in an equivalent volume and were run in parallel over identical sucrose gradients for each experiment.

Gel filtration chromatography was carried out on a Superose-6 column in Column Buffer plus 1 mM b-mercaptoethanol and 75 mM or 500 mM KCl, as indicated. The column was calibrated with standards of known stokes radii as indicated in the legend to Fig. 2. Stokes radii of protein complexes were estimated as described in Siegel and Monty (1966).

Sucrose gradient quantitation

Standards were TCA precipitated, electrophoresed on 8.5% or 11% polyacrylamide gels and stained with Coomassie blue. Gels were scanned into the computer using a UMAX scanner; NIH image was used to quantitate

Coomassie band intensities. Peak fraction number was assigned for each standard using Kaleidograph (Synergy Software, Reading, PA). Standard curves of peak fraction vs. sedimentation coefficient were then used to convert fraction number to S value (essentially $S_{20,w}$) for each sucrose gradient to allow direct comparison of protein complexes sedimented in 75 mM and 500 mM KCl. This use of standards to correct to $S_{20,w}$ from different buffers is valid as long as the partial specific volumes are the same for the the standard proteins and the protein complexes being studied (Martin and Ames, 1961).

Quantitative Western Blotting

For immunoblots, samples were precipitated by addition of trichloroacetic acid to 10% and resuspended in sample buffer before separation on 11% SDS-containing polyacrylamide gels. Proteins were then transferred to nitrocellulose (pore size 0.1 mm) in the presence of 25% methanol, 0.15 M glycine, 0.02% SDS. The blots were incubated for 20 min in Block (TBS containing 0.1% Tween-20, 3% nonfat dry milk and 10% glycerol). A chemiluminescent substrate system was used to detect the horseradish peroxidase-conjugated secondary antibodies. Developed film was scanned into the computer using a UMAX scanner and NIH image was used to quantitate band intensities. Serial dilutions of CP190, CP60 and γ–tubulin were blotted simultaneously with all experimental fractions, allowing us to determine the relative concentrations of CP190, CP60 and γ–tubulin in each fraction.

Immunoprecipitations

For each immunoprecipitation, 20 mgs of antibody was first coupled to 50 ml of packed Affiprep protein A beads (Bio-Rad, Hercules, CA). The beads were then mixed with antibody in PBST for 30 min at 22°C and were washed 3X with PBST before washing and resuspension in 0.2M Na Borate, pH 9.0. To couple the antibody to the beads, dimethyl pimelimidate was added to 20 mM and the beads were mixed at 22°C for 1 hour . To inactivate residual crosslinker, the beads were washed into 0.2 M ethanolamine, pH 8.0 and mixed at 22°C for two hours before use.

Beads were then pre-eluted 3 times with 500 ml of 100 mM Glycine, pH 2.3, before washing into Extract Buffer. 50 ml of packed beads were mixed with 300 ml of concentrated *Drosophila* embryo extract for 1 hour at 4°C. The beads were spun down and the supernatants sampled. The beads were washed 4 times with 500 ml Column Buffer plus 75 mM KCl, 0.05% NP-40 and protease inhibitor stock (1:200) and then once with the same buffer without NP-40. Proteins were eluted 3 times sequentially with 150 ul of 100 mM glycine, pH 2.3. The elutions were pooled and neutralized by addition of 200 ml of 0.5M HEPES, pH 7.6. For gel analysis, 20 mgs of porcine insulin was added as carrier and the samples were TCA precipitated.

Immunoprecipitations to test the salt sensitivity of the CP60/CP190 interaction were done without coupling the antibody to the beads. For each immunoprecipitation 10 mgs of antibody was bound to 25 mls of packed Affiprep protein A beads. The beads were then mixed for 1 hour at 4°C with 300 ml of extract + 142 ml of a mixture of extract buffer and extract buffer containing 2M KCl sufficient to bring the KCl concentration to the appropriate level. For gel analysis of the immunoprecipiated proteins, the beads were washed as described above and boiled in 60 mls of sample buffer.

Expression and purification of bacterially expressed fusion proteins

The expression and purification and of the 6XHis CP190 and CP60 fusion proteins was perfomed as described previously (Oegema et al., 1995). Fusion protein concentrations were determined from their OD_{280} using extinction coefficients calculated from the amino acid sequence (Gill and von Hippel, 1989).

Analytical ultracentrifugation

Analytical ultracentrifugation was performed in a Beckman XL-A analytical ultracentrifuge equipped with scanning absorption optics. All experiments were carried out at 4°C in Column Buffer containing 500 mM KCl to match the conditions used in the extract experiments. The equilibrium distributions of OD_{280} vs. radius were fit assuming a single ideal species model using the Beckman Optima software. Sedimentation velocity boundaries were analyzed according to the method of Van Holde and Weischet (1978) using XL-A UltraScan-Origin software (Borries Demeler, San Antonio, TX). Partial specific volumes used in the determination of molecular weight were calculated from amino acid sequence, and axial ratios of the equivalent prolate ellipsoids of revolution, $[a/b]_p$, were estimated according to Laue et al. (1992) using the method of Kuntz (1971) to estimate the degree of hydration from amino acid sequence.

Results

In *Drosophila*, CP190, CP60 and γ–tubulin are three characterized components of pericentriolar material that remain at centrosomes when

microtubules are depolymerized. How do these three proteins associate with themselves and with other proteins inside the cell? To address this question, we have determined the size and shape of the complexes containing these three centrosomal proteins in concentrated *Drosophila* embryo extracts. For CP190 and CP60, we have been able to compare the behaviour of native proteins in extracts to that of bacterially expressed fusion proteins that are able to mimic the localization patterns of the native proteins when fluorescently labeled and injected into *Drosophila* embyros (Oegema et al., submitted for publication).

CP190 and CP60 co-localize with γ–tubulin at centrosomes during part of the cell cycle in *Drosophila* embryos

To begin our analysis of the relationship between CP190, CP60 and γ–tubulin, we compared their localizations at centrosomes during the cell cycle. Figure 1 shows the result of double label immunofluorescence staining for γ–tubulin and either CP60 (Fig. 1A) or CP190 (Fig. 1B) in early *Drosophila* embryos. In syncytial *Drosophila* embryos during the surface divisions, nuclear cycles 10-14, γ–tubulin is found at centrosomes throughout the cell cycle. In mitosis, we also saw faint spindle staining that was most apparent at anaphase and weak staining of the midbody during telophase (see the γ–tubulin staining in Fig. 1A in the anaphase and telophase panels). This staining pattern is similar to that observed in other organisms (Julian et al., 1993, Lajoie-Mazenc et al., 1994, Shu et al., 1995).

The centrosomal localizations of CP190 and CP60 are more dynamic during the cell cycle than that of γ–tubulin. As has been previously described, both CP190 (Frasch et al., 1986, Whitfield et al., 1995) and CP60 (Kellogg et al., 1995, Oegema et al., submitted for publication) localize to both centrosomes

and nuclei, being primarily centrosomal during mitosis and primarily nuclear during interphase. CP190 is most prominent at centrosomes in metaphase (Fig. 1B) but persists at centrosomes at low levels into early interphase. Although there is some CP60 at centrosomes during interphase and metaphase, CP60 is most prominent at centrosomes during anaphase and telophase (see Fig. 1A). Our results show that, although CP190, CP60 and γ–tubulin do not have identical staining patterns, they do co-localize to centrosomes during part of the cell cycle in *Drosophila* embryos.

In embyro extracts, γ–tubulin is found in two distinct complexes, neither of which contain CP190 or CP60

Because γ–tubulin, CP190 and CP60 co-localize at centrosomes during part of the cell cycle and there was also previous evidence for a cytoplasmic complex containing CP190, CP60 and γ–tubulin (Raff et al., 1993), we decided to characterize complexes containing these proteins in concentrated *Drosophila* embryo extracts. To this end, concentrated embryo extracts were fractionated by both Superose-6 gel filtration chromatography and by sucrose gradient sedimentation. The same extract was simultaneously characterized by both techniques in identical buffers containing 75 or 500 mM KCl. The results of western blotting to detect CP190, CP60 and γ–tubulin after these fractionation steps are shown in Figure 2.

To facilitate the comparison between complexes containing γ–tubulin and those containing CP190 and CP60, we used a quantitative blotting technique that allowed us to determine the relative concentrations of CP190, CP60 and γ–tubulin in each fraction. Because sucrose gradients run in different salt concentrations cannot be directly compared due to differences in buffer density and viscosity that affect sedimentation rates, standard curves of

peak fraction vs. S value, generated by loading proteins of known S value over identical sucrose gradients in parallel with each experimental gradient, were used to convert fraction number to S value for each sucrose gradient. The quantitative analysis of the sucrose gradient and gel filtration data shown in Figure 2 is presented in Figure 3.

In buffer containing 75 mM KCl, most of the γ–tubulin is found in two complexes that can be separated by both sucrose gradient sedimentation and by gel filtration (see Fig. 3A and B, left panels, small dashed line corresponds to γ–tubulin). The large γ–tubulin complex, having both a greater hydrodynamic radius and a greater sedimentation coefficient, is converted to the small γ–tubulin containing complex by raising the KCl concentration (In Fig. 3A and B, compare the γ–tubulin profiles in the left panels (75mM KCl) to those in the right panels (500 mM KCl)). In addition, the gel filtration peak corresponding to the small γ–tubulin complex, which appears heterogeneous in 75 mM KCl, becomes much more homogeneous in 500 mM KCl. These results suggest that the small γ–tubulin complex is a subunit of the large γ–tubulin complex.

The sedimentation coefficients of the large and small γ–tubulin complexes are 36.9 S and 8.5 S, respectively. (The sedimentation coefficient of the large γ–tubulin complex was determined on a separate sucrose gradient using 30S ribosome particle as a standard in addition to the standards mentioned in the legend to Fig. 2 (data not shown)). The Stokes radii of the small and large γ–tubulin complexes, estimated from our gel filtration results, are 6.9 nm and about 20 nm, respectively (the large γ–tubulin complex fractionates close to the void volume of the Superose-6 column preventing a more precise determination). We can estimate the mass of the large and small γ–tubulin complexes from their sedimentation coefficients and Stokes

radii using the method of Siegel and Monty (1966). The estimated masses are 240,000 and about 3,000,000 Daltons for the small and large complexes respectively.

On sucrose gradients, CP60 co-migrates with the small γ–tubulin complex in both high and low salt (Compare CP60, solid line, with γ–tubulin, small dashed line in Fig. 3A). However, under the same buffer conditions, CP60 can be easily separated from the small γ–tubulin complex by gel filtration (compare the location of the CP60 peak with that of the small γ–tubulin complex in Fig. 3B). By gel filtration in 75 mM KCl (see Fig. 3B, left panel), CP60 elutes with the large γ–tubulin complex; but under identical conditions, CP60 and the γ–tubulin large complex are easily separated on sucrose gradients (see Fig. 3A, left panel). Similarly, CP190 can be separated from the small γ–tubulin complex by gel filtration (See Fig. 3B comparing γ–tubulin, small dashed line, to CP190, large dashed line) and from the γ–tubulin large complex on sucrose gradients (see Fig. 3A, left panel). These experiments suggest that neither CP60 nor CP190 are among the components of either the large or small γ–tubulin containing complexes.

γ–tubulin does not co-immunoprecipitate with either CP190 or CP60

To look for more subtle interactions between γ–tubulin and CP190 and CP60, antibodies were used to immunoprecipitate CP60, CP190 and γ–tubulin from concentrated embryo extracts. Since *Drosophila* γ–tubulin is exactly the same size as IgG heavy chain, special care was taken to remove contaminating IgG from the immunoprecipitation pellets (see Materials and Methods). Figure 4A shows an analysis of the immunprecipitation pellets by SDS polyacrylamide gel electrophoreses after staining with Coomassie blue. Antibodies to γ–tubulin immunoprecipitate γ–tubulin and a group of

associated proteins that are components of the *Drosophila* gTuRC (see Fig. 4A, last two lanes; Zheng,Y. and Alberts, B.M., unpublished experiments). Two antibodies to CP190 were used in immunoprecipitations, both bring down CP190 and a large fraction of the CP60 found in extracts. Antibodies to CP60 immunoprecipitate CP60 and a small fraction of the CP190 found in extracts.

Western blots of the supernatants and pellets from the immunoprecipiations were performed to confirm the identity of the Coomassie stained bands. Figure 4B shows the immunoprecipiation supernatants analyzed for CP190, CP60 and γ–tubulin. As expected, CP60 is depleted by the anti CP60 antibody, γ–tubulin is depleted by the anti-γ–tubulin C-terminal peptide antibody and CP190 is depleted by both of the antibodies to CP190. In addition, CP60 is largely depleted in the supernatants of extracts immunoprecipited with the anti-CP190 antibodies.

Pellets from immunprecipitations performed from concentrated extract (+) or from buffer controls (-) are shown in Fig. 4C. We could detect no CP190 or CP60 in the pellets from immunoprecipitations performed with the antibodies to γ–tubulin, nor was any γ–tubulin present in the pellets of immunprecipiations performed with antibodies to CP190 or CP60. The majority of the CP60 in extracts co-immunoprecipitates with CP190, however, and a small fraction of the CP190 co-immunoprecipitates with CP60. Two explanations consistent with these results are: (1) the majority of CP60 in extracts is associated with a small fraction of the extract CP190 or (2) although the majority of CP190 and CP60 are complexed in extracts, the anti-CP60 antibody interferes with the co-immunoprecipitation of CP190.

We tested the salt sensitivity of the interaction between CP190 and CP60 by doing immunoprecipitations with anti CP190 (amino acids 385-508)

after addition of a small amount of buffer or buffer containing additional KCl to the extracts (see Fig. 4D). Although robust co-imunoprecipitation was seen from extracts containing 75 mM KCl, only a small amount of CP60 co-immunoprecipitated when the salt concentration of the extract was raised to 150 mM KCl and no co-immunoprecipitation was seen at 300 mM KCl, suggesting that the interaction between CP190 and CP60 is salt sensitive.

These results clearly show that, although CP60 and CP190 associate in these extracts, neither CP190 nor CP60 are in a cytoplasmic complex with γ-tubulin.

CP60 and CP190 interact in concentrated embryo extracts

Knowing that CP190 and CP60 co-immunoprecipitate from concentrated *Drosophila* embryo extracts, we wanted to further characterize the interaction between these two proteins. Gel filtration was not useful here because both proteins on their own have such large hydrodynamic radii. Sucrose gradient sedimentation was therefore used to test for complexes containing CP60 and CP190. Since the interaction is salt sensitive, all analysis was done under low salt conditions (75 mM KCl).

We know that most of the CP190 population does not co-migrate with CP60 on sucrose gradients, even in low salt (see Fig. 3A, left panel). Therefore, a more sensitive test was tried: we immunodepleted extracts of CP190 or CP60 and then examined both the original and the depleted extracts to determine whether the S value of CP60 is affected by the presence of CP190, and vice versa. The CP190 was immunodepleted with either anti-CP190 amino acids 385-508 or with anti-CP190 amino acids 705-789. The latter antibody interferes with the interaction between CP190 and CP60 and therefore removes all of the CP190 while leaving the much of the CP60

behind (see legend to Fig. 5). Extracts were also immunoprecipitated with anti-CP60 (which removes CP60 and a small fraction of the CP190) and with a random IgG as a control. Figure 5C is a western blot that confirms these depletion results. The sedimentation analyses for each immunodepleted extract, compared to mock-treated control, are shown in Figure 5A and B. The corresponding quantitation of these western blots is shown in Figure 6A and B.

Depletion of CP190 results in a dramatic decrease in the CP60 sedimentation rate (see Figures 5B and 6B), demonstrating that when the complete (mock-treated) extract is sedimented, most of the CP60 spends at least part of the time associated with CP190 in a faster sedimenting complex. The CP60 distribution shifts in a similar fashion independent of the anti-CP190 antibody used, revealing that the CP60 displaced from the CP60/CP190 complex behaves identically to the non-complexed CP60 in extracts. (Note that the CP60 in the CP190-depleted extracts also has an S value similar to that of CP60 in 500 mM KCl).

The CP190 distribution shifts slightly to lower S values when CP60 is immunodepleted (see Figures 5A and 6A). However, the modest nature of this shift makes it impossible to determine whether the if entire population is shifting a small distance, or if a small part of the rapidly sedimenting population is instead shifting to a much smaller S value. However, one possibility, consistent with our immunoprecipitation results, is that the majority of the CP60 is tightly complexed with only a small fraction of the CP190 in extracts. As expected, the sedimentation of γ–tubulin is not affected by the depletion of either CP190 or CP60 (data not shown).

Both bacterially expressed and native CP60 form large asymmetric oligomers

We have also used sucrose gradient sedimentation and Superose-6 gel filtration to characterize two highly purified bacterially expressed 6XHis fusion proteins: full length CP60 and CP190 containing amino acids 167-1090 (the C-terminal 85% of the protein). These fusion proteins, when fluorescently labeled and injected into *Drosophila* embryos, localize in a manner identical to that of the native proteins (Oegema et al., submitted for publication). The N-terminal 166 amino acids of CP190 had to be omitted because they make the bacterially expressed fusion protein insoluble.

The results for CP60 are shown in Figure 7A and B. In 500 mM KCl, bacterially expressed 6XHis CP60 has a sedimentation coeffcient indistinguishable from that of the native protein in extracts (8.7 S compared to 8.9 S). The bacterially expressed and native CP60 also behave identically by gel filtration in 500 mM KCl (Figs. 7B and 3B), yielding Stokes radii of 146 and 149 angstoms, respectively.

These values are much larger than would be expected for monomeric CP60 and suggest that both bacterially expressed and native CP60 form identical large oligomers. Using the method of Siegel and Monty (1966), we obtain a molecular weight estimate of 523,000 daltons (10X the monomer molecular weight of 52,000) for the bacterially expressed protein and 546,000 for native CP60 in extracts (both in 500 mM KCl; see Tables I and II). The predicted molecular weight for the bacterially expressed protein in 75 mM KCl is 485,000 (Table II).

To test for heterogeneity in the oligomerization state of CP60, we analyzed sedimentation velocity data using the method of Van Holde and Weischet (1978) (Fig. 8A and B), finding that the bacterially expressed CP60 behaves as a single species with an S value of 8.7 S. We estimate $[a/b]_p$, the

axial ratio of the prolate ellipsoid of revolution, for CP60 oligomer to be 25, suggesting that CP60 forms a very asymmetric oligomer.

Native CP190 is also a asymmetric oligomer in extracts

A similar analysis was performed on bacterially expressed CP190. 6XHis CP190 (amino acids 167-1090) has a sedimentation coefficient of 3.3S and a predicted Stokes radius of 98 angstroms in 500 mM KCl (see Fig. 7C and D and Table II); this compares with values of 5.7 S and 146 angstoms for the native protein in extracts (Table I). Therefore, in contrast to bacterially expressed CP60, bacterially expressed 6XHis CP190 (amino acids 167-1090) does not behave like native CP190 in extracts.

Sedimentation equilbrium analysis was performed on CP190 under the same buffer and temperature conditions used in the extract experiments. For CP190 (amino acids 167-1090) we obtained a molecular weight of 105,000 +/- 10,000 Daltons (see Fig. 8C). Since the molecular weight of this fusion protein predicted from its amino acid sequence is 104,000 Daltons, the bacterially expressed CP190 fusion protein is monomeric. Its axial ratio, $[a/b]_p$, is 18 suggesting that it is also asymmetric.

The method of Sigel and Monty predicts a molecular weight of 343,000 for native CP190 in extracts in 500 mM KCl versus 129,000 for the bacterially expressed fusion protein. The difference in their molecular weights predicted from amino acid sequence is much smaller (104,000 for the bacterially expressed and 122,000 for native CP190). These results suggest that native CP190 is oligomeric. Because 343,000 is 2.8X the predicted monomeric molecular weight of CP190, CP190 could form a trimer in extracts. However, because of the tendency of this method to overestimate the molecular weight

of asymmetric molecules (Potschka, 1987), we suspect that CP190 is more likely dimeric.

CP190 and CP60 are present in approximately a 1:1 molar ratio in extracts

We have also used the bacterially expressed 6XHis fusion proteins as standards to determine the concentration of native CP190 and CP60 present in extracts. Known concentrations of the 6XHis fusion proteins were serially diluted in extract and quantitative Elisas were performed to determine the concentration of fusion protein required to double the amount of each protein present in the extract. We estimate that our extracts contain 8.2 E-8 M CP60 and 7.2 E-8 M CP190, corresponding to 8.8 ugs/ml and 3.9 ug/ml, respectively. The protein concentration of the extract determined by Bradford assay relative to bovine g globulin is 69 mg/ml, so CP190 and CP60 are present at approximately .013% and .0057% of total extract protein, respectively. We expect that the molar ratio of the two proteins is similar in embryos since 100% of the CP190 and about 80% of the CP60 present in the embryos is solublized by our extract conditions.

Discussion

In order to understand the centrosome and its dynamics at a molecular level, we began a characterization of protein complexes containing CP190, CP60 and γ–tubulin in concentrated *Drosophila* embryo extracts. *Drosophila* embryos are an especially good system for the biochemical characterization of centrosomal components because the proteins required for the extensive centrosome duplication that occurs during the early rapid embryo divisions are maternally deposited and are therefore both abundant and soluble.

To characterize cytoplasmic complexes containing CP190, CP60 and γ–tubulin in *Drosophila* embryos, we fractionated concentrated embryo extracts by gel filtration and sucrose gradient sedimentation. We found that in low salt, most of the γ–tubulin is found in two complexes, one large and one small, that can be separated by either sucrose gradients or by gel filtration. Furthermore, the large γ–tubulin containing complex can be converted into the smaller complex by raising the KCl concentration to 500 mM, suggesting that the small γ–tubulin complex is a subunit of the larger complex. We estimate the molecular masses of the small and large γ–tubulin complexes from their sedimentation coefficients and Stokes radii to be 240,000 and about 3,000,000 Daltons, respectively (see Table I).

The large γ–tubulin complex seen in these extracts has been purified to near homogeneity and is the *Drosophila* homolog of the γ–tubulin ring complex (gTuRC) isolated from *Xenopus* egg extracts (Zheng,Y. and Alberts, B.M., unpublished experiments). Purification of the small γ–tubulin complex indicates that the small γ–tubulin complex contains γ–tubulin and two other proteins that are also components of the large complex. Since the molecular weights of these three proteins estimated from SDS polyacrylamide gels total 240,000 (Zheng,Y. and Alberts, B.M., unpublished experiments) we conclude that each small complex contains one γ–tubulin molecule. Our predicted

molecular weight for the large γ–tubulin complex is about 13 times the molecular weight of the small γ–tubulin containing complex suggesting that the gTuRC could be in large part comprised of 13 small γ–tubulin containing complex subunits, perhaps one to nucleate each of the 13 microtubule protofilaments.

CP60 and CP190 can be separated from the small γ–tubulin complex by gel filtration and from the large γ–tubulin complex on sucrose gradients, demonstrating that neither CP60 nor CP190 are components of either the large or small γ–tubulin containing complexes. We also failed to detect any association between CP190 or CP60 and γ–tubulin in immunoprecipitations done under low salt conditions. How can we reconcile our data with previous results favoring a cytoplasmic complex containing CP190, CP60 and γ–tubulin? The previous evidence for such a complex was two-fold (Raff et al., 1993). First, CP60 and γ–tubulin, eluted from microtubule affinity columns in high salt (500 mM KCl), were shown to co-migrate at approximately 8S on sucrose gradients. This result is consistent with our data, we see CP60 co-migrating with the γ–tubulin small complex on sucrose gradients in 500 mM KCl (see Fig. 3C). However, under the same buffer conditions, CP60 can easily be separated from the γ–tubulin small complex by gel filtration (see Fig. 3B, right panel), demonstrating that the similarity in the sedimentation coefficients of CP60 and the γ–tubulin small complex is merely fortuitous and that CP60 is not a actually a component of the γ–tubulin small complex.

The other piece of evidence supporting an association between CP190, CP60 and γ–tubulin is the fact that γ–tubulin was detected by western blotting in elutions from immunoaffinity columns constructed from antibodies to both CP190 and CP60 (Raff et al., 1993). γ–tubulin was a very minor

component of these elutions, however, as the authors were never able to detect a band corresponding to γ–tubulin on Coomassie stained gels (Raff et al., 1993).

In order to determine the oligomerization state of CP60 and CP190, we compared the physical properties of bacterially expressed 6XHis CP60 and CP190 fusion proteins to those of the native proteins in extracts in 500 mM KCl, conditions that we believe allow us to measure the properties of the native proteins in extracts uncomplexed with other molecules. The 6XHis fusion proteins used are able to replicate the localization patterns of native CP190 and CP60 when fluorescently labeled and injected into Drosophila embryos (Oegema et al., submitted for publication). We found that bacterially expressed 6XHis CP60 has the same sedimentation coefficient and Stokes radius as native CP60 in extracts in 500 mM KCl (see Tables I and II), suggesting that native CP60, like the bacterially expressed fusion protein, is forming large oligomers. The molecular weight of the CP60 oligomer is predicted to be about 523,000 Daltons, or about 10X the monomer molecular weight. If we assume that the CP60 oligomer is a prolate ellipsoid, the axial ratio of CP60 predicted from data is 25, consistent with an asymmetric oligomer.

Unlike 6XHis CP60, 6XHis CP190 (amino acids 167-1090) is monomeric. Its molecular weight determined by sedimentation equilibrium analysis is 105,000 +/- 10,000, very close to the molecular weight of 104,000 predicted from its sequence. The molecular weight of the 6XHis CP190 fusion protein estimated using the method of Siegel and Monty (1966) is 129,000 (See Table II), about 1.25 times the monomer molecular weight. The overestimate of the molecular weight using this method is likely due to the asymmetric nature of the CP190 fusion protein which can result in an overestimate of the Stokes

radius by gel filtration (Potschka, 1987). Consistent with this, the axial ratio predicted for 6XHis CP190 (amino acids 167-1090), assuming a prolate model, is 18. Native CP190 in extracts in 500 mM KCl is much larger than the bacterially expressed fusion protein. The method of Siegel and Monty (1966) predicts a molecular weight of 343,000 (2.8X the predicted molecular weight of 122,000) implying that CP190 could be trimeric in extracts. Due to the tendency of this method to overestimate the molecular weight of asymmetric molecules however, we think it is more likely to be dimeric in extracts. If we assume that native CP190 is dimeric (i.e.- molecular weight= 244,000), then we can estimate an axial ratio for the native protein of 19 suggesting that native CP190, like the bacterially expressed fusion protein, is asymmetric. The N-terminal 15% (amino acids 1-167) of CP190, which is not present in the bacterially expressed fusion protein because it makes the fusion protein insoluble, probably contains sequences essential for the oligomerization of CP190.

Since the association between CP190 and CP60 is salt sensitive, we did experiments under low salt conditions to characterize the interaction between native CP190 and CP60 in extracts. In immunoprecipitations from concentrated extracts in 75 mM KCl, the majority of CP60 co-immunoprecipitates with CP190, but only a small amount of CP190 co-immunoprecipitates with CP60. This experiment suggests that the majority of CP60 in extracts is associated with CP190. However, the majority of the CP60 and CP190 populations are separated by fractionation of the extract on sucrose gradients. To determine if CP190 and CP60 interact in extracts, we fractionated extracts that had been immunodepleted for CP190 or CP60 on sucrose gradients to determine how the sedimentation of each protein depends on the presence of the other. We found that, in the absence of

CP190, CP60 shifts dramatically to a smaller S value peaking at nearly the same S value as the CP60 oligomer alone. This was true even when CP190 was immunoprecipitated with an antibody that immunoprecipitates CP190 while leaving much of the CP60 in the extract. This result demonstrates that the majority of CP60 does interact with CP190 during sucrose gradient sedimentation.

Depletion of CP60 also results in a shift in the CP190 sedimentation rate, demonstrating that CP190 does interact with CP60 in extracts. However, the nature of the CP190 shift prevents us from determining if the entire CP190 population is shifting a relatively small distance or if a small part of the rapidly sedimenting population is shifted to much smaller S values. Two models remain consistent with our data. The first possibility is that the majority of the CP60 is associated with a small fraction of the CP190 in extracts. A second possibility is that CP190 and CP60 are weakly associated and are therefore able to affect each other's sedimentation rates without being tightly complexed. It is interesting that in 75 mM KCl, CP190 remains heterogeneous in extracts depleted of CP60, suggesting that CP190 can form multiple complexes even in the absence of CP60, associating either with itself or with other molecules. The fact that CP190 contains four predicted zinc fingers in the middle of its coding region raises the possibility that CP190 could complex with nucleic acids.

Our results suggest that CP190 and CP60 are either weakly associated in extracts or that the CP60 in extracts is associated with only a small fraction of the CP190. These results are consistent with the complex temporal and spatial localizations of CP190 and CP60 that have been observed in embryos. Work in live and fixed embryos has demonstrated that CP190 and CP60 localize to nuclei and to centrosomes asynchronously in the early *Drosophila*

embryo (Oegema et al., submitted for publication). CP190 is prominently at centrosomes between nuclear envelope breakdown at prophase and telophase. In contrast, CP60 is found at centrosomes primarily between anaphase and early interphase. CP190 is nuclear between telophase and the following prophase; CP60 follows CP190 into nuclei between middle to late interphase and remains there until the following metaphase. CP190 and CP60 both localize to fibrous networks within the nucleus in the early embryo, but do not appear to co-localize with each other or with DNA (Oegema et al., submitted for publication). These temporal and spatial differences in the localizations of CP190 and CP60 are inconsistent with the existence of a tight single complex containing both proteins at all times during the cell cycle.

The dynamic asynchronous localization patterns of CP190 and CP60 are probably the result of cell cycle specific regulation. CP60 contains 6 consensus cdc2 phosphorylation sites and is phosphorylated in vivo (Kellogg et al., 1995). In most of our extract experiments, CP60 was in a lower phosphorylated form, but in some extracts, we could see some more highly phosphorylated form of CP60 that would migrate on gel filtration with an apparently smaller Stokes radius. We were unable to control the phosphorylation state of CP60 in our extracts, making it difficult to pursue this interesting avenue. Phosphorylation could regulate the oligomerization state of CP60 and/or its association with CP190. Solid correlations between cell cycle state and the existence of CP190 and CP60 containing protein assemblies at various locations within the cell await more detailed studies in a system with potential for control of cell cycle state, such as Xenopus egg extracts.

Acknowledgments

K. Oegema thanks Jack Barry for many helpful discussions and for protein purification assistance and advice. In addition, Michelle Moritz, Doug Kellogg and Arshad Desai made helpful comments and critically read the manuscript. This work was supported by a grant from The National Institutes of Health to B. Alberts (GM23928).

References

Boleti, H., Karsenti, E., and Vernos, I. (1996). Xklp2, a novel Xenopus centrosomal kinesin-like protein required for centrosome separation during mitosis. Cell.*84,* 49-59.

Doxsey, S. J., Stein, P., Evans, L., Calarco, P. D., and Kirschner, M. (1994). Pericentrin, a highly conserved centrosome protein involved in microtubule organization . Cell.*76,* 639-50.

Evans, L., Mitchison, T., and Kirschner, M. (1985). Influence of the centrosome on the structure of nucleated microtubules. J Cell Biol.*100,* 1185-91.

Frasch, M., Glover, D. M., and Saumweber, H. (1986). Nuclear antigens follow different pathways into daughter nuclei during mitosis in early Drosophila embryos. J Cell Sci.*82,* 155-72.

Gill, S., and von Hippel, P. (1989). Calculation of protein extinction coefficients from amino acid sequence data. Anal. Biochem.*182,* 319-326.

Joshi, H. C., Palacios, M. J., McNamara, L., and Cleveland, D. W. (1992). Gamma-tubulin is a centrosomal protein required for cell cycle-dependent microtubule nucleation. Nature.*356,* 80-3.

Julian, M., Tollon, Y., Lajoie-Mazenc, I., Moisand, A., Mazarguil, H., Puget, A., and Wright, M. (1993). gamma-Tubulin participates in the formation of the midbody during cytokinesis in mammalian cells. J Cell Sci.*105,* 145-56.

Kellogg, D. R., and Alberts, B. M. (1992). Purification of a multiprotein complex containing centrosomal proteins from the Drosophila embryo by chromatography with low-affinity polyclonal antibodies. Mol Biol Cell.*3*, 1-11.

Kellogg, D. R., Field, C. M., and Alberts, B. M. (1989). Identification of microtubule-associated proteins in the centrosome, spindle, and kinetochore of the early Drosophila embryo. J Cell Biol.*109*, 2977-91.

Kellogg, D. R., Moritz, M., and Alberts, B. M. (1994). The centrosome and cellular organization. Annu Rev Biochem.*63*, 639-74.

Kellogg, D. R., Oegema, K., Raff, J., Schneider, K., and Alberts, B. M. (1995). CP60: a microtubule-associated protein that is localized to the centrosome in a cell cycle-specific manner. Mol Biol Cell.*6*, 1673-84.

Keryer, G., Ris, H., and Borisy, G. G. (1984). Centriole distribution during tripolar mitosis in Chinese hamster ovary cells. J Cell Biol.*98*, 2222-9.

Kuntz, I. D. (1971). Hydration of macromolecules. IV. Polypeptide conformation in frozen solutions. J Am Chem Soc.*93*, 516-8.

Kuriyama, R., and Borisy, G. G. (1981). Microtubule-nucleating activity of centrosomes in Chinese hamster ovary cells is independent of the centriole cycle but coupled to the mitotic cycle. J Cell Biol.*91*, 822-6.

Lajoie-Mazenc, I., Tollon, Y., Detraves, C., Julian, M., Moisand, A., Gueth-Hallonet, C., Debec, A., Salles-Passador, I., Puget, A. and Mazarguil, H. (1994).

Recruitment of antigenic gamma-tubulin during mitosis in animal cells: presence of gamma-tubulin in the mitotic spindle. J Cell Sci.*107*, 2825-37.

Laue, T., Shah, B., Ridgeway, T., and Pelletier, S. (1992). Computer-Aided Interpretation of Analytical Sedimentation Data for Proteins. In: Analytical Ultracentrifugation in Biochemistry and Polymer Science, ed. S. Harding, A. Rowe, and J. Horton, Cambridge: The Royal Society of Chemistry, 90-125.

Martin, R., and Ames, B. (1961). A Method for Determining the Sedimentation Behaviour of Enzymes: Application to Protein Mixtures. J Biol Chem.*236*, 1372-1379.

Mazia, D. (1987). The chromosome cycle and the centrosome cycle in the mitotic cycle. Int Rev Cytol.*100*, 49-92.

Miller, K. G., Field, C. M., and Alberts, B. M. (1989). Actin-binding proteins from Drosophila embryos: a complex network of interacting proteins detected by F-actin affinity chromatography. J Cell Biol.*109*, 2963-75.

Moritz, M., Braunfeld, M. B., Sedat, J. W., Alberts, B., and Agard, D. A. (1995). Microtubule nucleation by gamma-tubulin-containing rings in the centrosome. Nature.*378*, 638-40.

Oakley, B. R., Oakley, C. E., Yoon, Y., and Jung, M. K. (1990). Gamma-tubulin is a component of the spindle pole body that is essential for microtubule function in Aspergillus nidulans. Cell.*61*, 1289-301.

Oegema, K., Whitfield, W. G., and Alberts, B. (1995). The cell cycle-dependent localization of the CP190 centrosomal protein is determined by the coordinate action of two separable domains. J Cell Biol.*131*, 1261-73.

Potschka, M. (1987). Universal Calibration of Gel Permeation Chromatography and Determination of Molecular Shape in Solution. Analytical Biochemistry.*162*, 47-64.

Raff, J. W., Kellogg, D. R., and Alberts, B. M. (1993). Drosophila gamma-tubulin is part of a complex containing two previously identified centrosomal MAPs. J Cell Biol.*121*, 823-35.

Rieder, C., and Borisy, G. (1982). The Centrosome Cycle in PtK2 Cells: Asymmetric Distribution and Structural Changes in the Pericentriolar Material. Biology of the Cell.*44*, 117-132.

Schatten, G. (1994). The centrosome and its mode of inheritance: the reduction of the centrosome during gametogenesis and its restoration during fertilization. Dev Biol.*165*, 299-335.

Shu, H. B., Li, Z., Palacios, M. J., Li, Q., and Joshi, H. C. (1995). A transient association of gamma-tubulin at the midbody is required for the completion of cytokinesis during the mammalian cell division. J Cell Sci.*108*, 2955-62.

Siegel, L. M., and Monty, K. J. (1966). Determination of molecular weights and frictional ratios of proteins in impure systems by use of gel filtration and

density gradient centrifugation. Application to crude preparations of sulfite and hydroxylamine reductases. Biochim Biophys Acta.*112*, 346-62.

Stearns, T., Evans, L., and Kirschner, M. (1991). Gamma-tubulin is a highly conserved component of the centrosome. Cell.*65*, 825-36.

Theurkauf, W. (1992). Behaviour of structurally divergent alpha-tubulin isotypes during Drosophila embryogenesis: evidence for post-translational regulation of isotype abundance. Dev. Biol.*154*, 205-217.

Van Holde, K., and Weischet, W. (1978). Boundary Analysis of Sedimentation-Velocity Experiments with Monodisperse and Paucidisperse Solutes. Biopolymers.*17*, 1387-1403.

Vorobjev, I. A., and Chentsov Yu, S. (1982). Centrioles in the cell cycle. I. Epithelial cells. J Cell Biol.*93*, 938-49.

Vorobjev, I. A., and Nadezhdina, E. S. (1987). The centrosome and its role in the organization of microtubules. Int Rev Cytol.*106*, 227-93.

Whitfield, W. G., Chaplin, M. A., Oegema, K., Parry, H., and Glover, D. M. (1995). The 190 kDa centrosome-associated protein of Drosophila melanogaster contains four zinc finger motifs and binds to specific sites on polytene chromosomes. J Cell Sci.*108*, 3377-87.

Whitfield, W. G., Millar, S. E., Saumweber, H., Frasch, M., and Glover, D. M. (1988). Cloning of a gene encoding an antigen associated with the centrosome in Drosophila. J Cell Sci.*89*, 467-80.

Zheng, Y., Jung, M. K., and Oakley, B. R. (1991). Gamma-tubulin is present in Drosophila melanogaster and Homo sapiens and is associated with the centrosome. Cell.*65*, 817-23.

Zheng, Y., Wong, M. L., Alberts, B., and Mitchison, T. (1995). Nucleation of microtubule assembly by a γ-tubulin-containing ring complex. Nature.*378*, 578-83.

Figure legends

Figure 1: CP60 and CP190 co-localize with γ–tubulin at centrosomes during part of the cell cycle. Double label immunofluorescence of γ–tubulin and CP60 (A) or CP190 (B) in syncytial *Drosophila* embryos. Scale bars are 10mm.

Figure 2: Behavior of CP60, CP190, and γ–tubulin during sucrose gradient sedimentation and Superose-6 gel filtration of concentrated *Drosophila*

embryo extracts. Each fraction was immunoblotted for CP190, CP60 and γ–tubulin following separation on SDS-containing 11% polyacrylamide gels. A single extract was first buffer-exchanged using spin columns into Column Buffer containing either 75 or 500 mM KCl. An aliquot was then sedimented through 5-40% sucrose gradients for 4 hours (A) or fractionated by Superose-6 gel filtration chromatography (B) in buffers containing 75 or 500 mM KCl . In (C), a separate extract was sedimented on a 5-20% sucrose gradient for 8 hours in 500 mM KCl to increase the separation between the smaller complexes present in the high salt. Sucrose gradient fractions were collected from the top of the gradient; gradient pellets are also shown (P). Standards were run in parallel with the extract over identical sucrose gradients. The location of the peak for each standard is indicated with an arrowhead above its S value (see Materials and Methods for determination of peak fractions). The sucrose gradient standards used were bovine serum albumin (4.4 S), rabbit muscle aldolase (7.35 S), bovine liver catalase (11.3 S) and porcine thyroglobulin (19.4 S). The Superose-6 column was calibrated with bovine thyroglobulin (Stokes radius= 8.5 nm), horse spleen ferritin (6.1 nm), bovine liver catalase (5.22 nm), rabbit muscle aldolase (4.81 nm) and hen egg ovalbumin (30.5 nm). The location of the peak for each standard is indicated with an arrowhead above its Stokes radius in (B).

Figure 3: A graphical representation of the sucrose gradient (A) and gel filtration data (B) in Fig. 2. The γ–tubulin is present in two distinct complexes; CP190 and CP60 are not components of either complex. For each fraction, standard curves were used to determine the corresponding S value and the relative concentrations of CP190, CP60 and γ–tubulin (see Methods).

Figure 4: Tests for complex formation by immunoprecipiation. Since *Drosophila* γ–tubulin is the same size as IgG heavy chain, the immunoprecipitations in (A-C) were carried out with special care to avoid any IgG contamination in the pellets (see Methods).

(A) Immunoprecipitation pellets after separation on an 11% polyacrylamide gel and staining with Coomassie blue. Anti-CP60 immunoprecipitates CP60 and a small fraction of the CP190. Both anti-CP190 antibodies immunoprecipitate CP190 and a large percentage of the CP60. Antibodies to γ–tubulin immunoprecipitate γ–tubulin and a group of γ–tubulin associated proteins. (The anti-γ–tubulin C-terminal peptide antibody was much more effective in immunoprecipitations than the antibody made to the whole γ–tubulin molecule.)

In (B) and (C), western blots to detect CP190, CP60 and γ–tubulin in immunoprecipitation supernatants (B) and pellets (C). In (C) beads were incubated in the presence (+) or absence (-) of extract to control for antibody contamination in the pellets.

In (D) immunoprecipitations with the anti-CP190 (385-508) antibody (right lane of each pair) or random IgG as a control (left lane of each pair) were carried out from extracts to which additional KCl had been added to to determine the salt sensitivity of the interaction between CP190 and CP60. The final salt concentrations are indicated. Immunoprecipiatation pellets are shown western blotted for CP60 and CP190.

Figure 5: Sedimentation of CP60 and CP190 from immunodepleted extracts. Concentrated embryo extracts were immunodepleted with either anti CP60, anti-CP190 (amino acids 385-508), anti CP190 (amino acids 705-789) or a random IgG (mock-depleted extract). The antibody to amino acids 705-789 of

CP190 is able to disrupt the interaction between CP190 and CP60 in a time dependent manner. If immunoprecipitations are allowed to go for about 2 hours, the antibody to CP190 amino acids 705-789 is able to largely disrupt the interaction between CP190 and CP60 whereas the additional time of immunoprecipitation has no effect on immunoprecipitations done with the antibody to amino acids 385-508 (data not shown). The immunodepleted extracts used are shown in (C) immunoblotted for CP190 and CP60.

Immunodepleted extracts were analyzed by SDS polyacrylamide gel electrophoreses after sedimentation through 5-20% sucrose gradients. Fractions are shown after immunoblotting for CP190 (A) and CP60 (B).

Figure 6: Quantitation of the immunoblotting data in Figure 5; graphs corresponding to the immunoblots in Figure 5A and B are shown in (A) and (B) respectively.

Figure 7: Characterization of purified bacterially expressed fusion proteins by sucrose gradient sedimentation and gel filtration.
(A) 0.5 mg/ml of 6XHis CP60 fusion protein was co-sedimented with 0.5 mg/ml each of bovine serum albumin (4.4 S), rabbit muscle aldolase (7.35 S) and bovine liver catalase (11.3 S) through 5-20% sucrose gradients in 75 or 500 mM KCl for 8 hours. Fractions were processed as described in Materials and Methods and the resulting Coomassie intensities for 6XHis CP60 are plotted in (A) vs. S-value.
(B) 0.5 mg/ml bacterially expressed 6XHis CP60 was gel filtered on a Superose-6 column in buffers containing 75 or 500 mM KCl. The 6XHis CP60 Coomassie intensity was quantitated as above and plotted vs. fraction number.

(C) Characterization of 6XHis CP190 (amino acids 167-1090); 0.5 mg/ml bacterially expressed CP190 (amino acids 167-1090) was sedimented through 5-20% sucrose gradients in 75 or 500 mM KCl for 14 hours. Fractions were analyzed as described in (A).

(D) 0.57 mg/ml bacterially expressed CP190 (amino acids 167-1090) was gel filtered on a superose-6 column in buffers containing 75 or 500 mM KCl and was processed as described in (B).

Figure 8: Analytical ultracentrifugation of bacterially expressed 6XHis CP60 and CP190 fusion proteins. A sedimentation-velocity experiment was performed on 6XHis CP60 at a concentration of 0.7 mg/ml at 4°C in Column buffer plus 500 mM KCl to test for heterogeneity. The moving boundary was analyzed by the method of Van Holde and Weischet (1978) and the results are shown in (A) and (B) . CP60 behaves as a single species with an S value of about 8.7 S. The apparent decrease in S value with increasing concentration is expected from hydrodynamics and is particularly pronounced for asymmetric molecules (Cantor and Schimmel, 1980).

The results of a sedimentation equilibrium experiment performed on 6X His CP190 amino acids 167-1090 are shown in (C). This experiment was performed at 4°C in Column Buffer plus 500 mM KCl to match the conditions used in the extract experiments. The initial fusion protein concentration was 0.28 mg/ml. A curve fit to a single ideal species model of the equilibrium distribution of OD_{280} vs. radius is shown. We obtained a value of 105,000 +/- 10,000 Daltons which is in good agreement with the predicted monomer molecular weight of 104,000.

Figure 1
Oegema et al.

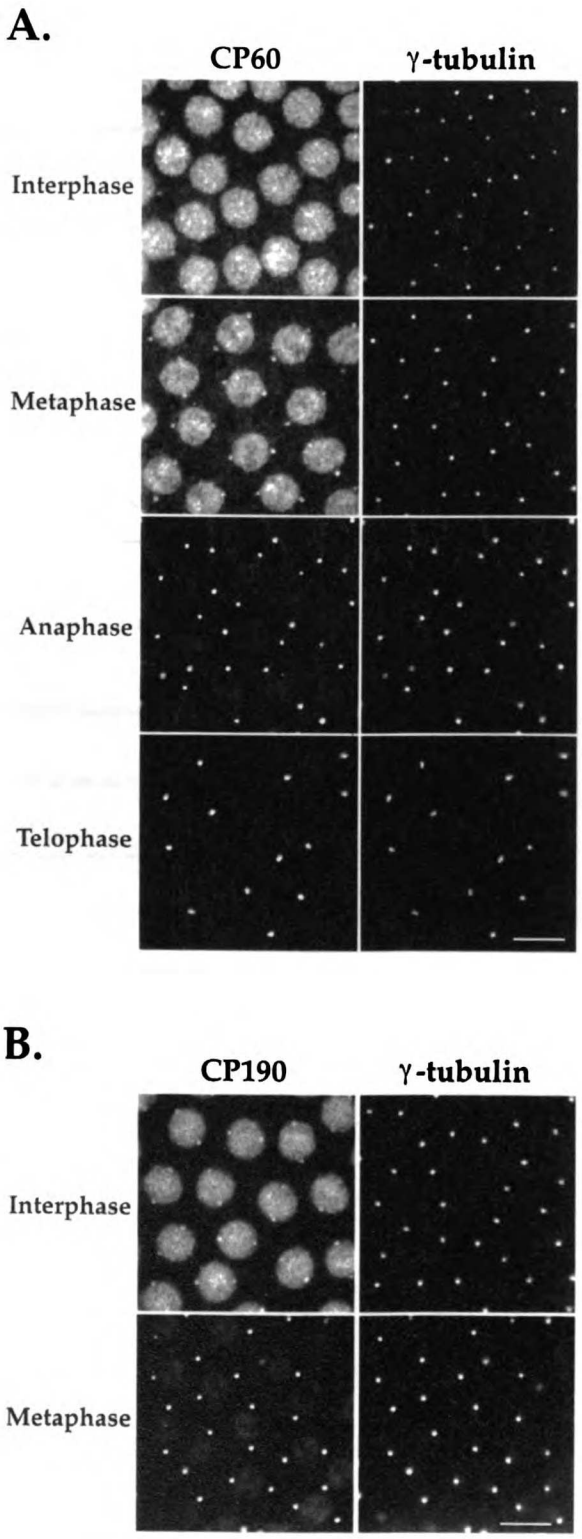

Figure 2
Oegema et al.

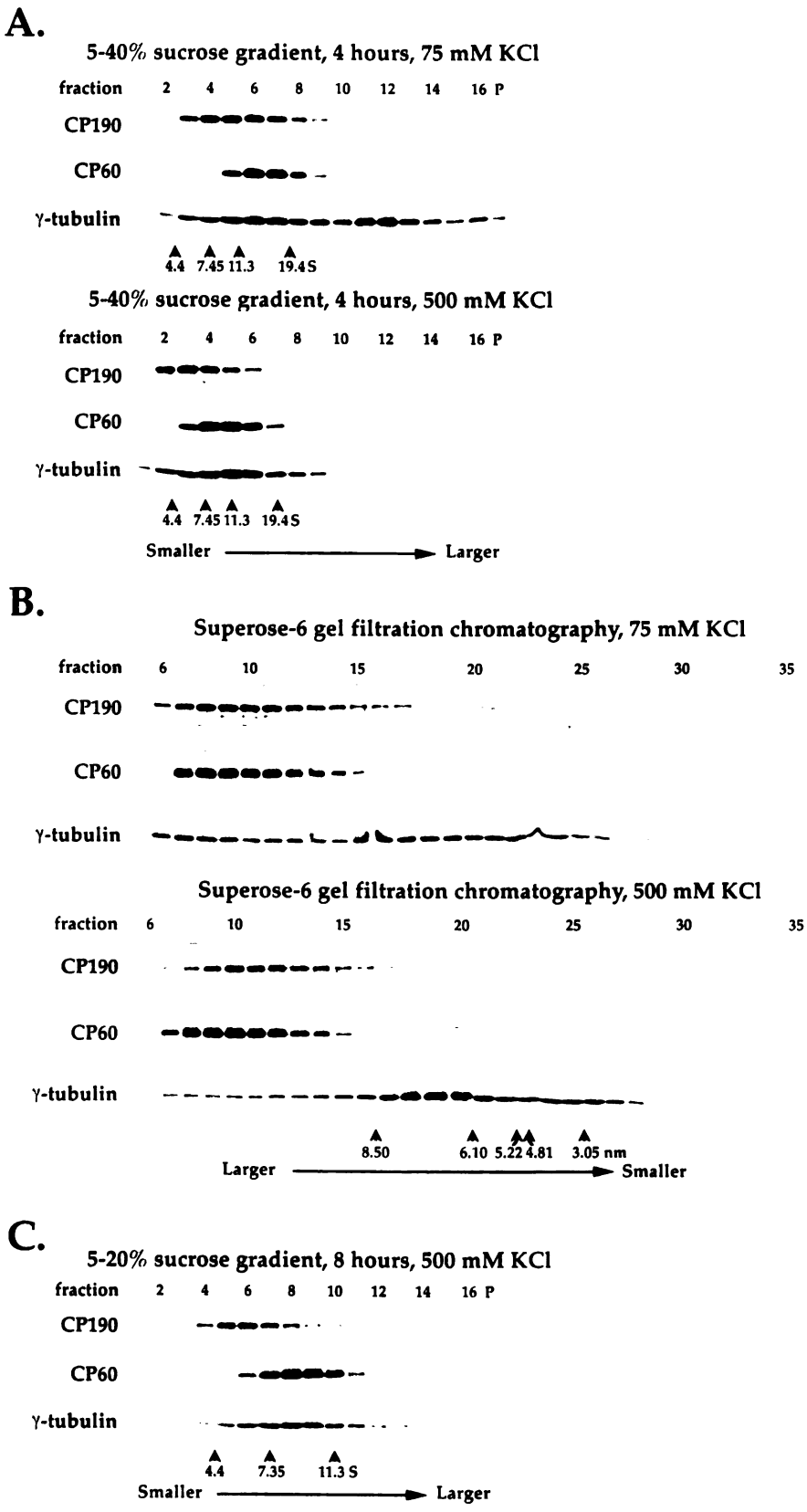

Figure 3
Oegema et al.

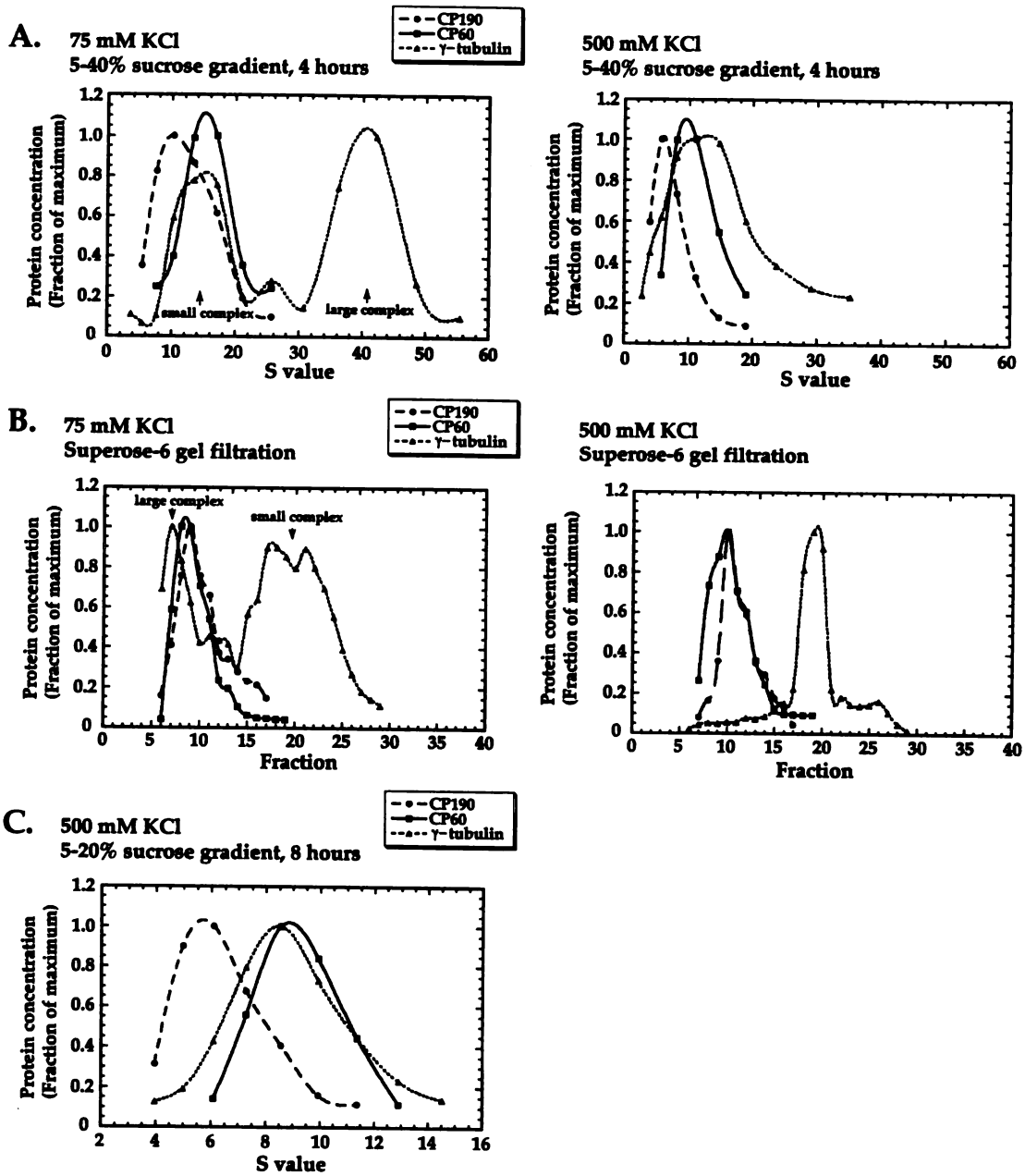

Figure 4
Oegema et al.

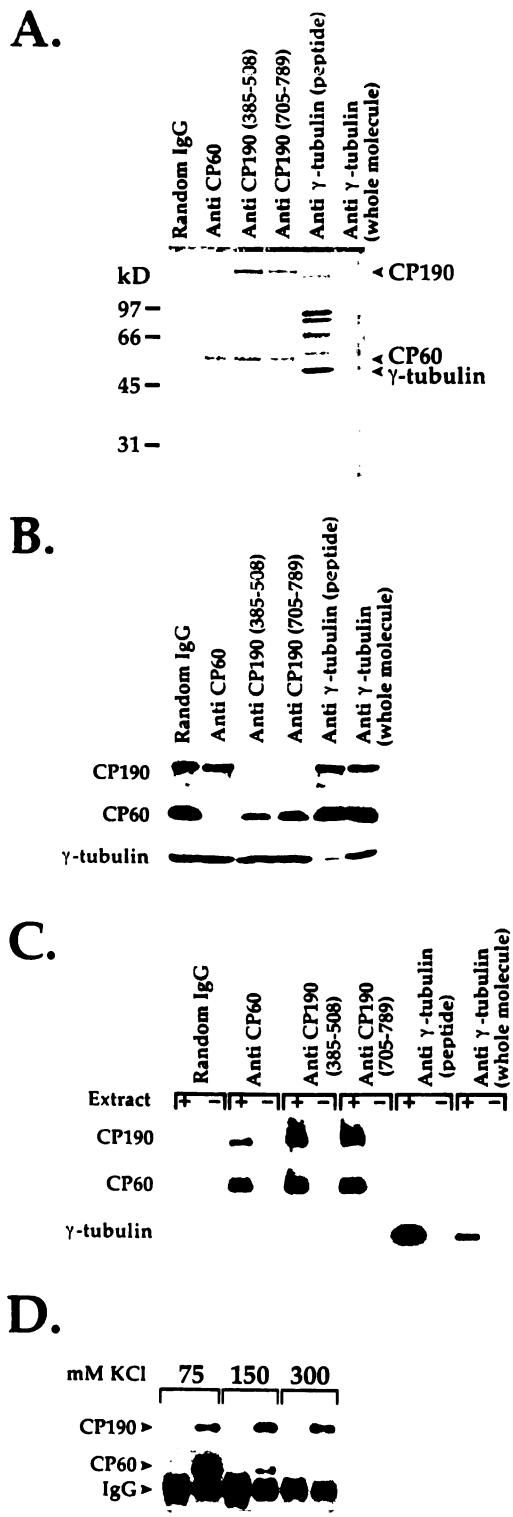

Figure 5
Oegema et al.

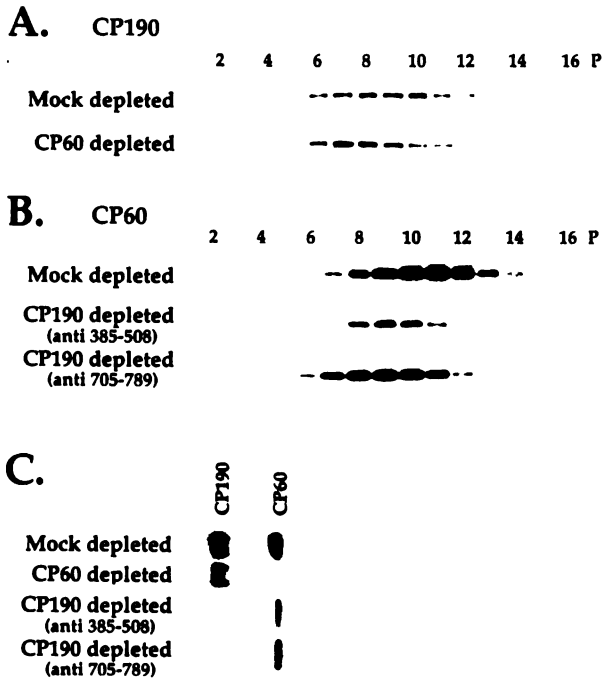

Figure 6
Oegema et al.

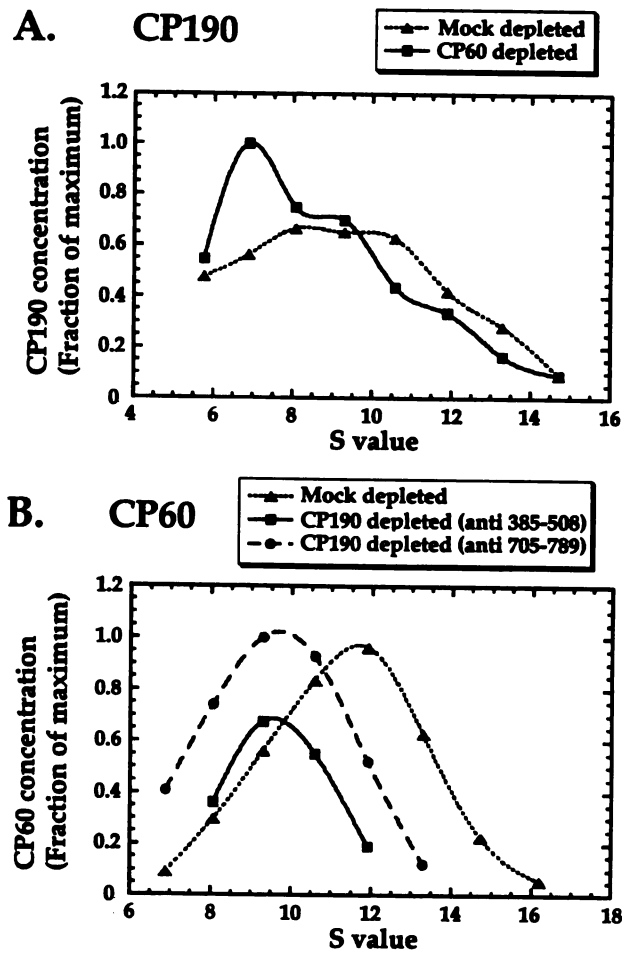

Figure 7
Oegema et al.

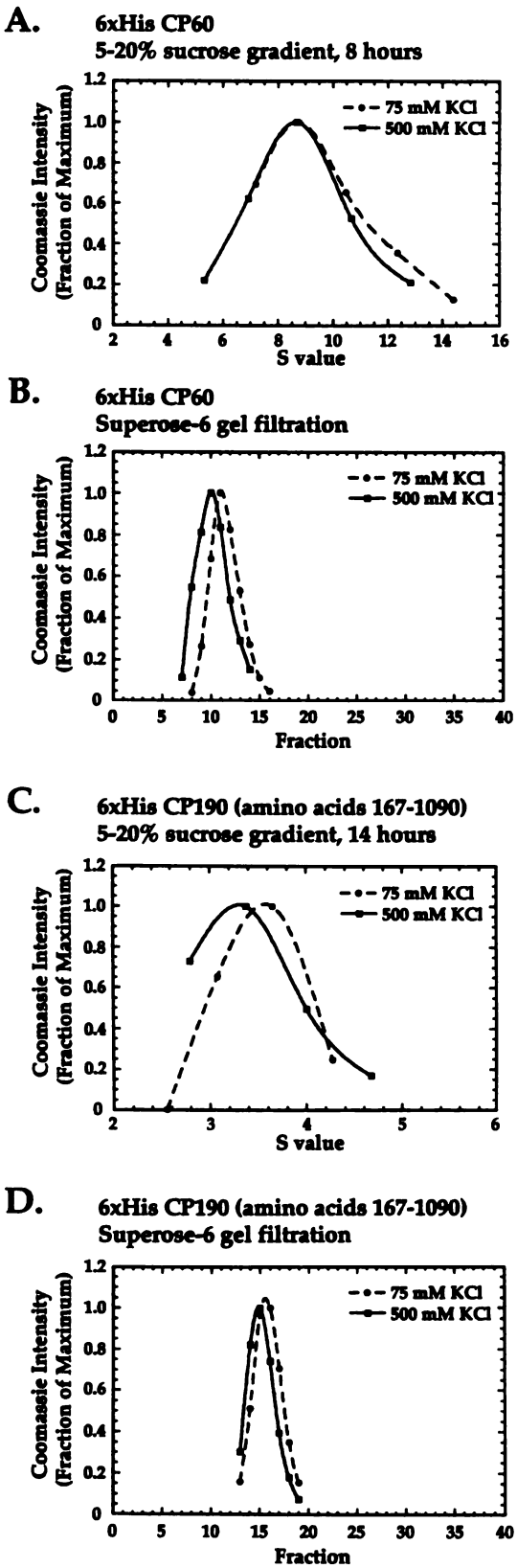

Figure 8
Oegema et al.

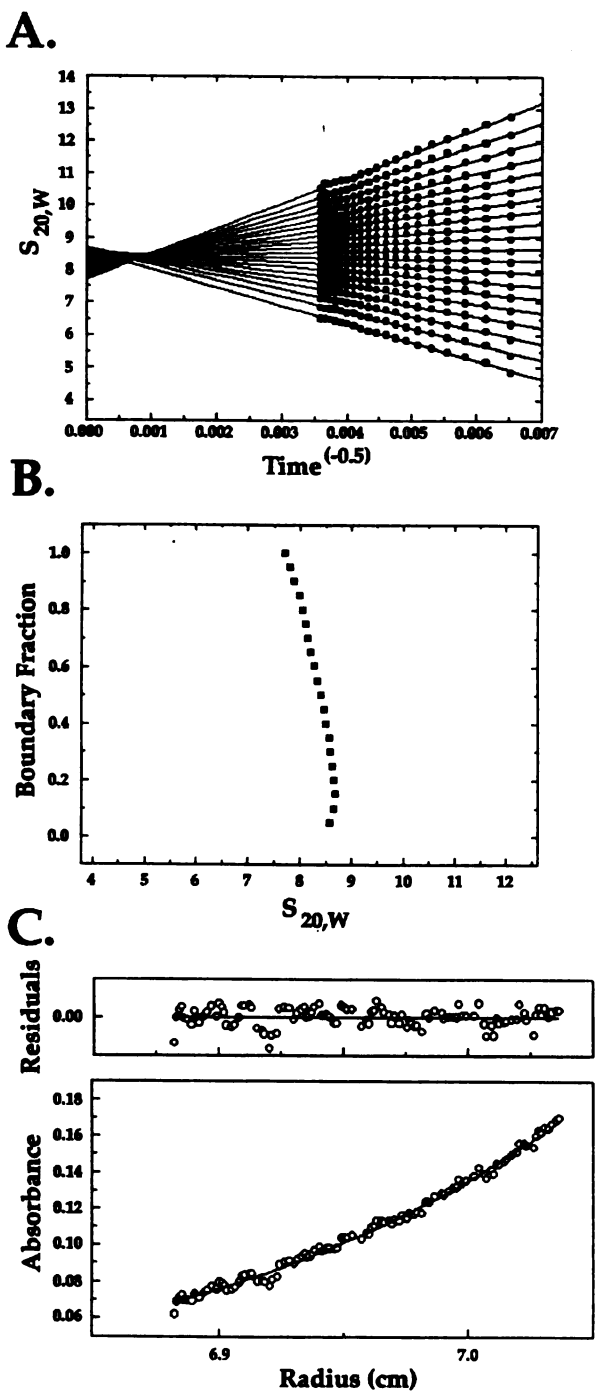

Table I

Properties of protein complexes in extracts

$S_{20,w}$	Rs (angstroms)	MW (estimated)	$[a/b]_p$
γ-tubulin- large complex (75 mM KCl)			
36.9 S	> 200	>3,040,000	
γ-tubulin- small complex (500 mM KCl)			
8.5 S	68.7	240,000	
CP190 (500 mM KCl)			
5.7 S	146	343,000	19
CP60 (500 mM KCl)			
8.9 S	149 s	546,000	23

A summary of the physical data presented for protein complexes containing CP190, CP60 and γ–tubulin present in concentrated *Drosophila* extracts. Molecular weights were estimated by the method of Siegel and Monty (1966). Axial ratios, $[a/b]_p$ were calculated after estimating the degree of hydration from amino acid sequence using the method of Kuntz (1971). The axial ratio of CP190 presented was calculated assuming the protein is dimeric (actual MW= 243,000), if the protein is trimeric (actual MW=365,000) then the calculated axial ratio would be 36.

Table II

Properties of bacterially expressed proteins

	$S_{20,w}$	Rs (angstoms)	Predicted MW (from sequence)	MW (estimated)	$[a/b]_p$
6XHis CP60					
75 mM KCl-	8.8 S	134	52,000	485,000	
500 mM KCl	8.7 S	146	52,000	523,000	25
6XHis CP190 (amino acids 167-1090)					
75 mM KCl	3.6 S	93.4	104,000	134,000	
500 mM KCl	3.3 S	98.1	104,000	129,000	18

Properties of bacterially expressed proteins. Data for bacterially expressed 6XHis CP60 and 6XHis CP190 (amino acids 167-1090) in 75 and 500 mM KCl. Molecular weights were estimated and axial ratios calculated as described in the legend to table I. The molecular weight of 6XHis CP190 was also determined by sedimentation equilibrium analysis to be 105,000 +/- 10,000.

Chapter 5
Conclusions

Our studies have led to a detailed characterization of the localization patterns of CP190 and CP60, the domain structure of CP190, and the hydrodynamic properties of protein complexes containing CP190, CP60 and γ-tubulin. However, the larger question of the functions of these proteins in embryos remains unanswered. Nevertheless, we believe that our work may, in conjunction with future studies, be useful in assigning function to CP190 and CP60 and in understanding the processes in which they are involved.

Do CP190 and CP60 bind microtubules?

CP190 was isolated by microtubule affinity chromatography (Kellogg et al., 1989) and CP60 is also found in eluates from microtubule affinity columns (Kellogg and Alberts, 1992). If microtubules are polymerized in extract by the addition of exogenous tubulin and taxol, both CP190 and CP60 pellet with the taxol stabilized microtubules (Raff et al., 1993). In addition, both bacterially expressed fragments of CP190 (Chapter 3) and full length 6XHis CP60 (Appendix) bind to microtubules in vitro, and the binding of CP60 to microtubules can be regulated by phosphorylation. The stoichiometry of binding of both proteins to microtubules is high, indicating that they bind along the lengths of microtubules in vitro and not just to microtubule ends. The domain of CP190 that confers the ability to bind to microtubules has been determined and is inseparable from its centrosomal localization domain (chapter 3).

CP190 and CP60 are nuclear during interphase and are presumably not in contact with microtubules (neither CP190 nor CP60 co-localize along the lengths of interphase microtubules). We have also looked carefully for any interaction that might occur following nuclear envelope breakdown or during mitosis. Microtubules are not required for either protein to attain or maintain its

centrosomal localization, and, by immunofluorescence, there is no obvious co-localization of either protein along the lengths of microtubules within the spindle. It remains possible that CP190 and CP60 interact with microtubules while at the centrosome, either anchoring microtubules in the pericentriolar material or as part of a role in the mitotic expansion, duplication or separation of the pericentriolar material. Alternatively, CP190 and CP60 could associate with γ-tubulin at the centrosome, as has been proposed (Raff et al., 1993). Another possibility is that these proteins interact with microtubules after nuclear envelope breakdown but while they are still attached to residual nuclear structures perhaps promoting spindle assembly. A final possibility is that the observed microtubule binding is an *in vitro* artifact.

Do CP190 and CP60 function in nuclei or at centrosomes?

CP190 and CP60 could function at centrosomes and be sequestered in nuclei to regulate their activity. In fixed embryos, the maximum immunofluorescence intensity of nuclei stained with anti CP190 or CP60 antibodies is about 20X that of the maximum centrosomal intensity. This could be due to differences in the accessibility of the epitopes recognized by these antibodies at centrosomes and in nuclei, but, if true, makes it seem unlikely that the nuclear localization of CP190 and CP60 serves solely to sequester these proteins until they are needed. At the other extreme, CP190 and CP60 could function primarily in nuclei and their centrosomal localization could contribute to their nuclear function. For example, concentration of CP190 at centrosomes could facilitate its initial recruitment to nuclei during interphase. A final possibility is that CP190 and CP60 function both at centrosomes and in nuclei. Because CP190 always accumulates before CP60, both at centrosomes and in

nuclei, it is possible that CP190 has a role in the recruitment of CP60 to centrosomes, to nuclei, or to both structures. But we also find that CP60 lingers both at centrosomes and in nuclei after the majority of the CP190 is gone, suggesting that CP60 may not require CP190 to remain localized to centrosomes or nuclei.

Do CP190 or CP60 have a role in microtubule nucleation?

Multiple lines of evidence suggest that CP190 and CP60 are not likely to have a direct role in microtubule nucleation. Microtubule nucleation is thought to be due to the presence of γ-tubulin containing ring complexes (γ-TuRCs) anchored within the PCM (Zheng et al., 1995; Moritz et al., 1995). Our work (chapter 4) suggests that CP190 and CP60 are not components of the soluble γ-TuRC or of the smaller γ-tubulin containing complex found in *Drosophila* embryo extracts. Consistent with this, experiments in which centrosomes are complemented with *Drosophila* embryo extracts after treatment with 2M KI have shown that CP190 and CP60 are not required for microtubule nucleation (Michelle Moritz, unpublished results). Treatment with KI abolishes the microtubule nucleating ability of the centrosomes and CP190 and CP60 are completely removed. The microtubule nucleating activity of the stripped centrosomes can be restored by incubation with extracts that have been depleted of CP190 or CP60 but not by incubation with extract depleted of γ-tubulin. These results suggest that, while γ-tubulin is required for microtubule nucleation from these centrosomes, CP190 and CP60 are not.

If not microtubule nucleation, then what? --possible functions for CP190 and CP60

Although we do not know what CP190 and CP60 are actually doing in embyros, their interesting cell cycle-dependent localization patterns may provide some clues. The centrosome cycle in the early Drosophila embryo is somewhat different than that characterized for somatic tissue culture cells (see Figure 1; Callaini and Riparbelli, 1990). In *Drosophila* embryos, the centriolar cylinders lose their perpendicular orientation in late metaphase, consistent with preparation for centrosome division; the centrosomes then become visibly less compact in early anaphase, forming ovoid plates by late anaphase. During telophase, the duplicated centrosomes physically separate.

CP190, present at centrosomes immediately following nuclear envelope breakdown, could function in the transition of the centrosomes from their interphase location and functions next to the nuclear envelope to their new roles at spindle poles. The localization of CP60 to centrosomes between anaphase and early interphase coincides with the period of centrosome duplication and separation and the transition back to an interphase state, making possible some role in these processes. One possibility, for example, is that CP190 could be involved in the expansion of the pericentriolar material that occurs at the onset of mitosis, and CP60 could be involved in the transition of the pericentriolar material back to the interphase state. We can extend our speculation to suggest that the pericentriolar material is in some way analogous to the nuclear structures that contain CP190 and CP60 and that CP190 and CP60 could function similarly at centrosomes and in nuclei.

Are CP190 and CP60 components of a multiprotein complex?

Immunoaffinity chromatography has identified a group of CP190 associated proteins (Kellogg et al., 1992) and previous results suggested that CP190, CP60 and γ-tubulin form a cytoplasmic complex in embryos. Our work suggests that neither CP190 nor CP60 is complexed with γ-tubulin in extracts but the majority of CP60 in extracts is complexed with CP190. In the absence of CP190, CP60 sediments as free oligomer, but CP190 remains heterogeneous in extracts depleted of CP60, suggesting that CP190 can form multiple complexes in the absence of CP60, associating either with itself or with other molecules. The proteins that CP190 is complexing with could include other proteins that were previously identified by anti-CP190 immunoaffinity chromatography. The fact that CP190 contains four predicted zinc fingers in the middle of its coding region also raises the possibility that CP190 could complex with nucleic acids.

Our results suggest that CP190 and CP60 are either weakly associated in extracts or that the CP60 in extracts is associated with only a small fraction of the CP190. This is consistent with the complex temporal and spatial localizations of CP190 and CP60 that we observed in embryos and suggests that the interaction between CP190 and CP60 is complex and likely to be regulated in a cell cycle-specific manner. Consistent with this CP60 contains 6 consensus cdc2 phosphorylation sites and western blotting of extracts reveals the existence of multiple phosphorylated forms in vivo (Kellogg et al., 1995). In addition, a kinase present in elutes from anti-CP190 immunoaffinity columns can phosphorylate CP60 in vitro (Kellogg et al., 1995), suggesting that the phosphorylation of CP60 could be in part regulated by its association with CP190. Bacterially expressed CP60 forms a higher order oligomer, which is also

formed by a poorly phosphorylated form of CP60 predominant in concentrated *Drosophila* extracts. One speculative possibility is that the dephosphorylation of CP60 during anaphase releases it from its attachment to residual nuclear structures and allows CP60 to oligomerize at centrosomes.

Assignment of function to CP190 and CP60 awaits genetic studies. These studies are currently underway in other laboratories, but obtaining mutations in the corresponding *Drosophila* genes is proving difficult. Some of our results suggest that CP190 and CP60 are likely to be conserved in other systems that offer distinct advantages for functional studies. In particular, our antibodies to CP60 and two of the existing antibodies to CP190 (Rb 188 and Bx63) recognize centrosomes in *C. Elegans* (Will Whitfield, personal communication) and CP190 fusion proteins will localize to nuclei and to centrosomes in Xenopus egg extracts in a cell cycle dependent manner (Karen Oegema and Steve Doxsey, unpublished experiments). If homologs to CP190 or CP60 are discovered by the C. Elegans genome sequencing project, injection of antisense RNA could provide a fast means to get at the phenotype of CP190 and CP60.

If the Xenopus homologs could be identified, use of cycling Xenopus extracts could also be useful for functional analysis. Depletion of the CP190 or CP60 homologs from Xenopus extracts could be used to test for possible roles in centrosome duplication or separation or in spindle function. In addition, more detailed biochemical analysis in a system with potential for control of cell cycle state, such as Xenopus egg extracts, could allow the establishment of solid correlations between cell cycle state and the existence of different CP190 and CP60 containing protein assemblies.

Appendix

CP60: A microtubule-associated protein that is localized to the centrosome in a cell cycle-specific manner

This appendix has been reproduced from Molecular Biology of the Cell, 1995, Volume 6, pp. 1673-1684 by copyright permission of the American Society for Cell Biology. I made and purified the bacterially expressed CP60 fusion protein used and did the microtubule spin down experiments.

Molecular Biology of the Cell
Vol. 6, 1673–1684, December 1995

CP60: A Microtubule-associated Protein that Is Localized to the Centrosome in a Cell Cycle–specific Manner

Douglas R. Kellogg,*† Karen Oegema, Jordan Raff, Ken Schneider, and Bruce M. Alberts

Department of Biochemistry and Biophysics, University of California, San Francisco, San Francisco, California 94143-0448

Submitted June 23, 1995; Accepted September 26, 1995
Monitoring Editor: J. Richard McIntosh

DMAP190 is a microtubule-associated protein from *Drosophila* that is localized to the centrosome. In a previous study, we used affinity chromatography to identify proteins that interact with DMAP190, and identified a 60-kDa protein that we named DMAP60 (Kellogg and Alberts, 1992). Like DMAP190, DMAP60 interacts with microtubules and is localized to the centrosome, and the two proteins associate as part of a multiprotein complex. We now report the cloning and sequencing of the cDNA encoding DMAP60. The amino acid sequence of DMAP60 is not homologous to any protein in the database, although it contains six consensus sites for phosphorylation by cyclin-dependent kinases. As judged by in situ hybridization, the gene for DMAP60 maps to chromosomal region 46A. In agreement with others working on *Drosophila* centrosomal proteins, we have changed the names for DMAP190 and DMAP60 to CP190 and CP60, respectively, to give these proteins a consistent nomenclature. Antibodies that recognize CP60 reveal that it is localized to the centrosome in a cell cycle–dependent manner. The amount of CP60 at the centrosome is maximal during anaphase and telophase, and then drops dramatically during late telophase or early interphase. This dramatic disappearance of CP60 may be due to specific proteolysis, because CP60 contains a sequence of amino acids similar to the "destruction box" that targets cyclins for proteolysis at the end of mitosis. Starting with nuclear cycle 12, CP60 and CP190 are both found in the nucleus during interphase. CP60 isolated from *Drosophila* embryos is highly phosphorylated, and dephosphorylated CP60 is a good substrate for cyclin B/p34^{cdc2} kinase complexes. A second kinase activity capable of phosphorylating CP60 is present in the CP60/CP190 multiprotein complex. We find that bacterially expressed CP60 binds to purified microtubules, and this binding is blocked by CP60 phosphorylation.

INTRODUCTION

The centrosome nucleates microtubules and plays a central role in the organization of dynamic microtubule arrays in all animal cells (for reviews see Karsenti and Maro, 1986; Vorobjev and Nadezhdina, 1987; Kalt and Schliwa, 1993; Kellogg *et al.*, 1994). Unfortunately, we know very little about this important organelle at the molecular level. The proteins that are responsible for microtubule nucleation remain largely unknown, as do the proteins that are responsible for centrosome assembly, duplication, and positioning. An important first step toward understanding the centrosome is to identify and characterize the many different proteins that function as its components.

We recently described the cloning of a partial cDNA encoding a *Drosophila* microtubule-associated protein that interacts with microtubules and is localized to the

* Corresponding author.
† Present Address: Sinsheimer Labs, Department of Biology, University of California, Santa Cruz, CA 95064.

centrosome in a cell cycle–specific manner (Kellogg and Alberts, 1992). We called this protein DMAP190 to indicate that it is a *Drosophila* microtubule-associated protein with an apparent molecular mass of 190 kDa. We later found that DMAP190 is identical to the protein recognized by the Bx63 monoclonal antibody (Whitfield *et al.*, 1988), which was originally isolated in a screen for monoclonal antibodies that recognize nuclear antigens in the early *Drosophila* embryo (Frasch *et al.*, 1986). To give this protein a consistent name in the literature, we have agreed with the other researchers in the field to rename the protein CP190 (centrosomal protein of 190 kDa).

We used a fusion protein produced from our CP190 clone to generate affinity-purified antibodies that recognize the CP190 protein, and these antibodies allowed us to construct an immunoaffinity column. When *Drosophila* embryo extracts were passed over such an anti-CP190 immunoaffinity column, we found that CP190 was specifically retained and could be eluted in highly purified form with 1.5 M $MgCl_2$ (Kellogg and Alberts, 1992). Additional proteins that bound specifically to the anti-CP190 column could be detected by washing the immunoaffinity column with 1 M KCl before the $MgCl_2$ elution. This wash released approximately 10 additional proteins, which represent candidates for proteins that interact with CP190 within the cell (Kellogg and Alberts, 1992).

To further study these potential centrosomal proteins, we initiated a characterization of a 60-kDa protein that is retained on the anti-CP190 immunoaffinity column. Antibodies that recognize the 60-kDa protein revealed that it colocalizes with CP190 at the centrosome. Western blotting experiments show that this 60-kDa protein is quantitatively retained on an anti-CP190 immunoaffinity column, indicating a tight association with CP190, and that it is retained on microtubule affinity columns in a manner identical to CP190 (Kellogg and Alberts, 1992). These experiments provide strong evidence that the 60-kDa protein interacts with CP190 as part of a multiprotein complex within the cell. We originally called this protein DMAP60 to indicate that it is a 60-kDa *Drosophila* microtubule-associated protein, but we now refer to it as CP60 in accordance with the new name for DMAP190.

In the present study, we have used mouse polyclonal antibodies against CP60 to isolate a cDNA clone from a *Drosophila* ovarian cDNA library, which has served as a starting point for further characterization of the CP60 protein.

MATERIALS AND METHODS

Buffers

The following buffers were used. Phosphate-buffered saline (PBS): 14 mM Na_2HPO_4, 1.8 mM KH_2PO_4, pH 7.2, 138 mM NaCl, 2.7 mM KCl. Lysis buffer: 50 mM *N*-2-hydroxyethylpiperazine-*N'*-2-ethanesulfonic acid (HEPES)-KOH, pH 7.6, 1.0 M NaCl, 2 mM Na_3EGTA, 2 mM Na_3EDTA, 0.25% Tween-20, 1 mm phenylmethylsulfonyl fluoride. Kinase buffer: 50 mM HEPES-KOH, pH 7.6, 1 mM $MgCl_2$, 1 mM Na_3EGTA, 0.1% Tween-20. Phosphatase buffer: 50 mM Tris-HCl, pH 7.8, 2.0 mM $MnCl_2$, 5 mM dithiothreitol (DTT), 100 μg/ml acetylated bovine serum albumin (New England Biolabs, Beverly, MA). Sample buffer: 65 mM Tris-HCl, pH 6.8, 3% SDS, 5% β-mercaptoethanol, 10% glycerol. Cosedimentation buffer: 50 mM HEPES-KOH, pH 7.6, 1 mM $MgCl_2$, 1 mM Na_3EGTA, 50 mM KCl. BRB80 buffer: 80 mM piperazine-*N,N'*-bis(ethansulfonic acid) (Pipes)-KOH, pH 7.6, 1 mM $MgCl_2$, 1 mM Na_3EGTA.

Cloning and In Situ Hybridization

Mouse polyclonal antibodies that recognize CP60 (Kellogg and Alberts, 1992) were used to screen an ovarian lambda gt11 cDNA library (Steinhauer *et al.*, 1989), as described by Kellogg and Alberts (1992). We obtained six positive plaques by screening 250,000 plaques. The sequence of the largest DNA insert (1.3 kb) contained a polyadenylation site at one end and a large open reading frame extending to the other end. To test whether this clone encodes CP60, we used the polymerase chain reaction (PCR) to amplify a 0.7-kb fragment, using two PCR primers (primer 1, GCGAATTCCTGTCCGCCGCCGC; primer 2, CGCGAATTCGCTCCAGCTTGGCGG). The PCR fragment was cloned into the *Eco*RI site of the vector pGEX.1, which directs expression of proteins fused to the enzyme glutathione-*S*-transferase (GST; Smith and Johnson, 1988). We thereby obtained a 45-kDa fusion protein, which was purified and used to generate affinity-purified antibodies according to the methods described by Kellogg and Alberts (1992). These antibodies recognized CP60 on Western blots and in fixed embryos in a manner identical to the original mouse polyclonal sera, demonstrating the correct identity of the clone.

Northern blot analysis was used to determine the size of the CP60 mRNA in RNA isolated from 0- to 3-h embryos. Based on the size of the mRNA (1.8 kb), and the presence of a polyadenylation site at one end of the partial CP60 cDNA, we concluded that our clone was lacking approximately 0.5 kb from the 5' end of the cDNA. We used a nested PCR approach to clone this missing DNA from a plasmid cDNA library (Brown and Kafatos, 1988; Gibbons *et al.*, 1991). A primer complementary to the cloning vector used for construction of the cDNA library (Brown and Kafatos, 1988), and a pair of nested primers taken from the sequence of the partial CP60 cDNA were used. A single 0.5-kb DNA fragment was obtained in the nested PCR reaction. The fragment was subcloned and sequenced, and the overlap of its sequence with that of the partial cDNA clone demonstrated that it was indeed the 5' end of the CP60 cDNA.

To confirm that the open reading frame of the full-length cDNA encodes a protein of the expected size (60 kDa), PCR was used to amplify the open reading frame and clone it into the vector pTrcHis (Invitrogen, San Diego, CA), which directs expression of proteins fused to six histidines. The fusion protein was expressed in bacteria according to the protocol supplied by Invitrogen.

The location of the CP60 gene on polytene chromosomes was determined using a digoxigenin-dUTP–labeled probe as previously described (de Frutos *et al.*, 1989).

Sequencing

Both strands of the CP60 cDNA were sequenced by using either the Sequenase protocol (United States Biochemical, Cleveland, OH), or the fluorescent dye-labeled terminator chemistry employed by the Biomolecular Resource Center at UCSF.

Immunofluorescence

Embryos were fixed with formaldehyde and stained according to the method of Theurkauf (1992). The affinity-purified rabbit antibodies against CP190 and CP60 were prepared as described by

Kellogg and Alberts (1992), and were used for immunofluorescence experiments at a concentration of 1–2 μg/ml. These antibodies stain only CP190 or CP60 in Western blotting experiments using crude embryo extracts, and the affinity-purified anti-CP60 antibodies used for this study stain the centrosome in a manner identical to the mouse serum used in our previous study (Kellogg and Alberts, 1992). For the triple label experiment shown in Figure 4, we used the same anti-CP60 mouse serum that we used previously (Kellogg and Alberts, 1992). Photomicrographs were taken on a Nikon Microphot FXA using a Nikon 60X plan apo objective and Kodak technical pan film at ASA 400 (see Figure 2A).

Immunoaffinity Chromatography

Immunoaffinity chromatography was carried out according to the methods described in our previous study (Kellogg and Alberts, 1992), with several modifications. High affinity polyclonal antibodies, rather than low affinity antibodies, were used, and the extract and wash buffers contained 70 mM KCl rather than 50 mM KCl (see Figure 5). Gel electrophoresis was carried out as previously described (Anderson *et al.*, 1973).

Immunoprecipitation, Dephosphorylation, and Phosphorylation of CP60

To prepare beads for the immunoprecipitation of CP60, 100 μl of protein A-Sepharose (Bio-Rad, Richmond, CA) were mixed with 100 μg of affinity-purified anti-CP60 antibody in a volume of 1 ml of PBS for 1 h. The bound antibody was then covalently linked to the beads with dimethylpimelimidate according to the method of Harlow and Lane (1988). After the coupling reaction, the beads were washed three times with 0.1 M glycine (pH 3.0) before use to remove any antibody not covalently linked, followed by PBS to remove the glycine buffer.

To immunoprecipitate CP60, a *Drosophila* embryo extract was made by homogenizing 1 g of embryos (age 1 to 2.5 h) in 2 ml of lysis buffer using a motor-driven Dounce homogenizer. The extract was centrifuged at 4°C for 1 h at 100,000 × *g*, and 1 ml of the supernatant was mixed with 100 μl of anti-CP60 beads. After mixing for 1 h at 4°C, the beads were pelleted and washed three times with 15 vol of lysis buffer, followed by two times with 15 vol of kinase buffer. For dephosphorylation of CP60, 10 μl of beads are washed once with 20 vol of phosphatase buffer, and then brought to a total volume of 25 μl with the same buffer. Lambda phosphatase (200 U; New England Biolabs) was added and the reaction was incubated at 30°C for 30 min. The beads were then washed once with 50 vol of kinase buffer, resuspended in 250 μl of sample buffer, and incubated at 100°C for 3 min to release the CP60 from the antibody. For Western blots, 10 μl of the CP60 released from the beads was loaded onto a 10% polyacrylamide gel, which was blotted onto nitrocellulose and probed with anti-CP60 antibody.

To phosphorylate CP60, 10 μl of beads carrying dephosphorylated CP60 (prepared as described above) were washed two times with kinase buffer, and then brought to a total volume of 25 μl with kinase buffer containing 300 uM ATP, 0.1 mCi/ml [γ-^{32}P]ATP (10 mCi/ml, 3000 Ci/mmole), and 1 mM DTT. Purified GST-cyclin B/p34^{cdc2} kinase (5 μl) was then added and the reaction was allowed to proceed for 45 min at room temperature. (The GST-cyclin B/p34^{cdc2} kinase was purified from *Xenopus* embryos as previously described [Kellogg *et al.*, 1995], and was at 0.7 mg ml in 30 mM Tris-HCl, pH 7.6, 75 mM KCl, 1 mM $MgCl_2$, 1 mM EGTA, 5 mM reduced glutathione, 10% glycerol). After the reaction, the beads were washed twice with 50 vol of kinase buffer and resuspended in 40 μl of sample buffer. After incubation at 100°C for 3 min, 15 μl was loaded onto a 10% polyacrylamide gel, which was dried and exposed to film to detect ^{32}P incorporation into CP60. For Western blotting, the CP60 released from the beads was diluted 10-fold and 15 μl was loaded onto a 10% polyacrylamide gel.

Proteins that interact with CP60 and CP190 were prepared for phosphorylation reactions by concentrating the fractions from the immunoaffinity purification experiment shown in Figure 5. To lower the salt concentration in these fractions, 100 μl of the elution from each column was diluted 1 to 5 with 50 mM HEPES, pH 7.6, 1 mM Na_3EGTA, 1 mM $MgCl_2$, 0.1% Tween-20, 0.5 mM DTT, and then concentrated fivefold using a Microcon-10 filtration device (Amicon, Beverly, MA). The concentrate was diluted 1 to 5 again with the same buffer, and then concentrated to a final volume of 15 μl. Phosphorylation reactions were carried out as described above, using 7.5 μl of the concentrated elutions for each reaction.

Cosedimentation of CP60 with Microtubules

Purified 6× His-tagged CP60 was prepared as described elsewhere (Oegema *et al.*, 1995). The CP60 fusion protein concentration was determined from the absorbance at 280 nm using an extinction coefficient calculated from the primary amino acid sequence (0.41 ml mg^{-1} cm^{-1}). The purified CP60 fusion protein was prespun at 100,000 rpm for 10 min in a TLA 100 rotor (Beckman, Fullerton, CA). Purified bovine tubulin (Mitchison and Kirschner, 1984) at 10 mg/ml in BRB80 was polymerized by the addition of an equal volume of BRB80 buffer containing 20% dimethyl sulfoxide and 2 mM GTP at 37°C. Microtubules were stabilized following polymerization by the addition of taxol to 100 uM. Fusion protein (7.6 μg) in cosedimentation buffer (10 μl) was diluted to 90 μl with the appropriate amount of either cosedimentation buffer or cosedimentation buffer containing 2 M KCl to give the desired salt concentrations, and either 10 μl of microtubules or 10 μl of control buffer were then added. The mixtures were layered over 100 μl cushions of cosedimentation buffer containing 50% glycerol and spun at 100,000 rpm for 10 min in the TLA 100 rotor. Finally, supernatants and pellets were analyzed by electrophoresis on 11.5% polyacrylamide gels and stained with Coomassie blue.

To determine the stoichiometry of binding at saturation, cosedimentation of CP60 with microtubules was carried out as above at saturating ratios of CP60 to microtubules. Instead of cosedimentation buffer, 80 mM Pipes-KOH, pH 6.8, 1 mM $MgCl_2$, 1 mM Na_3EGTA, 50 mM KCl was used. Pellets were electrophoresed on an 11.5% polyacrylamide gel alongside CP60 and tubulin standards and stained with Coomassie blue. Tubulin standards were prepared according to the method of Butner and Kirschner (1991). An image of the gel was transferred into the computer using a CCD camera attached to a Foto/Eclipse imaging system from Fotodyne (Hartland, WI). The resulting bands were quantitated using the histogram function of Adobe Photoshop (Mountain View, CA). Standard curves were generated using the curve fitting functions of KaleidaGraph (Synergy Software, Reading, PA).

To determine whether phosphorylation affects the ability of CP60 to cosediment with MTs, purified 6× His CP60 was phosphorylated with purified *Xenopus* cyclin B/p34^{cdc2} kinase in a reaction containing 20 μl kinase buffer, 2.5 μl 6× His CP60, 2.5 μl kinase, and 0.5 mM ATP. The CP60 was at 0.9 mg/ml in 50 mM sodium phosphate (pH 8.0), 250 NaCl, 1 mM β-mercaptoethanol, while the cyclin B/p34^{cdc2} kinase was as described in the previous section. As controls, identical reactions were set up that lacked either the kinase or ATP, and the reactions were incubated at room temperature for 2 h.

For cosedimentation assays, KCl was added to each reaction to 50 mM, as well as 10 μg of carrier protein (the bacteriophage T4 gene 45 protein in cosedimentation buffer containing 0.05% Tween-20 and 1 mM DTT [Morris *et al.*, 1979]). The final volume of each sample was 28 μl. Twelve microliters of each CP60 sample were mixed with 10 μl of microtubules or control buffer; microtubules had been prepared as above but were diluted to 1 mg/ml in cosedimentation buffer containing 0.05% Tween and 1 mM DTT before mixing with the CP60. Samples were layered over 100 μl cushions of cosedimentation buffer containing 0.05% Tween-20, 1 mM DTT, and

50% glycerol, and were spun at 80,000 rpm for 10 min in a TLA 100 rotor (Beckman). Samples of the supernatant and pellet were electrophoresed on an SDS-polyacrylamide gel, transferred to nitrocellulose, and probed with antibodies that recognize CP60.

RESULTS

Cloning and Sequencing of the CP60 cDNA

In a previous study we produced mouse polyclonal antibodies that recognize CP60 by injecting mice with protein purified by chromatography on an anti-CP190 immunoaffinity column (Kellogg and Alberts, 1992). To isolate a cDNA clone for CP60, we used these antibodies to screen a lambda gt11 library constructed with *Drosophila* ovarian cDNAs. We obtained five clones, each of which contained a 1.2-kb insert, and one clone carrying a 1.3-kb insert. Partial sequencing of the 1.3-kb insert and two of the 1.2-kb inserts revealed that they all were derived from a common cDNA. To confirm that these clones encode CP60, we subcloned a fragment of the largest cDNA clone into the vector pGEX.1, which directs expression of proteins fused to the enzyme GST (Smith and Johnson, 1988). Affinity-purified antibodies obtained using the resulting fusion protein recognize a 60-kDa protein that is localized to the centrosome in a manner identical to the protein recognized by the original mouse serum, thus demonstrating the correct identity of the clone.

Northern blot analysis revealed that the CP60 protein is encoded by an approximately 1.8-kb mRNA, indicating that our largest cDNA clone was lacking approximately 0.5 kb. We used nested PCR to amplify a clone containing the remainder of the coding sequences for CP60 from a plasmid cDNA library (see MATERIALS AND METHODS). The full length sequence of the CP60 cDNA is shown in Figure 1. The cDNA contains a 1.2-kb open reading frame that encodes a protein with a predicted molecular mass of 48 kDa. Because this is somewhat smaller than the expected size of 60 kDa, we generated a PCR fragment that carried the putative open reading frame and cloned it into a vector that directs the expression of proteins fused to six histidines. This CP60 fusion protein migrates slightly more slowly on polyacrylamide gels than CP60 from *Drosophila* embryos, consistent with the presence of the polyhistidine tag. This confirms the correct identity of the open reading frame.

CP60 is not homologous to any known proteins, although it has six potential sites for phosphorylation by cyclin-dependent kinases or MAP kinases (Figure 1) (Nigg, 1993). In situ hybridization of a CP60 DNA probe to polytene chromosomes reveals that the CP60 gene maps to chromosomal location 46A. We know of no mutations that map to this site, although we have not checked more recently obtained collections of P-element–induced lethal mutations.

CP60 Localizes to the Centrosome in a Cell Cycle–specific Manner

We have used affinity-purified rabbit polyclonal antibodies raised against a CP60-GST fusion protein to follow the localization of CP60 during nuclear cycle 10 in fixed *Drosophila* embryos. As shown in Figure 2, the amount of CP60 that can be detected at the centrosome peaks during late anaphase and telophase, and there is an abrupt loss of most of this centrosome staining in late telophase or early interphase. Figure 2A shows CP60 staining during interphase, when it is barely detectable at the centrosome, while Figure 2I shows CP60 staining during telophase, just before the loss of CP60 from the centrosome. As judged by the observation of many embryos, this loss appears to coincide with the time when the daughter centrosomes complete their migration to opposite sides of the nucleus (the early nuclear divisions in the *Drosophila* embryo take place very rapidly, and the centrosome divides and migrates immediately after chromosome segregation, during late telophase and early interphase (Kellogg *et al.*, 1988). The amount of CP60 at the centrosome remains low through the remainder of interphase and prophase, and then increases somewhat during metaphase before dramatically rising during anaphase. Thus, CP60 is localized to the centrosome in a cell cycle–specific manner. The CP60 antibody also stains the spindle region weakly during metaphase and anaphase.

There are two subtle differences in the centrosomal localizations observed for CP60 and CP190 in the early embryo. First, whereas the amount of CP60 at the centrosome appears relatively low during metaphase, and then rises dramatically during anaphase and telophase, the amount of CP190 at the centrosome is relatively high during metaphase and rises less dramatically during anaphase. The other difference appears only when embryos are fixed according to a different protocol. The embryos shown in Figure 2 were fixed with formaldehyde. If the embryos are fixed using methanol (Kellogg *et al.*, 1988), the weak staining of the spindle region by anti-CP60 during anaphase and telophase is somewhat more pronounced, whereas the anti-CP190 staining is unchanged. The formaldehyde fixation is known to give superior preservation of microtubules (Theurkauf, 1992), but the methanol fixation may be more likely to minimize artifacts due to epitope masking. Because of limitations inherent in immunofluorescence techniques, no strong conclusions can be derived from these subtle differences in the distributions of CP60 and CP190. Techniques utilizing fluorescently labeled proteins are currently being developed to learn more about the relative

```
                                                                                         TATATAAAAACAAGCGGA
     TCCTAGTTACATATACCAATTCGTGTGTCGCGTGTTATCAAAACAGCCTCCAAAATTATCAGGAACGCGCAACCAGCGGGCCGCAAGTCGCTGACTAAG

1    M   A   I   Q   L   D   K   I   L   Q   D   I   A   K   E   K   V   L   H   P   N   N   G   G   A
1    ATG GCA ATC CAA CTG GAC AAG ATT CTG CAG GAC ATC GCC AAA GAA AAG GTG CTG CAT CCA AAC AAT GGC GGC GCC

26   S   K   Q   E   Q   E   E   A   W   A   R   I   G   R   L   N   K   L   S   V   H   E   S   R   S
76   AGC AAG CAG GAG CAG GAG GAG GCG TGG GCC AGG ATC GGG CGT CTC AAC AAG CTC TCT GTG CAC GAA TCG CGC TCC

51   I   F   I   V   L   Q   K   K   Y   E   Q   E   K   L   K   G   N   S   A   W   K   L   F   S   L
151  ATC TTC ATA GTG CTC CAA AAG AAG TAC GAG CAG GAA AAG CTA AAG GGC AAT TCG GCG TGG AAG CTC TTC AGT CTG

76   M   H   Q   I   H   Q   D   P   K   I   S   I   K   E   E   N   D   Q   V   P   M   E   E   V   E
226  ATG CAT CAG ATC CAT CAG GAC CCT AAA ATC TCA ATC AAG GAG GAG AAT GAT CAA GTA CCC ATG GAG GAG GTG GAG

101  E   Y   E   M   L   E   V   Q   E   F   E   D   E   D   D   A   H   Q   Y   G   Q   H   T   N   S
301  GAG TAC GAA ATG CTG GAG GTG CAG GAG CCT GAG GAC GAG GAT GAC GCC CAT CAG TAC GGA CAG CAC ACC AAC TCT

126  T   G   S   A   S   S   D   G   E   S   P   T   K   S   H   S   T   G   S   P   E   K   D   E   R
376  ACC GGC TCG GCG TCC TCC GAC GGC GAA AGC CCC ACA AAG TCA CAC AGC ACC GGT TCG CCA GAA AAG GAC GAG CGG

151  L   A   Y   A   K   P   N   V   D   T   P   R   P   A   I   E   E   K   K   L   L   N   T   L   A
451  TTG GCG TAC GCC AAA CCC AAC GTC GAC ACT CCT CGC CCA GCC ATC GAG GAG AAA AAG CTG CTC AAC ACA CTG GCT

176  N   N   T   P   R   S   S   S   L   S   A   A   A   A   V   L   Q   K   K   G   I   T   V   K   K
526  AAC AAC ACA CCG CGA AGT AGC TCG CTG TCC GCC GCC GCA GCA GTA CTG CAA AAG AAG GGA ATT ACT GTG AAG AAG

201  T   P   S   S   A   A   A   P   K   P   A   I   G   Q   Q   A   P   A   S   G   Q   R   S   S   S
601  ACG CCC AGC TCC GCA GCA GCA CCG AAA CCG GCT ATT GGG CAA CAG GCG CCA GCC AGT GGG CAA AGA TCA AGC TCC

226  S   R   T   T   I   Q   L   P   D   S   L   K   R   K   L   S   E   E   Y   T   S   S   S   A   Q
676  TCG CGC ACC ACC ATT CAG CTG CCA GAT TCT TTG AAG CGC AAA CTT TCG GAG GAG TAC ACC TCG TCA TCG GCG CAA

251  K   K   Q   T   K   T   T   S   P   K   Q   A   A   S   S   A   G   A   T   S   V   H   T   S   V
751  AAA AAG CAG ACC AAG ACC ACG AGC CCG AAA CAA GCC GCT TCA TCG GCA GGC GCA ACT TCA GTG CAC ACC AGC GTT

276  P   D   Q   L   P   A   G   N   N   V   V   H   T   T   T   A   Q   L   M   Q   V   K   K   E   R
826  CCA GAT CAA CTG CCG GCG GGA AAC AAT GTG GTG CAC ACA ACC ACT GCC CAG CTG ATG CAG GTT AAG AAG GAG CGT

301  E   D   N   Q   T   P   P   P   G   I   N   I   I   T   I   P   S   E   Q   Q   I   N   G   G   G
901  GAG GAC AAC CAG ACA CCA CCG CCG GGT ATC AAC ATC ATC ACC ATT CCA TCG GAA CAA CAG ATA AAC GGT GGT GGT

326  G   G   T   N   S   S   T   A   A   T   I   A   S   T   S   V   A   S   T   N   G   F   S   P   H
976  GGG GGA ACG AAC TCA TCG ACA GCC GCC ACC ATT GCT TCC ACC TCG GTG GCT TCC ACA AAC GGC TTT TCG CCA CAC

351  I   E   E   L   D   F   K   N   D   I   I   F   G   P   K   I   N   A   A   S   S   N   T   P   E
1026 ATC GAG GAG CTG GAC TTT AAG AAT GAC ATT ATC TTC GGG CCG AAG ATC AAC GCC GCC TCC TCC AAT ACA CCC GAG

376  I   I   N   L   G   N   F   D   N   S   V   P   P   T   F   F   K   N   L   C   N   S   S   R   H
1101 ATT ATC AAC CTG GGC AAC TTT GAC AAC TCG GTG CCG CCA ACC TTT TTC AAG AAT CTA TGC AAC TCG TCG CGA CAC

401  E   S   L   G   L   Y   V   A   N   V   M   N   R   L   S   S   R   A   S   A   K   L   E   L   S
1176 GAG TCT CTC GGG CTG TAC GTG GCC AAT GTG ATG AAC AGA CTC TCT TCG CGT GCC TCC GCC AAG CTG GAG CTG TCC
             *   *   *   *   *   *   *   *
426  I   L   R   A   I   L   D   V   Q   S   D   E   L   E   Q   *
1251 ATC TTG CGC GCC ATC CTC GAT GTG CAG AGC GAC GAA CTG GAG CAG TAG ACCGACTGATACTCGCAATTTAAATGATTACTCAG

     CTTACTTATTAGACAAACTAAAAAGGTAGTTATGTAGTAGGCCTGTCTGAACCATTTCTCGTATTTATCGTATTATTTTTTCCGTGTTCAAACGTCTGC
     GTTCTGTGCCGCCCACTTGTAAAATGTATTTACTCACAGTTCTGGTATGAGTGTTCATAGCATTTACGCATGAATTTTAAAGCTAAATTTAAAATGTAT
     TTCTAATATTTGAGATTTCGAATTTGTCCCTATTTAAGGTTGAATATGCTACTTGATTTTAAAATACGTTTATATGCAAATAAATCTACATAACTTAAA
     AAAAAAA
```

Figure 1. The sequence of the CP60 cDNA. Potential sites for phosphorylation by the cyclin-dependent protein kinase $p34^{CDC2}$ are underlined. The potential destruction box near the C-terminus is marked by an asterisk above each of the underlined amino acids. Sequence available through GenBank accession number U38248.

localizations of CP60 and CP190 in living embryos (Oegema *et al.*, 1995).

CP60 Has a Potential Destruction Box

The mechanism by which CP60 is localized to the centrosome in a cell cycle–specific manner is unknown. The fact that CP60 has a number of potential phosphorylation sites for cyclin-dependent kinases or MAP kinases suggests that it is regulated by post-translational modification. Another possibility, however, is that the loss of CP60 at the centrosome at the end of mitosis is due to specific proteolysis. A number of proteins are known to be proteolytically destroyed at the end of mitosis, including the B-type cyclins, CENP-E, and CENP-F (Evans *et al.*, 1983; Brown *et al.*, 1994; Liao *et al.*, 1995). The existence of additional proteins that are destroyed at the end of mitosis has been inferred from studies using inhibitors of protein degradation (Holloway *et al.*, 1993). In the case of the cyclins, it has been shown that specific proteolysis is mediated by a sequence of amino acids called a "destruction box," which targets the protein for proteolysis by a ubiquitin-dependent pathway (Glotzer *et al.*, 1991). We found that CP60 has a good match to the destruction box sequence near its C-terminus; this sequence is

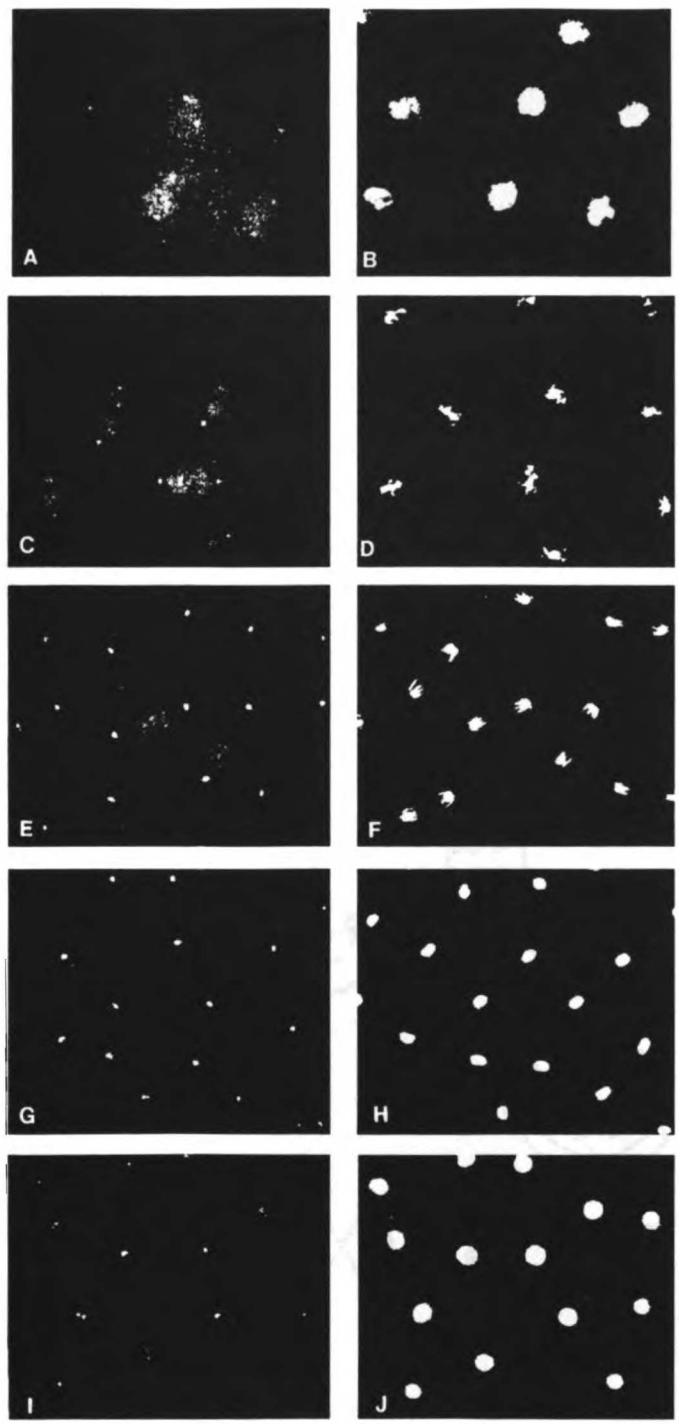

Figure 2. CP60 is localized to the centrosome in a cell cycle-dependent manner. A double-label immunofluorescence experiment showing the distribution of CP60 (A, C, E, G, and I) and DNA (B, D, F, H, and J). The distribution of the DNA was revealed by staining with Hoechst 33258. The photomicrographs show a small section of the embryo surface during nuclear cycle 10 (see Kellogg *et al.*, 1988, for the distribution of microtubules at this stage). The antibody staining shown in each panel was photographed and printed using the same exposures, with the exception of panel A, which was printed somewhat lighter to help bring out the weak staining of the centrosome. Bar, 10 μm.

marked in Figure 1, and is compared with destruction boxes from other proteins in Figure 3. The existence of a potential destruction box on CP60 is consistent with the possibility that it is proteolytically destroyed at the end of mitosis.

CP60 Localizes to the Nucleus during Interphase of Later Cell Cycles

During the early nuclear cycles that occur in the *Drosophila* embryo, CP60 is mainly detected at the centrosome, with faint staining over the nuclear region during interphase. Starting with nuclear cycle 12, staining of the nucleus during interphase becomes much more prominent. The intensity of this nuclear staining increases with each nuclear cycle, reaching a maximum during nuclear cycle 13 or 14. From this time of development onward, CP60 is found at the centrosome during mitosis, and within the nucleus during interphase. An example of this distribution is shown in Figure 4. Perhaps the relatively low level of nuclear staining in early embryos reflects the extremely short duration of interphase during these nuclear cycles: the time available may be insufficient for transport of CP60 into the nucleus (Foe and Alberts, 1983).

The nuclear staining observed with the CP60 antibody in early embryos appears uniform throughout the nucleus; however, in embryos that are undergoing gastrulation, one often sees a number of bright dots staining within the nucleus (arrowhead, Figure 4A). These dots do not correspond to the centrosome, because one often sees four to six of them scattered within the nucleus. They also do not correspond to heterochromatic or highly condensed regions of the chromatin (Figure 4, compare A and B with C). Not all nuclei have these spots, and more work needs to be done to determine whether they appear at a specific time during the cell cycle.

It appears that CP60 and CP190 colocalize in the nucleus at all stages, being found in the same intranuclear dots (Figure 4, compare A and B); however, the nuclear localization of CP190 can often be detected in the syncytial blastoderm embryo earlier than can that of CP60.

CP60	R	A	I	L	D	V	Q	S	D
B -Type Cyclins									
CLB2	R	L	A	L	N	N	V	T	N
Human B1	R	T	A	L	G	D	I	D	P
Xenopus B1	R	T	A	L	G	D	I	G	N
Human B2	R	T	V	L	E	E	I	G	N
S. purp.	R	A	A	L	G	N	I	S	N
Arbacia	R	A	A	L	G	N	I	S	M
Starfish	R	G	A	L	E	N	I	S	N
Clam	R	N	T	L	G	D	I	G	N
Drosophila	R	A	A	L	G	D	L	Q	N
Cdc13	R	H	A	L	D	D	V	S	N
A Cyclins									
Human	R	A	A	L	A	V	L	K	S
Xenopus	R	T	V	L	G	V	I	G	D
Clam	R	A	A	L	G	V	I	T	N
Drosophila	R	S	I	L	G	V	I	Q	S

Figure 3. CP60 has a potential destruction box. A comparison of the potential destruction box in CP60 with destruction boxes found in A and B type cyclins from a variety of organisms.

Immunoaffinity Chromatography with Anti-CP60 Antibodies

CP60 was originally identified in an immunoaffinity chromatography experiment designed to identify proteins that interact with CP190 (Kellogg and Alberts, 1992). In that experiment, we constructed an immunoaffinity column using antibodies that recognize CP190. The column was loaded with a *Drosophila* embryo extract, washed extensively with buffer, and then eluted with 1.0 M KCl to release proteins that associate with CP190, while leaving CP190 itself bound to the antibody on the column. We found that the 1.0 M KCl elution released a number of proteins, including CP60. It was of interest, therefore, to perform the reciprocal immunoaffinity chromatography experiment using a column that contains antibodies that recognize CP60. This would provide further information on the multiprotein complex containing CP190 and CP60, and might also lead to the identification of new proteins. For example, proteins that interact only with the fraction of CP60 that are not complexed with CP190 would not be detected on an anti-CP190 immunoaffinity column.

We constructed immunoaffinity columns with antibodies that recognize CP60 or CP190. As a control, we used a column containing nonimmune rabbit IgG. A *Drosophila* embryo extract was loaded onto each of the three columns, and the columns were then washed extensively with buffer and eluted with 1.5 M KCl to release proteins that interact with CP190 or CP60. Figure 5 shows a polyacrylamide gel analysis of the proteins that were eluted from each of these columns. The group of proteins eluted from the anti-CP190 column is very similar to the group of proteins observed in the eluates from our original experiments (Kellogg and Alberts, 1992). However, we washed the columns in the present experiment under more stringent conditions to select only for more tightly bound proteins, and the pattern of proteins obtained is therefore slightly different. The most notable difference is that CP60 is more prominent. In experiments using even more stringent wash conditions (a greater volume of wash at a higher salt concentration), we find

that CP60 is the only protein remaining bound to CP190.

The 1.5 M KCl elution from the anti-CP60 column shows a prominent 190-kDa protein band, and Western blotting confirms that this is CP190, as expected. The fact that CP190 is the major protein that is retained on the anti-CP60 column suggests that these two proteins interact directly. A number of additional proteins are also retained on the anti-CP60 column, which appear to be identical to proteins retained on the anti-CP190 column. We see no major proteins interacting uniquely with the anti-CP60 column. In contrast, a number of proteins are retained on the anti-CP190 column that are not retained on the anti-CP60 column. These could be proteins that interact only with CP190 that is not bound to CP60, or the antibodies against CP60 might block the interaction of some proteins with the CP60/CP190 complex. Alternatively, the additional proteins seen binding to the anti-CP190 column could interact directly with CP190, in which case, the binding of these proteins to the anti-CP60 column would be due to tertiary interactions that might be preferentially lost during the extensive wash used in these experiments (60 column volumes). Further experiments will need to be done to determine whether CP60 and CP190 exist in a number of different complexes. Because none of the proteins are retained on the control column, it is likely that most of the interactions that we observe are biologically significant.

Phosphorylation of CP60 by p34^{cdc2}

Antibodies against CP60 recognize a number of closely spaced bands on Western blots, suggesting that CP60 is post-translationally modified within the cell. Because CP60 has six consensus sites for phosphorylation by cyclin-dependent kinases or MAP kinases, we suspected that these different forms were due to phosphorylation. To test this possibility, we immunoprecipitated CP60 from embryo extracts and then treated it with lambda phosphatase. This treatment caused a dramatic shift in the electrophoretic mobility of CP60 (Figure 6, compare lanes 1 and 2), confirming that CP60 is phosphorylated. To test whether CP60 is indeed a substrate for cyclin-dependent kinases, we incubated the phosphatase-treated CP60 with purified cyclin B/p34^{cdc2} kinase complexes. This caused CP60 to shift up to five different bands (Figure 6, compare lanes 3 and 4), which agrees well with the number of predicted phosphorylation sites for cyclin-dependent kinases on CP60.

We next wanted to determine whether we could identify any additional kinase activities that can phosphorylate CP60. Such kinases might be present in the complex of proteins that interact with CP60 and CP190. We therefore tested the CP60 and CP190-binding proteins isolated by immunoaffinity chromatography for the presence of kinase activity using dephosphorylated CP60 as a substrate. We found that the proteins that interact with CP190 contain a kinase activity that can phosphorylate CP60, whereas the proteins that interact with CP60 and control IgG do

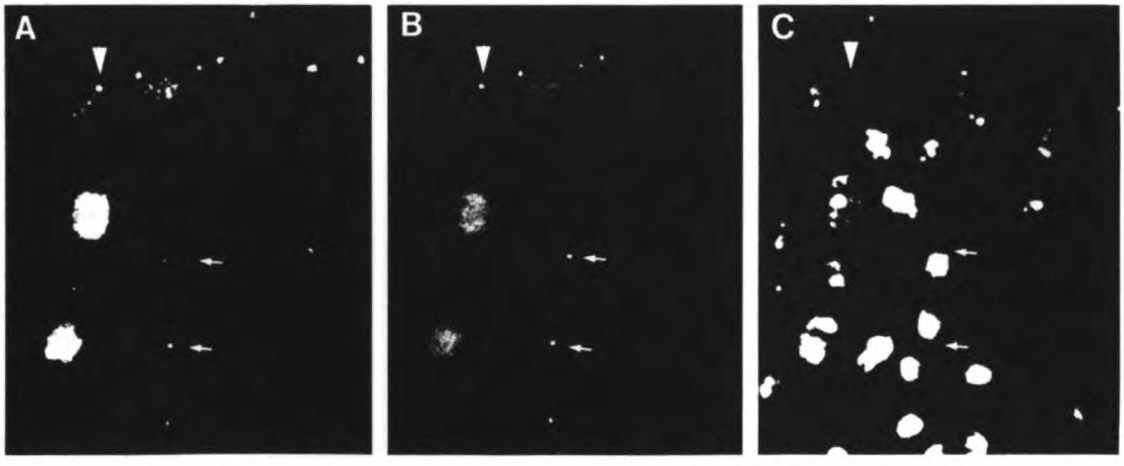

Figure 4. In embryos older than cycle 12, CP60 and CP190 localize to the centrosome during mitosis, and to the nucleus during interphase. A triple-label immunofluorescence experiment showing the distribution of CP60 (A), CP190 (B), and DNA (C) in an embryo undergoing gastrulation. The photomicrographs show a small section of the embryo surface. Staining of the centrosomes in a cell undergoing anaphase is marked by arrows. An example of the staining of dots within the nucleus during interphase is marked by an arrowhead in the upper left corner; these are not centrosomes (see text). A more diffuse staining of the nucleus that is typical of interphase can also be seen in this cell.

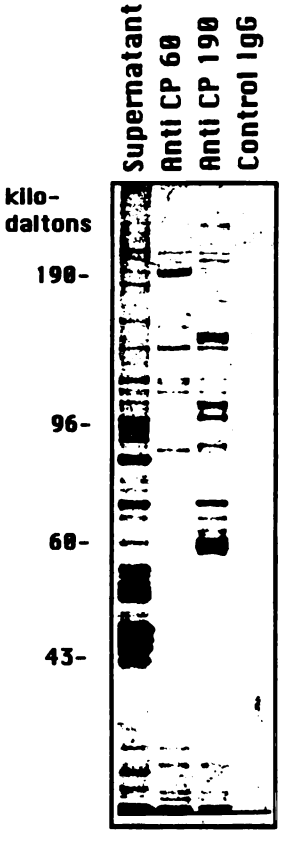

Figure 5. Immunoaffinity chromatography with anti-CP60 and anti-CP190 antibodies. Immunoaffinity chromatography was carried out as described in MATERIALS AND METHODS, and protein samples were analyzed on a 10% polyacrylamide gel. The lane marked "supernatant" is 15 μg of the high-speed supernatant that was loaded onto the columns, while the next three lanes show the proteins that elute from an anti-CP60 column (5 μg), an anti-CP190 column (5 μg), and an IgG control column with 1.5 M KCl. The gel is stained with Coomassie blue. For this experiment, three 1-ml columns were prepared, each containing 3 mg of antibody. The columns were loaded at 10 ml/h with extract made from 34 g of 0- to 4-h embryos. After loading, the columns were washed overnight with 60 column volumes of buffer containing 70 mM KCl, and then eluted with buffer containing 1.5 M KCl. The elutions from the anti-CP60 and anti-CP190 columns each contained 100 μg of protein, while the elution from the IgG control column contained no protein that could be detected by a Bradford assay (Bradford, 1976).

not (Figure 6, lanes 7–9). These results suggest that the CP190/CP60 complex contains a kinase that phosphorylates CP60. The absence of this kinase activity in the proteins that bind to CP60 could be due to any of the reasons discussed in the previous section to account for the differences in the proteins binding to the anti-CP60 and CP190 immunoaffinity columns.

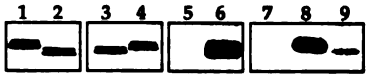

Figure 6. Phosphorylation of CP60. CP60 was immunoprecipitated as described in MATERIALS AND METHODS, treated with phosphatases or kinases, and analyzed by polyacrylamide gel electrophoresis. Lanes 1–4 are Western blots using anti-CP60 antibody to show shifts in electrophoretic mobility, while lanes 5–9 are autoradiographs showing incorporation of ^{32}P into CP60. (Lane 1) Immuno-precipitated CP60 that has been subjected to no treatment; (lane 2) immuno-precipitated CP60 treated with lambda phosphatase; (lane 3) immunoprecipitated CP60 treated with lambda phosphatase and then incubated in kinase reaction buffer; (lane 4) the same as lane 3 but incubated with purified cyclin B/p34cdc2 kinase; and (lanes 5 and 6) the same as lanes 3 and 4, but the gel has been exposed to film to show that CP60 has incorporated ^{32}P from ATP$\gamma^{32}P$. In lanes 7–9, dephosphorylated CP60 was incubated in the presence of [γ-^{32}P]ATP and the CP60- and CP190-binding proteins isolated by immunoaffinity chromatography in Figure 5. (Lane 7) incubation with the elution from the IgG control column; (lane 8) incubation with CP190-binding proteins; and (lane 9) incubation with CP60-binding proteins. Western blotting reveals that there is a corresponding shift in the electrophoretic mobility of the CP60 in lane 8, confirming that it is CP60 that is incorporating ^{32}P in this experiment.

CP60 Binds to Microtubules in a Phosphorylation-dependent Manner

In previous studies, we demonstrated that CP60 and CP190 bind to microtubules when a *Drosophila* embryo extract is passed over a microtubule affinity column. This experiment does not, however, tell us whether these proteins bind directly to microtubules, because they could bind by virtue of secondary interactions with other proteins that bind directly. To test whether CP60 is able to interact with microtubules directly, we expressed CP60 as a 6× His fusion protein in bacteria, and purified it by metal affinity and gel filtration chromatography. We then determined whether purified CP60 would interact with purified tubulin, using a cosedimentation assay. We found that CP60 binds quantitatively to microtubules at physiological ionic strength, and that significant binding occurs at salt concentrations as high as 250 mM (Figure 7A). We carried out similar cosedimentation experiments to quantitate the stoichiometry of binding at saturating conditions, and found that approximately 1.4 molecules of CP60 are bound per tubulin dimer (not shown).

We next determined whether phosphorylation of CP60 affects its ability to bind to microtubules. We used purified cyclin B/p34^{cdc2} complexes to phosphorylate the purified 6× His CP60 fusion protein, and we obtained quantitative phosphorylation of CP60, as seen by a quantitative shift of the CP60 protein to a slower-migrating form on polyacrylamide gels (Figure 7B, compare lanes 1 and 2). This phosphorylation of CP60 completely blocked its ability to

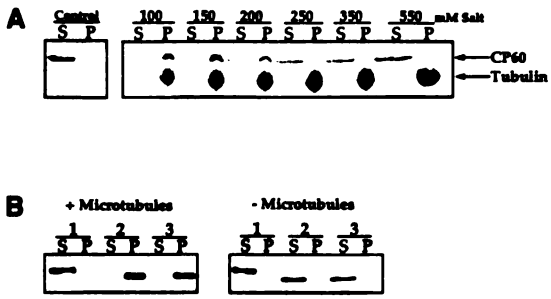

Figure 7. Binding of CP60 to microtubules. (A) Purified 6× His CP60 was tested for binding to microtubules using a cosedimentation assay as described in MATERIALS AND METHODS, and samples of the supernatant and pellet were analyzed by polyacrylamide gel electrophoresis. For each pair of lanes, the lane labeled "S" is the supernatant, and the lane labeled "P" is the pellet. The first panel labeled "control" shows the behavior of CP60 alone, demonstrating that it does not pellet in the absence of microtubules. The next panel shows a series of microtubule-binding tests carried out in successively higher concentrations of salt, demonstrating that CP60 binds quantitatively to microtubules at physiological salt concentrations. The indicated salt concentrations are the sum of the buffer (50 mM HEPES-KOH, pH 7.6) and added KCl. The gel is stained with Coomassie blue. (B) Purified 6× His CP60 was phosphorylated with cyclin B/p34^{cdc2} and tested for binding to microtubules as described in MATERIALS AND METHODS. The supernatants and pellets were analyzed on an SDS-polyacrylamide gel, transferred to nitrocellulose, and probed with an antibody against CP60. In the first panel, the first pair of lanes shows the behavior of phosphorylated CP60, demonstrating that it fails to cosediment with microtubules. Lanes 2 and 3 show the behavior of CP60 from control phosphorylation reactions that lacked either ATP or kinase, respectively. The second panel shows the results of control binding experiments that lack microtubules.

bind to microtubules in the cosedimentation assay (Figure 7B).

DISCUSSION

We have cloned and sequenced a cDNA encoding CP60, a protein that interacts with microtubules and is localized to the centrosome. We originally identified CP60 by virtue of its interaction with CP190, another *Drosophila* microtubule-associated protein that is localized to the centrosome, and these two proteins are components of a multiprotein complex (Kellogg and Alberts, 1992). The fact that CP60 shows no homology to any known proteins is perhaps not surprising, because so few centrosomal proteins have been cloned and sequenced. The centrosome is undoubtedly a complex organelle composed of many different proteins, and the identification and cloning of genes encoding new centrosomal proteins are important steps toward understanding its function and behavior.

Antibodies that recognize CP60 demonstrate that it localizes to the centrosome in a cell cycle–specific manner. The amount of CP60 at the centrosome is maximal during anaphase and telophase, and then drops dramatically sometime during late telophase or early interphase (see Figure 2). Our results suggest two possible mechanisms for regulating the association of CP60 with the centrosome. One possibility is that the disappearance of centrosomal CP60 at the end of mitosis is due to proteolytic destruction of CP60. A number of other proteins are known to be degraded at the end of mitosis, including the B-type cyclins, CENP-E, and CENP-F (Evans *et al.*, 1983; Brown *et al.*, 1994; Liao *et al.*, 1995). The idea that CP60 is degraded at the end of mitosis is supported by our finding that it has a sequence of amino acids similar to the destruction box that is known to be required for specific degradation of the B-type cyclins at the end of mitosis (Glotzer *et al.*, 1991). The dynamic changes in localization of CP60 might also be due to changes in its phosphorylation state, because our results demonstrate that CP60 has multiple phosphorylation sites for cyclin-dependent kinases or MAP kinases.

Although we observe phosphorylation of CP60 by cyclin-dependent kinases in vitro, it remains unclear which kinase or kinases actually phosphorylate CP60 in vivo. The substrate specificity of cyclin-dependent kinases and MAP kinases are found to overlap when studied in vitro (Nigg, 1993), and members of both of these large kinase families are known to be activated during mitosis (Gotoh *et al.*, 1990; Heider *et al.*, 1994; Minshull *et al.*, 1994). One criteria that can be used to suggest in vivo specificity is the finding of a kinase and its substrate together in a complex. For example, in the budding yeast mating pheromone signaling pathway, a number of kinases and their substrates have been identified by genetic and biochemical criteria, and these are found together in a large multiprotein complex (Marsh *et al.*, 1991; Reed, 1991; Choi *et al.*, 1994; Marcus *et al.*, 1994). It is therefore of interest that we found a CP60 kinase activity present in the group of proteins that form a complex with CP190. This kinase activity would seem to represent a good candidate for a protein that phosphorylates CP60 in vivo, and identification of this kinase should be possible by further purification followed by peptide sequencing.

The centrosome in animal cells undergoes a number of characteristic changes during mitosis, including a dramatic increase in the amount of pericentriolar material and in the number of microtubules nucleated by the centrosome (Kuriyama and Borisy, 1981; Voronova *et al.*, 1984; Vorobjev and Nadezhdina, 1987). There is also a dramatic increase in the presence of phosphorylated epitopes at the centrosome, as revealed by an antibody that recognizes a mitosis-specific phosphorylated epitope (Vandre *et al.*, 1984). It is interesting to note that the increased abundance of CP60 and CP190 at the centrosome is correlated with these events, suggesting that they may play a role.

Because CP60 is a highly phosphorylated protein, it may contribute substantially to the increase in phosphorylated epitopes seen at the centrosome during mitosis.

The CP60/CP190 complex binds to microtubules when a *Drosophila* embryo extract is passed over a microtubule affinity column. To determine whether CP60 alone is capable of interacting with microtubules, we obtained purified CP60 from a bacterial expression system, and tested whether or not it is capable of binding to purified microtubules in a cosedimentation assay. We found that CP60 binds quantitatively to microtubules under physiological salt conditions, and that binding is completely blocked by phosphorylation of CP60 with the cyclin-dependent kinase $p34^{cdc2}$. The fact that the binding of CP60 to microtubules is regulated by phosphorylation argues that it is a genuine in vivo activity, rather than the result of an in vitro artifact. However, because we do not know when the phosphorylations that inactivate microtubule binding occur during the cell cycle, the function of the microtubule-binding activity of CP60 is unclear.

CP60 and CP190 can be added to a growing list of proteins that localize to both the nucleus and to microtubule structures (Barnes *et al.*, 1992; Kuriyama and Nislow, 1992; Nislow *et al.*, 1992; Yang *et al.*, 1992). The significance of the nuclear localization of these proteins remains unclear, although one can imagine a number of possibilities. Proteins like CP190 and CP60 could be bifunctional, carrying out one function involving microtubules, and an independent function in the nucleus. Alternatively, certain proteins that function in the cytoplasm could be moved into the nucleus to sequester their activity away from cytoplasmic proteins. In our case, when the nuclear envelope breaks down at the beginning of mitosis, CP60 and CP190 would be released into the cytoplasm to play a specific role in the microtubule-based activities of mitosis.

When we used immunoaffinity chromatography to identify proteins that interact with CP60, we found that CP190 is the major protein that interacts with CP60 under the conditions used for our experiment. A number of additional proteins that interact with the anti-CP60 immunoaffinity column also interact with an anti-CP190 immunoaffinity column. These results provide further support for the idea that CP60 and CP190 are components of a multiprotein complex.

The cloning and sequencing of the CP60 cDNA is an important step toward understanding the functions of CP60 and the centrosome. Most recently, we have used the CP60 cDNA sequence in a bacterial expression system to obtain large amounts of purified CP60 protein. The purified CP60 can be fluorescently labeled and injected into embryos to follow its behavior in living cells (Oegema and Alberts, unpublished data). When combined with site-directed mutagenesis, this approach should allow us to determine how the putative destruction box and specific phosphorylations play a role in the cell cycle–dependent behavior of CP60. This approach may also allow us to create dominant mutations that can be used to disrupt the functions carried out by CP60 within the cell. Finally, the sequence of CP60 provides a first step toward identification of its homologues in other organisms that offer specific technical advantages for centrosome studies.

ACKNOWLEDGMENTS

We thank Christine Field, Nora Kury, Mercedes Rojas, Bill Sullivan, and Bill Theurkauf for providing helpful advice and support. We also thank Christine Field for providing adult supervision. This work was supported by National Institutes of Health grant GM-23928.

REFERENCES

Anderson, C.W., Baum, P.R., and Gesteland, R.F. (1973). Processing of adenovirus 2-induced proteins. J. Virol. *12*, 241–252.

Barnes, G., Louie, K.A., and Botstein, D. (1992). Yeast proteins associated with microtubules in vitro and in vivo. Mol. Biol. Cell *3*, 29–47.

Bradford, M. (1976). A rapid and sensitive method for the quantification of microgram quantities of protein utilizing the principle of protein-dye binding. Anal. Biochem. *72*, 248–254.

Brown, K.D., Coulson, R.M., Yen, T.J., and Cleveland, D.W. (1994). Cyclin-like accumulation and loss of the putative kinetochore motor CENP-E results from coupling continuous synthesis with specific degradation at the end of mitosis. J. Cell Biol. *125*, 1303–1312.

Brown, N.H., and Kafatos, F.C. (1988). Functional cDNA libraries from *Drosophila* embryos. J. Mol. Biol. *203*, 425–437.

Butner, K., and Kirschner, M.W. (1991). Tau protein binds to microtubules through a flexible array of distributed weak sites. J. Cell Biol. *115*, 717–730.

Choi, K.Y., Satterberg, B., Lyons, D.M., and Elion, E.A. (1994). Ste5 tethers multiple protein kinases in the MAP kinase cascade required for mating in *S. cerevisiae*. Cell *78*, 499–512.

de Frutos, R., Kimura, K., and Peterson, K.R. (1989). In situ hybridization of *Drosophila* polytene chromosomes with digoxigenin-dUTP labelled probes. Trends Genet. *5*, 366.

Evans, T., Rosenthal, E.T., Youngblom, J., Distel, D., and Hunt, T. (1983). Cyclin: a protein specified by maternal mRNA in sea urchin eggs that is destroyed at each cleavage division. Cell *33*, 389–396.

Foe, V.E., and Alberts, B.M. (1983). Studies of nuclear and cytoplasmic behavior during the five mitotic cycles that precede gastrulation in *Drosophila*. J. Cell Sci. *61*, 31.

Frasch, M., Glover, D., and Saumweber, H. (1986). Nuclear antigens follow different pathways into daughter nuclei during mitosis in early *Drosophila* embryos. J. Cell Sci. *82*, 155–172.

Gibbons, I.R., Asai, D.J., Ching, N.S., Dolecki, G.J., Mocz, G., Phillipson, C.A., Ren, H., Tang, W.J., and Gibbons, B.H. (1991). A PCR procedure to determine the sequence of large polypeptides by rapid walking through a cDNA library. Proc. Natl. Acad. Sci. USA *88*, 8563–8567.

Glotzer, M., Murray, A.W., and Kirschner, M.W. (1991). Cyclin is degraded by the ubiquitin pathway. Nature *349*, 132–138.

Gotoh, Y., Niishida, E., Yamashita, T., Hoshi, M., Kawakamii, M., and H. Sakai (1990). Microtubule-associated-protein (MAP) kinase activated by nerve growth factor and epidermal growth factor in PC12 cells. Eur. J. Biochem. *193*, 661–669.

Harlow, E., and Lane, D. (1988). Antibodies: A Laboratory Manual, Cold Spring Harbor, New York: Cold Spring Harbor Laboratory Press.

Heider, H., Hug, C., and Lucocq, J.M. (1994). A 40-kDa myelin basic protein kinase, distinct from erk1 and erk2, is activated in mitotic HeLa cells. Eur. J. Biochem. *219*, 513–520.

Holloway, S.L., Glotzer, M., King, R.W., and Murray, A.W. (1993). Anaphase is initiated by proteolysis rather than by the inactivation of MPF. Cell *73*, 1393–1402.

Kalt, A., and Schliwa, M. (1993). Molecular components of the centrosome. Trends Cell Biol. *3*, 119–128.

Karsenti, E., and Maro, B. (1986). Centrosomes and the spatial organization of microtubules in animal cells. Trends Biochem. Sci. *11*, 460–463.

Kellogg, D.R., and Alberts, B.M. (1992). Purification of a multiprotein complex containing centrosomal proteins from the *Drosophila* embryo by chromatography with low-affinity polyclonal antibodies. Mol. Biol. Cell *3*, 1–11.

Kellogg, D.R., Kikuchi, A., Fujii-Nakata, T., Turck, C.W., and Murray, A. (1995). Members of the NAP/SET family of proteins interact specifically with B-type cyclins. J. Cell Biol. *130*, 661–673.

Kellogg, D.R., Mitchison, T.J., and Alberts, B.M. (1988). Behavior of microtubules and actin filaments in living *Drosophila* embryos. Development *103*, 675–686.

Kellogg, D.R., Moritz, M., and Alberts, B.M. (1994). The centrosome and cellular organization. Annu. Rev. Biochem. *63*, 639–674.

Kuriyama, R., and Borisy, G.G. (1981). Microtubule-nucleating activity of centrosomes in Chinese hamster ovary cells is independent of the centriole cycle but coupled to the mitotic cycle. J. Cell Biol. *91*, 822–826.

Kuriyama, R., and Nislow, C. (1992). Molecular components of the mitotic spindle. BioEssays *14*, 81–8.

Liao, H., Winkfein, R.J., Mack, G., Rattner, J.B., and Yen, T.J. (1995). CENP-F is a protein of the nuclear matrix that assembles onto kinetochores at late G2 and is rapidly degraded after mitosis. J. Cell Biol. *130*, 507–518.

Marcus, S., Polverino, A., Barr, M., and Wigler, M. (1994). Complexes between STE5 and components of the pheromone-responsive mitogen-activated protein kinse module. Proc. Natl. Acad. Sci. USA *91*, 7762–6.

Marsh, L., Neiman, A.R., and Herskowitz, I. (1991). Signal transduction during pheromone response in yeast. Annu. Rev. Cell Biol. *7*, 699–728.

Minshull, J., Sun, H., Tonks, N.K., and Murray, A.W. (1994). MAP-kinase–dependent mitotic feedback arrest in *Xenopus* egg extracts. Cell *79*, 475–486.

Mitchison, T.J., and Kirschner, M.W. (1984). Microtubule assembly nucleated by isolated centrosomes. Nature *312*, 232–237.

Morris, C.F., Hama-Inaba, H., Mace, D., Sinha, N.K., and Alberts, B.M. (1979). Purification of the gene 43, 44, 45 and 62 proteins of the bacteriophage T4 DNA replication apparatus. J. Biol Chem 254, 6787–6796.

Nigg, E.A. (1993). Cellular substrates of $p34^{cdc2}$ and its companion cyclin-dependent kinases. Trends Cell Biol. *3*, 296–301.

Nislow, C., Lombillo, V.A., Kuriyama, R., and McIntosh, J.R. (1992). A plus-end-directed motor enzyme that moves antiparallel microtubules in vitro localizes to the interzone of mitotic spindles. Nature *359*, 543–547.

Oegema, K., Whitfield, W.G.F., and Alberts, B.M. (1995). The cell cycle-dependent localization of the CP190 centrosomal protein is determined by the coordinate action of two separable domains. J. Cell Biol. *131*, 1–13.

Reed, S.I. (1991). Pheromone signalling pathways in yeast. Curr. Opin. Genet. Dev. *1*, 391–396.

Smith, D.B., and Johnson, K.S. (1988). Single-step purification of polypeptides expressed in *Escherichia coli* as fusions with glutathione *S*-transferase. Gene *67*, 31–40.

Steinhauer, W.R., Walsh, R.C., and Kalfayan, L.J. (1989). Sequence and structure of the *Drosophila melanogaster* ovarian tumor gene and generation of an antibody specific for the ovarian tumor protein. Mol. Cell. Biol. *9*, 5726–5732.

Theurkauf, W.E. (1992). Behavior of structurally divergent alpha tubulin isotypes during *Drosophila* embryogenesis: evidence for post-translational regulation of isotype abundance. Dev. Biol. *154*, 205–217.

Vandre, D.D., Davis, F.M., Rao, P.N., and Borisy, G.G. (1984). Phosphoproteins are components of mitotic microtubule-organizing centers. Proc. Natl. Acad. Sci USA *81*, 4439–4443.

Vorobjev, I.A., and Nadezhdina, E.S. (1987). The centrosome and its role in the organization of microtubules. Int. Rev. Cytol. *106*, 227–293.

Voronova, A.F., Buss, J.E., Patschinsky, T., Hunter, T., and Sefton, B.M. (1984). Characterization of the protein apparently responsible for the elevated tyrosine protein kinase activity in LSTRA cells. Mol. Cell. Biol. *4*, 2705–2713.

Whitfield, W.G., Millar, S.E., Saumweber, H., Frasch, M., and Glover, D.M. (1988). Cloning of a gene encoding an antigen associated with the centrosome in *Drosophila*. J. Cell. Sci. *89*, 467–480.

Yang, C.H., Lambie, E.J., and Snyder, M. (1992). NuMA: an unusually long coiled-coil related protein in the mammalian nucleus. J. Cell. Biol. *116*, 1303–1317.

References

Bailly, E., M. Doree, P. Nurse, and M. Bornens. 1989. p34cdc2 is located in both nucleus and cytoplasm; part is centrosomally associated at G2/M and enters vesicles at anaphase. *Embo J.* 8:3985-95.

Boleti, H., E. Karsenti, and I. Vernos. 1996. Xklp2, a novel Xenopus centrosomal kinesin-like protein required for centrosome separation during mitosis. *Cell.* 84:49-59.

Buendia, B., G. Draetta, and E. Karsenti. 1992. Regulation of the microtubule nucleating activity of centrosomes in Xenopus egg extracts: role of cyclin A-associated protein kinase. *J Cell Biol.* 116:1431-42.

Centonze, V. E., and G. G. Borisy. 1990. Nucleation of microtubules from mitotic centrosomes is modulated by a phosphorylated epitope. *J Cell Sci.* 95:405-11.

Doxsey, S. J., P. Stein, L. Evans, P. D. Calarco, and M. Kirschner. 1994. Pericentrin, a highly conserved centrosome protein involved in microtubule organization [see comments]. *Cell.* 76:639-50.

Endow, S. A., R. Chandra, D. J. Komma, A. H. Yamamoto, and E. D. Salmon. 1994. Mutants of the Drosophila ncd microtubule motor protein cause centrosomal and spindle pole defects in mitosis. *J Cell Sci.* 107:859-67.

Engle, D. B., J. H. Doonan, and N. R. Morris. 1988. Cell-cycle modulation of MPM-2-specific spindle pole body phosphorylation in Aspergillus nidulans. *Cell Motil Cytoskeleton.* 10:434-7.

Evans, L., T. Mitchison, and M. Kirschner. 1985. Influence of the centrosome on the structure of nucleated microtubules. *J Cell Biol.* 100:1185-91.

Felix, M. A., C. Antony, M. Wright, and B. Maro. 1994. Centrosome assembly in vitro: role of γ-tubulin recruitment in Xenopus sperm aster formation. *J Cell Biol.* 124:19-31.

Frasch, M., D. M. Glover, and H. Saumweber. 1986. Nuclear antigens follow different pathways into daughter nuclei during mitosis in early Drosophila embryos. *J Cell Sci.* 82:155-72.

Gould, R. R., and G. G. Borisy. 1977. The pericentriolar material in Chinese hamster ovary cells nucleates microtubule formation. *J Cell Biol.* 73:601-15.

Heuer, J. G., K. Li, and T. C. Kaufman. 1995. The Drosophila homeotic target gene centrosomin (cnn) encodes a novel centrosomal protein with leucine zippers and maps to a genomic region required for midgut morphogenesis. *Development.* 121:3861-76.

Joshi, H. C., M. J. Palacios, L. McNamara, and D. W. Cleveland. 1992. Gamma-tubulin is a centrosomal protein required for cell cycle-dependent microtubule nucleation. *Nature.* 356:80-3.

Kallajoki, M., K. Weber, and M. Osborn. 1991. A 210 kDa nuclear matrix protein is a functional part of the mitotic spindle; a microinjection study using SPN monoclonal antibodies. *Embo J.* 10:3351-62.

Kalnins, V. 1992. The centrosome. *In* Cell Biology: A Series of Monographs. D. Buetow, G. Padilla, I. Cameron, and A. Zimmerman, editors. Academic Press, Inc., San Diego.

Kellogg, D. R., and B. M. Alberts. 1992. Purification of a multiprotein complex containing centrosomal proteins from the Drosophila embryo by chromatography with low-affinity polyclonal antibodies. *Mol Biol Cell.* 3:1-11.

Kellogg, D. R., C. M. Field, and B. M. Alberts. 1989. Identification of microtubule-associated proteins in the centrosome, spindle, and kinetochore of the early Drosophila embryo. *J Cell Biol.* 109:2977-91.

Kellogg, D. R., M. Moritz, and B. M. Alberts. 1994. The centrosome and cellular organization. *Annu Rev Biochem.* 63:639-74.

Kellogg, D. R., K. Oegema, J. Raff, K. Schneider, and B. M. Alberts. 1995. CP60: a microtubule-associated protein that is localized to the centrosome in a cell cycle-specific manner. *Mol Biol Cell.* 6:1673-84.

Keryer, G., H. Ris, and G. G. Borisy. 1984. Centriole distribution during tripolar mitosis in Chinese hamster ovary cells. *J Cell Biol.* 98:2222-9.

Kuriyama, R., and G. G. Borisy. 1981. Microtubule-nucleating activity of centrosomes in Chinese hamster ovary cells is independent of the centriole cycle but coupled to the mitotic cycle. *J Cell Biol.* 91:822-6.

Li, K., and T. Kaufman. 1996. The homeotic target gene centrosomin encodes an essential centrosomal component. *Cell*. 85:585-596.

Mazia, D. 1987. The chromosome cycle and the centrosome cycle in the mitotic cycle. *Int Rev Cytol*. 100:49-92.

Mitchison, T., and M. Kirschner. 1984. Microtubule assembly nucleated by isolated centrosomes. *Nature*. 312:232-7.

Moritz, M., M. B. Braunfeld, J. W. Sedat, B. Alberts, and D. A. Agard. 1995. Microtubule nucleation by gamma-tubulin-containing rings in the centrosome. *Nature*. 378:638-40.

Oakley, B. R., C. E. Oakley, Y. Yoon, and M. K. Jung. 1990. Gamma-tubulin is a component of the spindle pole body that is essential for microtubule function in Aspergillus nidulans. *Cell*. 61:1289-301.

Oakley, C. E., and B. R. Oakley. 1989. Identification of gamma-tubulin, a new member of the tubulin superfamily encoded by mipA gene of Aspergillus nidulans. *Nature*. 338:662-4.

Price, C. M., and D. E. Pettijohn. 1986. Redistribution of the nuclear mitotic apparatus protein (NuMA) during mitosis and nuclear assembly. Properties of purified NuMA protein. *Exp Cell Res*. 166:295-311.

Raff, J.W., D.R. Kellogg and B.M. Alberts. 1993. *Drosophila* γ-tubulin is part of a complex containing two previously identifed centrosomal MAPs. *J Cell Biol.* 121:823-835.

Rieder, C., and G. Borisy. 1982. The Centrosome Cycle in PtK2 Cells: Asymmetric Distribution and Structural Changes in the Pericentriolar Material. *Biology of the Cell.* 44:117-132.

Robbins, E., G. Jentzsch, and A. Micali. 1968. The centriole cycle in synchronized HeLa cells. *J Cell Biol.* 36:329-39.

Schatten, G. 1994. The centrosome and its mode of inheritance: the reduction of the centrosome during gametogenesis and its restoration during fertilization. *Dev Biol.* 165:299-335.

Stearns, T., L. Evans, and M. Kirschner. 1991. Gamma-tubulin is a highly conserved component of the centrosome. *Cell.* 65:825-36.

Stearns, T., and M. Kirschner. 1994. In vitro reconstitution of centrosome assembly and function: the central role of γ-tubulin. *Cell.* 76:623-37.

Tousson, A., C. Zeng, B. R. Brinkley, and M. M. Valdivia. 1991. Centrophilin: a novel mitotic spindle protein involved in microtubule nucleation. *J Cell Biol.* 112:427-40.

Vandre, D. D., and G. G. Borisy. 1989. Anaphase onset and dephosphorylation of mitotic phosphoproteins occur concomitantly. *J Cell Sci.* 94:245-58.

Vorobjev, I. A., and S. Chentsov Yu. 1982. Centrioles in the cell cycle. I. Epithelial cells. *J Cell Biol.* 93:938-49.

Vorobjev, I. A., and E. S. Nadezhdina. 1987. The centrosome and its role in the organization of microtubules. *Int Rev Cytol.* 106:227-93.

Whitfield, W. G., M. A. Chaplin, K. Oegema, H. Parry, and D. M. Glover. 1995. The 190 kDa centrosome-associated protein of Drosophila melanogaster contains four zinc finger motifs and binds to specific sites on polytene chromosomes. *J Cell Sci.* 108:3377-87.

Whitfield, W. G., S. E. Millar, H. Saumweber, M. Frasch, and D. M. Glover. 1988. Cloning of a gene encoding an antigen associated with the centrosome in Drosophila. *J Cell Sci.* 89:467-80.

Wilson, E. B. 1925. The Cell in Development and Heredity. Macmillian, New York. 1232.

Zheng, Y., M. K. Jung, and B. R. Oakley. 1991. Gamma-tubulin is present in Drosophila melanogaster and Homo sapiens and is associated with the centrosome. *Cell.* 65:817-23.

Zheng, Y., M. L. Wong, B. Alberts, and T. Mitchison. 1995. Nucleation of microtubule assembly by a gamma-tubulin-containing ring complex. *Nature.* 378:578-83.